

FINAL TECHNICAL REPORT

CONTRACT N°: FIGE-CT-2000-00108

PROJECT N°: FIS5-1999-00353

ACRONYM: ADVANCE

TITLE : SOURCE-SPECIFIC ECOSYSTEM TRANSFER OF ACTINIDES UTILISING
ADVANCED TECHNOLOGIES

CO-ORDINATOR : NATIONAL UNIVERSITY OF IRELAND
UNIVERSITY COLLEGE DUBLIN (UCD) IE

PARTNERS: UNIVERSIDAD DE SEVILLA (USEV) E
MIDDLESEX UNIVERSITY (MU) UK
AGRICULTURAL UNIVERSITY OF NORWAY (AUN) NO
NORWEGIAN RADIATION PROTECTION AUTHORITY (NRPA) NO

REPORTING PERIOD: FROM January 1, 2001

TO December 31, 2003

PROJECT START DATE: January 1, 2001

DURATION: 36 months

DATE OF ISSUE OF THIS REPORT: May 2004



EURATOM

Project funded by the European Commission under its RTD programme
(Nuclear Energy, EURATOM Framework Programme V, 1998-2002)

Table of Contents

Executive Summary	3
Objectives and Strategic Aspects	5
Scientific and technical description of the results	7
WP1. Review of existing information on sources and analytical tools	7
WP2. Characterisation of particles	8
Nuclear weapons tests: Semipalatinsk, Kazakhstan	9
Nuclear weapons disintegration: Palomares and Thule	15
Nuclear reactors accidents: Chernobyl	22
Reprocessing facilities: Mayak and Sellafield	25
Depleted uranium munitions: Kosovo, Serbia and Kuwait	32
WP3. Terrestrial ecosystems affected by actinide contamination	37
Palomares	37
Semipalatinsk nuclear test site	40
Mayak PA	44
Source-term characteristics and transfer in terrestrial ecosystems	46
WP4. Mobility in fresh water systems	49
Semipalatinsk nuclear test site	49
Mayak PA	59
Improvement of migration models (Mayak)	62
WP5. Transfer processes in marine (saline) environments	68
Sellafield	68
Palomares	75
Source-term characteristics and transfer in marine ecosystems	77
WP6. Comparative assessment	78
Semipalatinsk	79
Palomares and Thule	79
Chernobyl	80
Sellafield and Mayak	81
Kosovo and Kuwait	82
Recommendations regarding the characterisation of samples containing radioactive particles	83
Conclusions	88
References	89

Executive Summary

The ADVANCE project, carried out under the EC's Fifth Framework Programme, was initiated in January 2001 as a co-ordinated effort to investigate the influence of source term and ecosystem related characteristics on the transfer of actinides in different terrestrial, freshwater and marine ecosystems using advanced technologies.

The main objectives of the ADVANCE project were to (i) identify source- and ecosystem-related characteristics influencing the transfer of actinides in different terrestrial, freshwater and marine ecosystems, using advanced technologies; (ii) investigate the effect of source- and ecosystem-related characteristics on the transfer of actinides to biological endpoints (including humans); and (iii) significantly strengthen the European scientific competence and analytical technological skills within the field of radioecology.

To achieve these goals, a number of contaminated sites, chosen to represent different source-term and ecosystem characteristics, were systematically studied using a wide range of advanced analytical techniques. The selected study sites included a former nuclear test site (Semipalatinsk, Kazakhstan), sites affected by nuclear accidents involving the disintegration of nuclear weapons (Palomares, Spain; Thule, Greenland), areas affected by releases from reprocessing operations (Sellafield, UK; Mayak PA, Russia) and regions where depleted uranium munitions were used in recent conflicts (Kuwait and Kosovo).

A substantial effort was directed at the identification and characterisation of particles (heterogeneities) in samples collected at each of the selected sites. Particles identified either by sub-sampling and non-destructive gamma spectroscopy or by autoradiography were analysed using electron microscopy techniques. Scanning electron microscopy (SEM) using backscattered electrons provided information on the structure of the particles, as well as on the distribution of high atomic number elements on particle surfaces, while transmission electron microscopy (TEM) was used to identify electron-dense colloidal-sized structures. X-ray microanalysis (XRMA) was also used, in conjunction with electron microscopy techniques, to obtain information on the elemental composition of the particles. A selection of samples of particular interest were subjected to synchrotron-based techniques (μ -XRD, μ -tomography, μ -XANES) to obtain information on elemental distributions, crystallographic structures and oxidation states of actinides on individual micro-sized particles.

In addition, a comprehensive toolbox combining established (low-background alpha, beta and gamma spectroscopy) and novel (ICP-MS, AMS, RIMS) analytical techniques were used, in conjunction with speciation techniques, to identify the distribution, isotopic composition and physico-chemical speciation of actinides in different environmental compartments at each of the study sites. Finally, the bioavailability of actinides was investigated by a series of *in vitro* solubility tests.

The presence of radioactive particles and fragments varying in size, shape, structure, morphology, density, oxidation state distribution and charge was confirmed at all of the sites. Bioavailability and sequential extraction experiments conducted in the course of the project clearly demonstrated that failure to recognise the presence of these particles and their weathering characteristics may lead to analytical inconsistencies, irreproducible results and, ultimately, to erroneous conclusions regarding the mobility of these radionuclides in a given ecosystem.

Moreover, the study makes clear that any realistic assessment of the short- and long-term impact of actinide releases to a particular ecosystem should include, in addition to a programme to evaluate the radionuclide distribution in the ecosystem compartments, a suitable strategy to identify, isolate and characterise radioactive particles present at the site. Information on the physical and chemical characteristics of the particles, and kinetic information on processes influencing particle weathering, mobility and bioavailability of released radionuclide species associated with these particles should also form part of any such assessment.

Characterisation of source-terms, including radioactive particles in the submicrometer to micrometer range, certainly represents an analytical challenge. However, as demonstrated in the course of the ADVANCE project, application of emerging, state-of-the-art, advanced technologies in conjunction with more traditional techniques, can undoubtedly provide much of the required information.

2.1. Objectives and Strategic Aspects

The main objectives of the ADVANCE project were to:

- Identify source- and ecosystem-related characteristics influencing the transfer of actinides in different terrestrial, freshwater and marine ecosystems, using advanced technologies;
- Investigate the effect of source- and ecosystem-related characteristics on the transfer of actinides to biological endpoints (including humans); and
- Significantly strengthen the European scientific competence and analytical technological skills within the field of radioecology.

To achieve these goals, a number of sites, chosen to represent different source-term and ecosystem characteristics, were systematically studied using advanced technologies. The selected study sites included:

- The vicinity of ‘Ground Zero’ at the Semipalatinsk Nuclear Test Site (NTS) in present-day Kazakhstan, where 116 atmospheric nuclear tests were conducted in the period 1949–63 by the former Soviet Union;
- The Tel’kem I and Tel’kem II freshwater crater lakes within the Semipalatinsk NTS, created by the explosion of one and three 0.24 kT nuclear (plutonium) devices, respectively, in 1968;
- The Balapan (Atomic) lake within the Semipalatinsk NTS, created by the Chagan cratering thermonuclear explosion (140 kT) in 1965;
- The terrestrial and marine environments in the vicinity of Palomares (Spain), site of a nuclear accident involving the dispersion of insoluble plutonium oxide from fractured nuclear weapons in 1966;
- The marine environment in the vicinity of Thule (Greenland), site of a nuclear accident involving the disintegration of a number of nuclear weapons in 1968;
- The terrestrial and freshwater environments in the vicinity of the Mayak PA reprocessing plant in the SE Urals;
- The marine environment in the vicinity of the Sellafield reprocessing plant in Cumbria, UK;
- The terrestrial environment in the vicinity of Chernobyl, site of a nuclear reactor accident in 1986; and
- Target sites in Kosovo and Kuwait where depleted uranium (DU) ammunition was used during the Balkans and Gulf War conflicts in the 1990’s.

For each of these sites, contaminated as they are with actinides, archive and new samples (gathered in the course of field work undertaken as part of this project), were analysed using a combination of advanced speciation and low-level measurement techniques, with a view to identifying the key source- and ecosystem-related characteristics influencing the mobility and bioavailability of these radionuclides.

The form in which actinides are present in soil, sediment and water greatly influences their mobility and potential transfer. Actinides released from a source may be present as fragments, particles, aerosols or in the form of pseudocolloidal, colloidal or low molecular mass species. It is well established that a significant fraction of actinides released during

nuclear tests or accidents (such as those which are the subject of study here) may be present as discrete particles varying in structure and composition, and that effluents from reprocessing plants may also contain numerous radioactive particles and colloids. Following their release, radioactive particles represent point sources of short- and long-term radioecological significance, and the failure to recognise their presence (as has been the case in many monitoring and assessment programmes) may lead to significant errors in the short- and long-term radiological evaluation of the impact of actinide contamination at a particular site.

It is for this reason that in this project a substantial effort was directed at the identification and characterisation of particles (heterogeneities) present in the different environmental compartments of the study sites. Particles identified either by sub-sampling and non-destructive gamma spectroscopy or by autoradiography, were analysed using electron microscope techniques. Scanning electron microscopy (SEM) using backscattered electrons provided information on the structure of the particles, as well as on the distribution of high atomic number elements on particle surfaces, while transmission electron microscopy (TEM) was used to identify electron-dense colloidal-sized structures. X-ray microanalysis (XRMA) was also used, in conjunction with electron microscopy techniques, to obtain information on the elemental composition of the particles.

A selection of samples of particular interest were subjected to synchrotron-based techniques (μ -XRD, μ -tomography, μ -XANES) to obtain information on elemental distributions, crystallographic structures and oxidation states of actinides on individual micro-sized particles. The data obtained using these novel, state-of-the-art techniques have provided new information on particle characteristics influencing weathering rates and subsequent actinide mobilisation.

In addition, a comprehensive toolbox combining established (low-background alpha, beta and gamma spectrometry) and novel (ICP-MS, AMS, RIMS) analytical techniques were used, in conjunction with speciation techniques (i.e. dual tracer co-precipitation, in-situ fractionation, tangential-flow ultrafiltration), to identify the distribution, isotopic composition and physico-chemical speciation of actinides in different environmental compartments at each of the study sites. Finally, the bioavailability of actinides was investigated by a series of *in vitro* solubility experiments using simulated gastrointestinal fluid.

The findings of the ADVANCE project will be available for incorporation, in the form of revised model parameters, into models employed for the purposes of emergency planning and preparedness. The data generated are particularly relevant, as they have been gathered at accident sites within Europe (Palomares) and the former CIS (Mayak, Chernobyl), and should prove invaluable in helping to increase Europe's collective preparedness to face and manage future nuclear accidents.

In addition, the data generated should also be relevant to the assessment of the environmental impact of routine and authorised releases of radioactivity to the marine environment. Similarly, they should be of direct applicability to hazard identification at existing contaminated environments such as Mayak and the Semipalatinsk test site. For these latter, international agencies have recognised an urgent priority for site hazard identification and remediation, and have called upon international agencies to fund studies in co-operation with local responsible organisations. It is anticipated that the data generated in the course of the project, ranging from the simple analysis of contamination levels to the measurement of

actinide contamination of workers and local inhabitants, will be used to assess the hazards associated with local actinide deposits and to develop appropriate strategies for economic site remediation and/or exclusion. The data will be made available to those charged with the responsibility for site surveillance and will thus form part of the common database concerning contamination at these sites. The project has also provided new data that can be used for the optimisation of routine monitoring strategies within contaminated sites, including new, state-of-the-art methods and technologies, which can be implemented, where appropriate.

2.2. Scientific and technical description of the results

In order to facilitate the achievement of the objectives stated above, the project was divided into six distinct work-packages, each of them sub-divided into a set of relevant research activities. The work packages included • a review of existing information on sources and analytical tools, • the characterisation of isolated radioactive particles, • a study of terrestrial ecosystems affected by actinide contamination, • a study of actinide mobility in freshwater systems, • a study of actinide transfer processes in marine (saline) ecosystems, and • a comparative assessment of source-specific and ecosystem specific characteristics influencing the transfer of actinides in the different ecosystems considered.

In the next sections, a description of the scientific and technical progress achieved in each of these work-packages by the end of the project is given, including an assessment of the main results and the key conclusions. A listing of the publications that have issued as a result of the project is also provided in the attached final management report.

WP1. Review of existing information on sources and analytical tools

Existing data and information regarding source-term characteristics, spatial and temporal distributions of actinides, isotopic composition and actinide speciation (including heterogeneities) at each of the study sites were collated by the participants at the outset, with a view to obtaining an up-to-date picture of the breadth of existing data on actinide contamination at these sites. This information was made available to the Commission as one of the project's deliverables (deliverable D2, submitted with the first annual report). A careful scrutiny of this updated literature database allowed the collaboration to identify knowledge gaps and helped in the planning of necessary field work. For each of the study sites, the corresponding literature database was synthesised in the form of summary reports for internal circulation amongst the project's participants. Periodic updates of the existing database were carried out in the course of the project, and resulted in an extensive bibliography covering the period up to the end of 2003. This bibliography represents the final version of deliverable D2, which is appended at the end of this report.

In addition, a review report on the analytical techniques being used in the project was prepared by the collaboration and made available to the Commission as a project deliverable (deliverable D1, also submitted with the first annual report). The report included a synthesis of the theory and operating principles of radionuclide speciation analysis, a discussion on sampling and pre-analysis strategies, a review of fractionation techniques for radionuclides in water, sediments and soils (including electron microscopy and high energy X-ray tomography), a discussion on kinetic experiments and models, and their use in radionuclide

speciation studies, a review of radiochemical techniques, and a description of low-level radionuclide measurement systems (including advanced mass spectrometric methods).

WP2. Characterisation of particles

The objective of this important work-package was to identify source-related characteristics of released particles (of relevance for ecosystem transfer) using a combination of advanced analytical tools. Particles were identified and isolated from archive samples and from samples collected in the course of field work carried as part of the ADVANCE project. A summary of the location, source term and matrix of the particles studied is given in Table 1.

Table 1. Particle-contaminated samples included in the ADVANCE project

Source-term	Site	Location	Matrix
Nuclear weapons tests	Semipalatinsk NTS, Kazakstan	Tel’kem 1	Crater spoil (soil)
		Tel’kem 2	Crater spoil (soil)
		Ground Zero	Surface soil
		Lake Balapan	Crater spoil (sediment)
Nuclear weapons accidents	Palomares, Spain	Palomares	Surface soil
	Thule, Greenland	Bylot Sound	Sediments
Nuclear reactor accident	Chernobyl, Ukraine	West & North	Dust and soil
Reprocessing facilities	Sellafield, UK	Irish Sea	Sediment profile
		Ravenglass estuary	Surface sediments
	Mayak PA, Russia	Reservoirs Techa River	Sediments Soil profile
DU munitions	Kosovo	Ceja Mountain	Surface soil
	Kuwait	Al Doha	Surface soil
		Manageesh	Surface soil
		Um Al Kwaty	Surface soil

Information on particle characteristics was obtained using a combination of autoradiography, gamma spectroscopy, scanning electron microscopy (SEM) interfaced with X-ray microanalysis (XRMA), as well as with four different synchrotron-based X-ray microscopic techniques. Inhomogeneous distribution of radionuclides in environmental samples (as determined by, for example, gamma spectrometry) reflected the presence of heterogeneities (radioactive particles). For such samples, autoradiography using phosphor imaging was performed to locate and isolate the spatial region of a sample containing such heterogeneities. Following a series of sample subdivisions, leaving only a relatively small number of grains, SEM combined with XRMA were used to identify high atomic element particles prior to the synchrotron experiments.

During the duration of the project, the collaboration had access to the second generation synchrotron *Hasylab* in Hamburg and the third generation synchrotron *European Synchrotron Radiation Facility (ESRF)* in Grenoble. Several experiments were performed at *Hasylab*, Beamline L, and at three different beamlines at *ESRF*, namely ROBL, ID18 and ID22.

Synchrotron-based microscopic techniques (μ -XAS, μ -XRD, μ -tomography and μ -XANES) were used on selected particles to obtain information on elemental distributions, crystallographic structures and oxidation state distribution on individual micro-sized particles. A summary of the results obtained is given below.

Nuclear Weapons Tests: Semipalatinsk, Kazakhstan

The Semipalatinsk Nuclear Test Site (STS), located in the north-east of present day Kazakhstan (Figure 1), was the first and one of the main proving grounds for the testing of nuclear weapons by the former Soviet Union. The test site, situated 150 km west of Semipalatinsk, a city of 700,000 inhabitants, extends over an area of 18,500 km² – a territory comparable in size to, for example, Northern Ireland (14,100 km²) or Wales (20,800 km²). The site is a relatively flat area, with a landscape typical of the plains of the dry Eurasian steppe.



Figure 1. Location of the STS in Kazakhstan (reproduced from: Stone, 2003)

Over the period 1949-1989, a total of 456 nuclear test explosions were fielded at the STS. Of these, 116 were atmospheric tests (30 surface tests and 86 air tests), with the remaining 340 carried out underground (IAEA, 1998).

Testing at the site was conducted in four main ‘technical areas’ (*ploshchadkas*), referred to as Technical Areas Sh, B, G and M (Figure 2). The early surface and air tests were carried out in the northern technical area Sh. The first Soviet atomic test was conducted at the centre of this area, often referred to as ‘Ground Zero’, on 29th August 1949. Up to December 1962, a further 115 atmospheric explosions were carried out in this zone, giving an estimated total energy release equivalent to 6.62 megatons (Mt) of TNT (Bennett *et al.*, 2000).

Following the signing of the limited test ban treaty in 1963, testing moved underground, mainly to Technical Areas G (*Degelen Massif*) and B (*Balapan*). In all, 318 test explosions were performed underground between 1961 and 1989 at these two sites. A further 22 tests were conducted in Technical Area M, also known as *Sary-Uzen* (Figure 2), bringing the total number of underground explosions to 340.

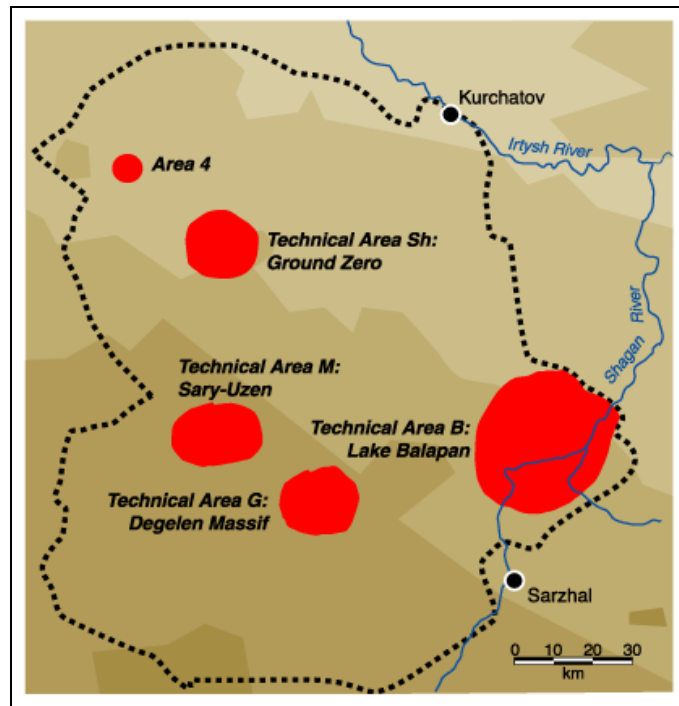


Figure 2. Map of the STS. Extensive testing was carried out at four main technical areas: Ground Zero (Sh), Balapan (B), Degelen Mountains (G) and Sary-Uzen (M) (reproduced from: Stone, 2003)

The above total includes four cratering nuclear explosions (Chagan, Sary-Uzen, Tel’kem 1 and Tel’kem 2) carried out in order to evaluate the potential of using nuclear explosions for civil engineering purposes. The Chagan explosion ($49^{\circ}56'N$ $78^{\circ}29'E$), carried out in January 1965 at the confluence of two rivers (Chagan and Aschy-Su), was the first and largest of these tests, and resulted in the creation of an artificial lake about 0.5 km in diameter, 100 m deep and with cliffs of up to 100 m high, known as ‘*Lake Balapan*’ or ‘*Atomic Lake*’ (Figure 3). The assembly employed consisted of a 140 kiloton (TNT equivalent) nuclear device, which was detonated at a depth of 175 m in slightly watered sandstone with an admixture of lignite-clayey schist (Izrael *et al.*, 2000).

The Tel’kem 1 and Tel’kem 2 tests, conducted in a zone between Technical Areas B and G, employed comparatively low-yield nuclear devices. The Tel’kem 1 explosion ($49^{\circ}43.40'N$ $78^{\circ}29.10'E$), carried out on 21st October 1968, consisted of a single, 0.24 kiloton nuclear device, detonated at a depth of 31.4 m. The explosion resulted in a circular crater about 70 m in diameter, surrounded by a ring of spoil several metres high. The Tel’kem 2 test ($49^{\circ}42.46'N$ $78^{\circ}27.39'E$), carried out on 12th November 1968 some 1.5 km to the west of the Tel’kem 1 site, employed three fission devices similar to that used in the Tel’kem 1 explosion. The simultaneous detonation of these devices, also buried at 31.4 m, resulted in an elliptical crater, approximately 142 m long \times 64 m wide (Figure 4) (Stukin and Izrael, 1998). Both craters, subsequently, became filled with freshwater to a depth of 7–10 m.



Figure 3. Atomic Lake, created by the first cratering explosion in January 1965

As part of the field work carried out during the ADVANCE project, samples were collected from Ground Zero, Lake Balapan, Tel’kem 1 and Tel’kem 2. Sampling took place in the course of field campaigns conducted in July 2000 and July 2001, in support of a multinational collaboration to evaluate the radiological situation in the Sarzhal region of the STS (Priest *et al.*, 2003). Sampling at Ground Zero was carried out close to the site of the first Soviet nuclear explosion, and included surface soil and vitrified soil/rock. At Lake Balapan, surface soil was taken from along the top of the crater rim surrounding the lake. In addition, samples of water and underlying spoil were collected close to the shoreline. At the Tel’kem craters, surface soils were collected at four locations along the ring of spoil surrounding each lake. Water samples and underlying spoil were also collected from the middle of each lake with the aid of a small inflatable.



Figure 4. A view of the Tel’kem 2 site, showing the elliptical crater lake produced by the simultaneous detonation of three 0.24 kt fission devices. The crater rim rises up to 25 m above the surface of the water

Digital phosphor autoradiography carried out on soil samples from Tel'kem 1 and Tel'kem 2 (Figure 5), as well as sediments from the shoreline of Lake Balapan (Figure 6), demonstrated the presence of particles of various sizes and activity concentrations. The most pronounced 'hot spots', however, were evident in autoradiography images corresponding to surface soils from Ground Zero (Figure 7). Clearly, all samples from sites in the Semipalatinsk test site were contaminated with radioactive particles.



Figure 5. Digital phosphor imaging (autoradiography) of dried surface soils (1-5 cm) from the outer rim (south-east) of the Tel'kem 1 crater (upper) and from the outside (north) of the Tel'kem 2 crater (lower), respectively

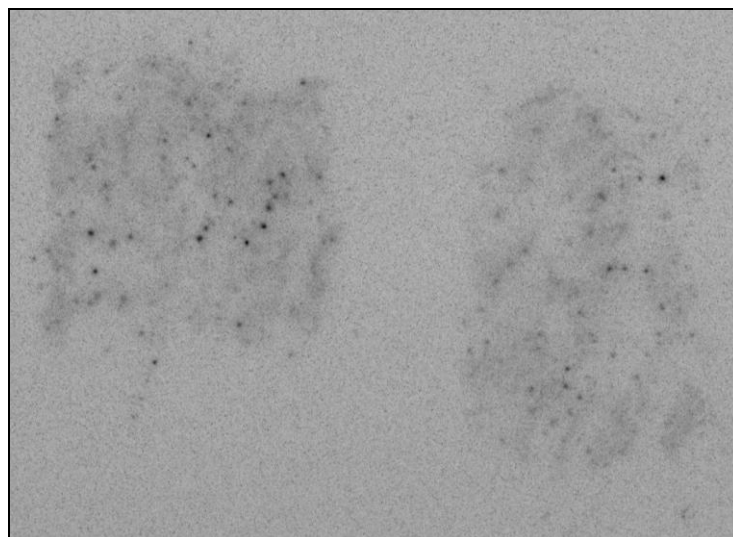


Figure 6. Digital phosphor imaging (autoradiography) of dried surface sediments collected from within the fusion explosion crater of Lake Balapan (Atomic Lake)

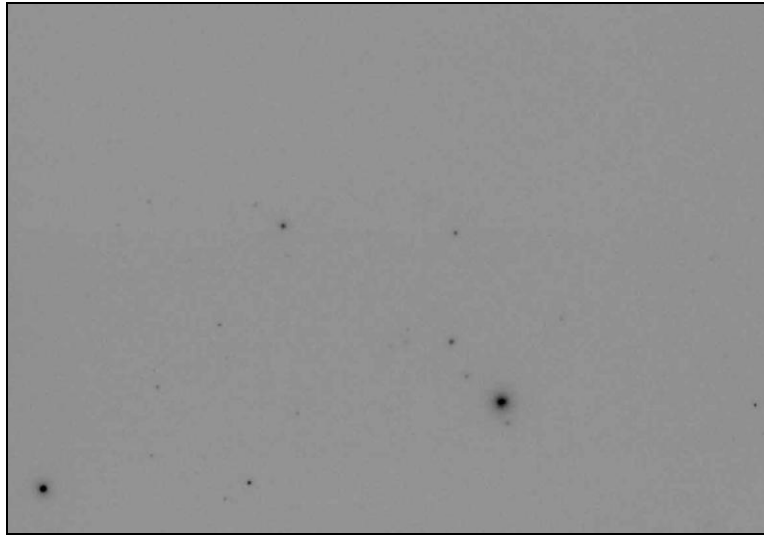


Figure 7. Digital phosphor imaging of Ground Zero soil sample

The gamma activity of selected radioactive particles was measured by high-resolution gamma spectrometry, while scanning electron microscopy, interfaced with an X-ray microanalyser, was employed to characterise the surface structure of the particles prior to synchrotron experiments at *HasyLab*. Several particles, with sizes ranging from a few hundred micrometres to a few millimetres, were isolated from Ground Zero samples. All particles appeared to be vitrified (Figures 8 and 9), most likely due to the extremely high-temperatures involved.

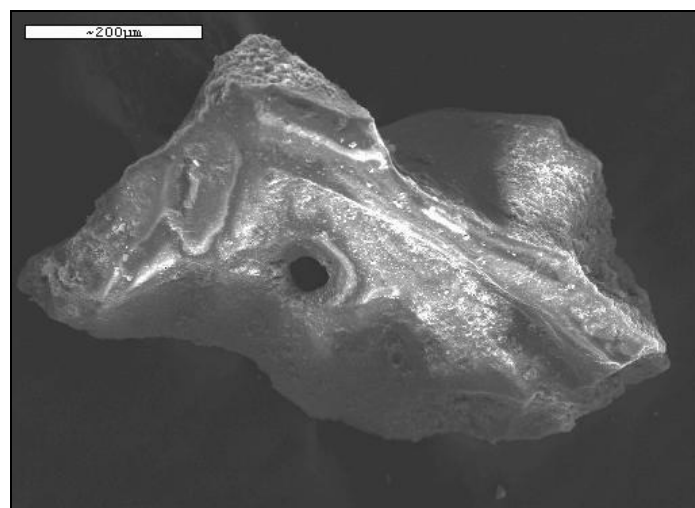


Figure 8. Electron micrograph of a radioactive vitrified particle isolated from Ground Zero, Semipalatinsk test site. Bar = 200 μm

Accelerator mass spectrometry (AMS) measurements of aqua regia leachates of the particles yielded a $^{240}\text{Pu}/^{239}\text{Pu}$ atom ratio of 0.040 ± 0.009 , a value which is in good agreement with the value of 0.0438 ± 0.0001 reported by Beasley *et al.* (1998) for a single surface soil sample collected at Ground Zero.

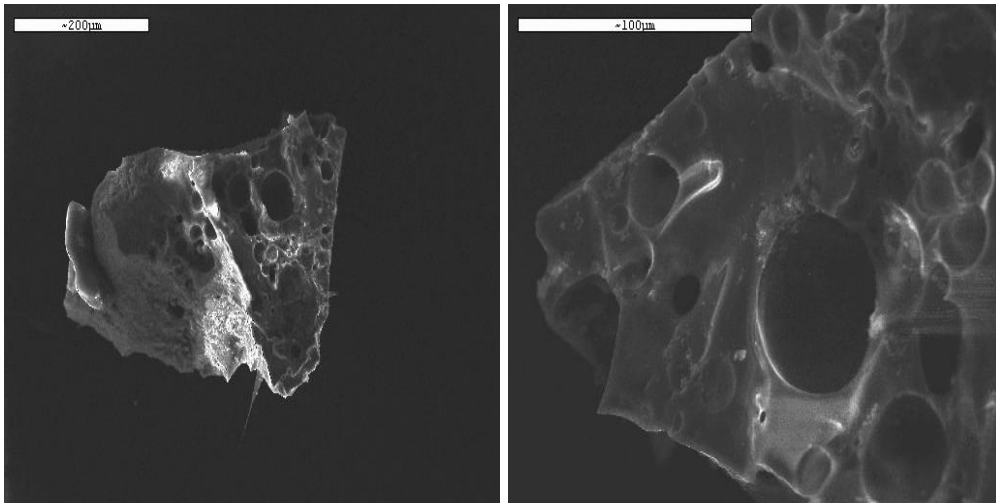


Figure 9. Electron micrographs of a radioactive vitrified particle isolated from Ground Zero, Semipalatinsk. Overview (left, bar = 200 μm), Close up (right, bar = 200 μm)

The X-ray microprobe at the synchrotron facility *HASYLAB* (beam line L), in Hamburg, was used to study the distribution of major, minor and trace constituents within a number of particles. Special attention was given to traces of U and Pu (present at the 10-100 ppm level) and their spatial correlation inside the particles. An X-ray microbeam of $E = 21 \text{ keV}$, focussed by a polycapillary X-ray lens, was used to excite local X-ray fluorescence in the sample. The beam diameter at this energy was approximately 15 μm .

Figure 10 shows the electron micrograph and elemental distributions of Ca and Fe (major constituents), and of U and Pu (trace constituents) in one of the investigated particles (600 μm in length) from the Tel'kem 2 crater. The distributions of U and Pu were almost overlapping, with no correlation with the major constituents Ca and Fe.

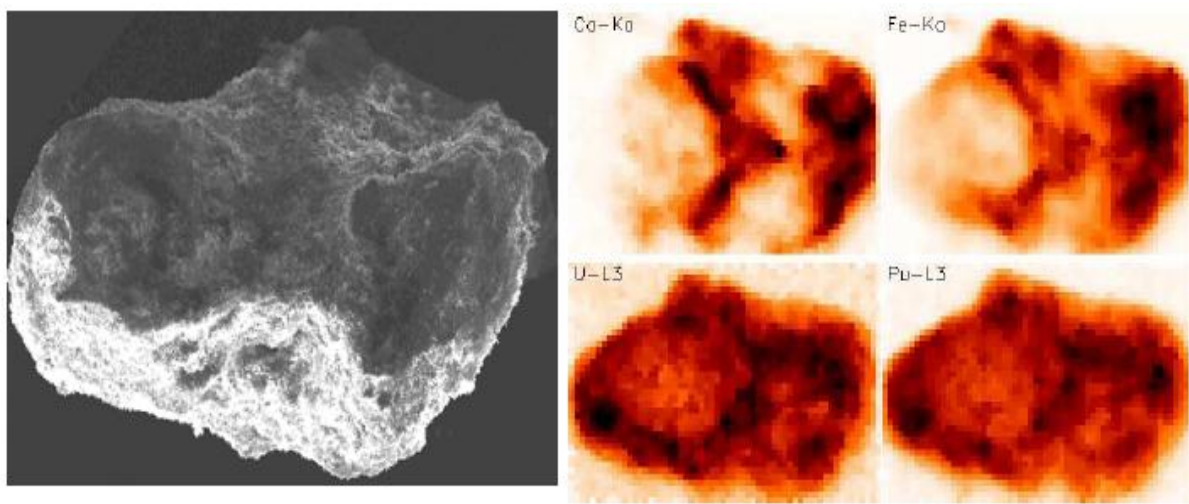


Figure 10. Electron micrograph and elemental distributions of Ca and Fe (major constituents) and of U and Pu (trace constituents) in one of the investigated particles (600 μm in length) from the Tel'kem 2 crater lake.

Based on the spatial distribution of U and Pu within particles (Figure 10), the presence of highly concentrated small grains (<50 µm in size) is evident. As illustrated in Figure 11, there is a very good linear correlation between the distributions of U and Pu within the particles.

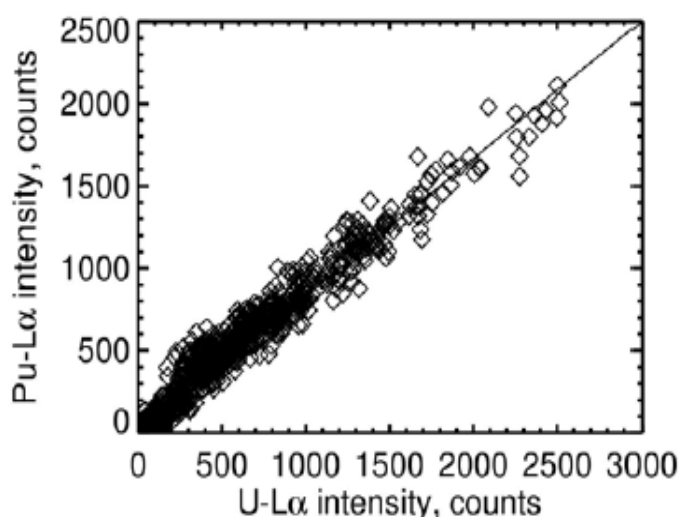


Figure 11. Linear correlation between U-La and Pu-La X-ray intensities in the particle shown in Figure 10

Nuclear weapons disintegration: Palomares (Spain) and Thule (Greenland)

In January 1966, four plutonium-bearing nuclear weapons were released at an altitude of 8500 m above the Mediterranean village of Palomares (Spain) following a mid-air collision between two US aircraft, namely a B-52 bomber and a KC-135 refuelling tanker. Although two of the weapons were reported to have been recovered intact (one from the seabed in the nearby Gulf of Vera), the chemical explosive component of the other two detonated on impact on land, and plutonium was dispersed over an area of approximately 500 ha (NEA, 1981). To date, the quantity of plutonium released does not appear to have been published. However, allowing for clean-up, it has been estimated that the total residual $^{239,240}\text{Pu}$ inventory is in the order of 0.1 TBq (Aarkrog, 1995). A small fraction of this would appear to have found its way to the local marine environment as it has been reported that traces of plutonium of accident origin have been detected in sediments from the submarine canyon system situated south of the mouth of the (almost always) dry Almanzora river (Romero, Lobo, Holm & Sánchez, 1991; Antón, Gascó, Sánchez Cabeza & Pujol, 1994). Similar traces have been found in marine algae sampled in the vicinity of Palomares (Manjón, García León, Ballestra & López, 1995).

Two years later, a second B-52 bomber, also carrying four plutonium-bearing weapons, crashed on Arctic ice in Bylot Sound (Greenland), 11 km west of the Thule Air Base. The plane and the chemical explosive component of all four weapons exploded on impact, causing the release of kilogramme quantities of insoluble plutonium oxide to the snow-pack in the locality (Risø, 1970; Aarkrog, 1977; Facer, 1980). The contamination was in the form of particles ranging in size from submicrometres up to several millimetres. The particle distribution was found to be lognormal, with a mean particle diameter of 2 µm. Although it was initially estimated that the bulk of the plutonium was removed in the ensuing clean-up operation, leaving a residual contamination totalling 1 TBq($^{239,240}\text{Pu}$) in a seabed area in the

order of 1000 km² (Aarkrog, Dahlgaard, Nilsson & Holm, 1984; Smith, Ellis, Aarkrog, Dahlgaard & Holm, 1994), a recent re-assessment of this figure (taking into account the presence of heterogeneities in the sediments) suggests 10 TBq as a more realistic estimate of the remaining inventory (Ericsson, 2002).

Measurement of ²³⁸Pu/^{239,240}Pu ratios in filtered waters at Thule have shown that, in contrast to the seabed sediment, there is virtually no weapons-grade plutonium in the Thule water column at the present time (McMahon *et al.*, 2000). A similar observation was made in the early 1990s in waters from the Palomares area (Mitchell *et al.*, 1995), which suggests that plutonium dispersed from fractured nuclear weapons is present in a rather insoluble form.

In the course of the ADVANCE project, uranium and plutonium particles from Palomares soil and Thule sediments were characterised with respect to size, elemental distribution, morphology and actinide oxidation states.

Particle size distribution and structure determined by SEM/XRMA and XRF

Based on scanning electron microscopy with XRMA, carried out prior to μ -XANES, particles ranging from about 1 to 50 μ m were isolated from Palomares soils (Figures 12–15), whereas isolated ‘Thule’ particles ranged from 20 to 40 μ m (Figures 16-18). SEM in secondary electron imaging (SEI) mode in these figures shows the morphological structure of the particles, while the bright areas obtained in back-scattered electron imaging (BEI) mode reflect the distribution of high atomic number elements such as uranium and plutonium. The XRMA and μ -XRF mapping of uranium and plutonium superimposed on a BEI mode image demonstrated that uranium and plutonium were homogeneously distributed throughout all the particles, indicating that uranium and plutonium were fused.

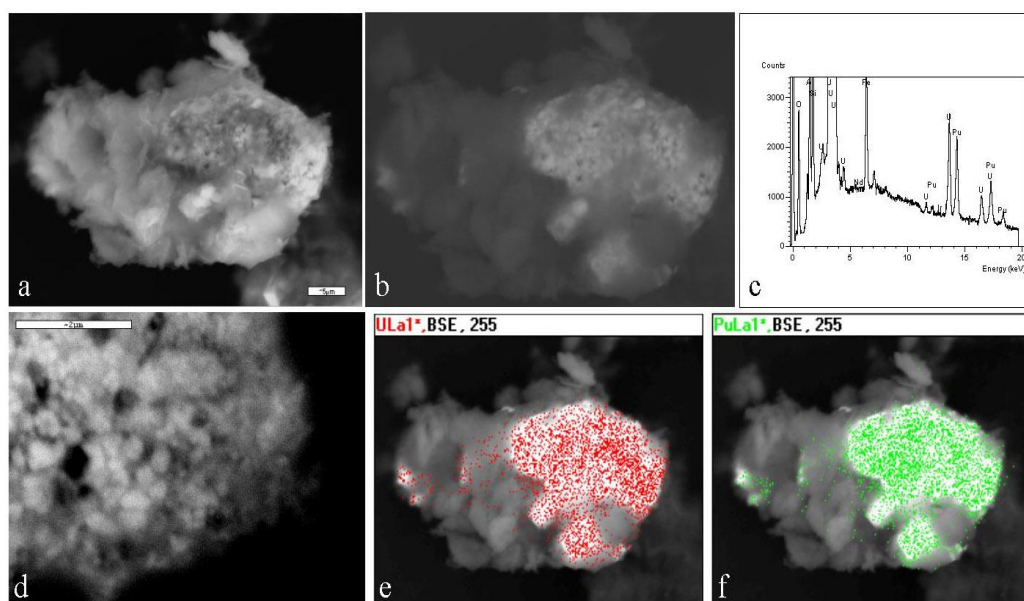


Figure 12. Scanning electron microscopy of particle #128 isolated from soils collected at Palomares, Spain (Lind *et al.*, *in prep.*): (a) Secondary Electron Imaging (SEI) mode image reflecting the morphological structure of the particle, bar 5 μ m, (b) Backscattered Electron Imaging (BEI) mode image, where bright areas reflect high atomic number elements; (c) elemental spot analysis by XRMA, (d) Close up of the particle, in BEI mode, bar = 2 μ m; (e and f) X-ray mapping of U and Pu, respectively, superimposed on a BEI mode image

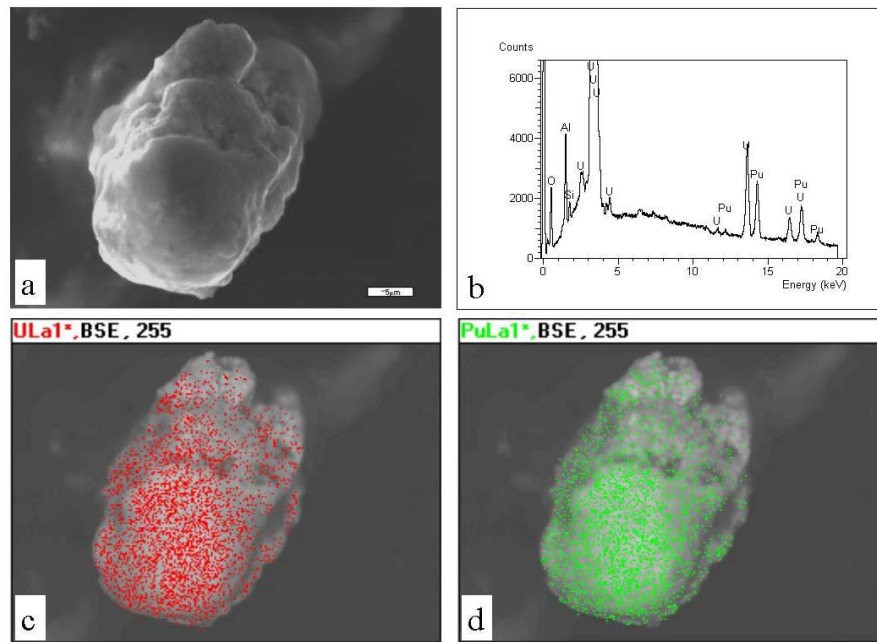


Figure 13. Scanning electron microscopy of particle #129 isolated from soils collected at Palomares, Spain (Lind et al., in prep.): (a) Secondary Electron Imaging (SEI) mode image reflecting the morphological structure of the particle, (b) elemental spot analysis by XRMA, (c) X-ray mapping of U superimposed on a Backscattered Electron Imaging (BEI) mode image, (d) X-ray mapping of Pu superimposed on a BEI mode image. Bar = 5 μm in all cases

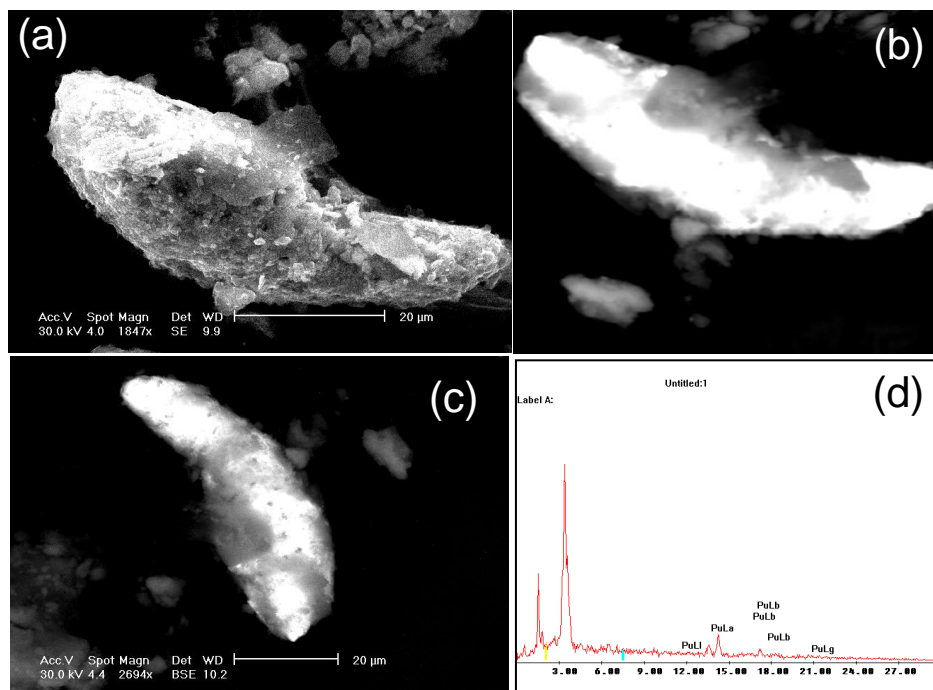


Figure 14. Scanning electron microscopy of a particle isolated from a soil collected at Palomares, Spain: (a) Secondary Electron Imaging (SEI) mode image reflecting the morphological structure of the particle, (b and c) Backscattered Electron Imaging (BEI) mode image of the particle at different angles, (d) elemental spot analysis by XRMA. Bar = 20 μm in all cases

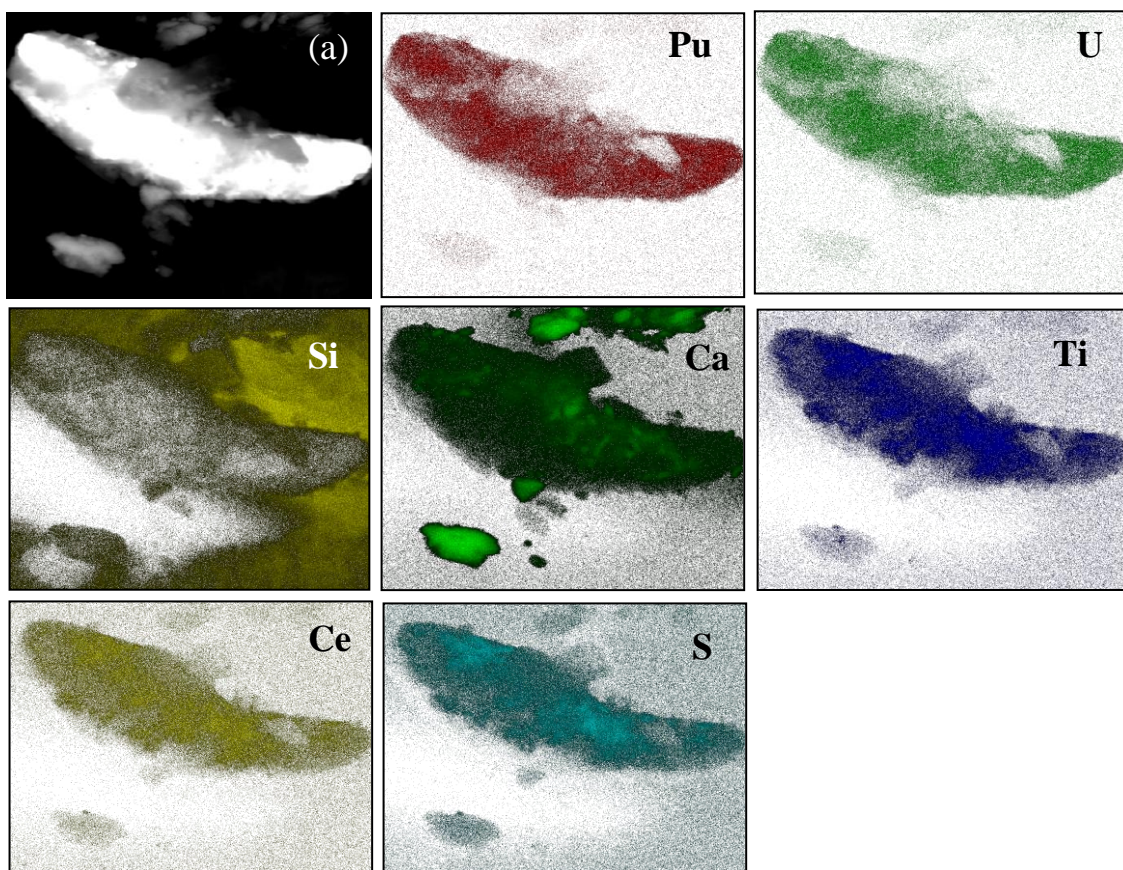


Figure 15. X-ray mapping of different elements for the Palomares particle shown in Figure 14

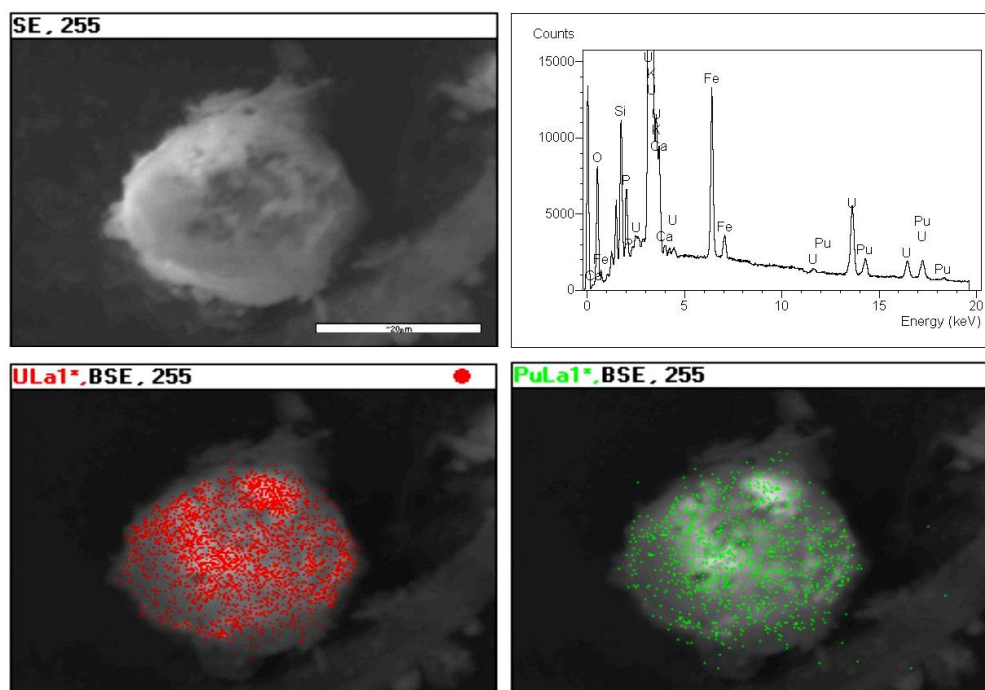


Figure 16. Scanning electron microscopy of particle #132 isolated from sediments collected at Bylot Sound, Greenland (Lind et al., in prep.): (a) Secondary Electron Imaging (SEI) mode image reflecting the morphological structure of the particle, (b) elemental spot analysis by XRMA, (c) X-ray mapping of uranium superimposed on a Backscattered Electron Imaging (BEI) mode image, (d) X-ray mapping of Pu superimposed on a BEI mode image. Bar = 20 μm in all cases

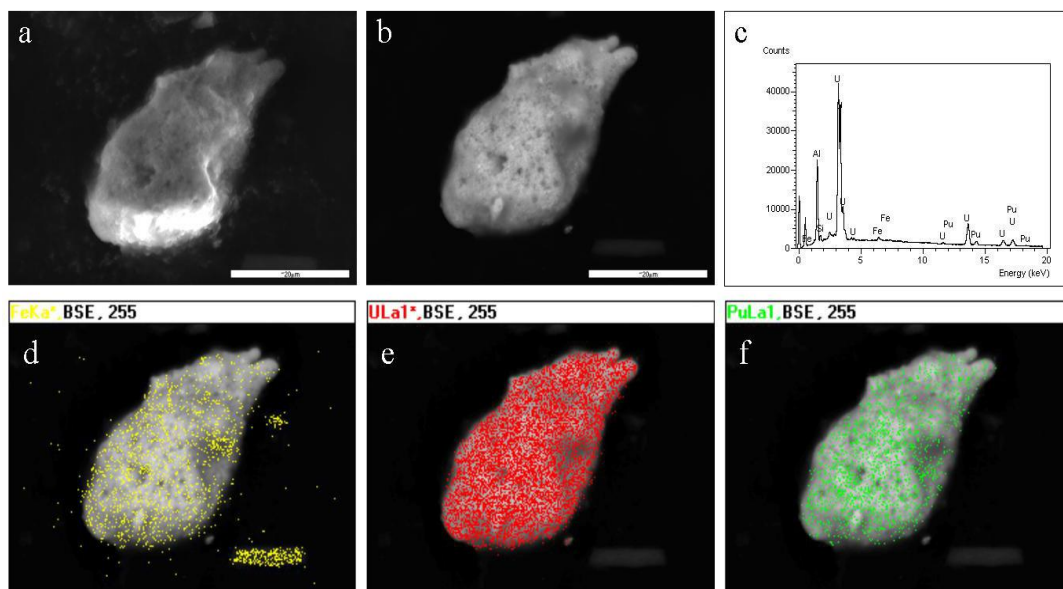


Figure 17. Scanning electron microscopy of particle #133 isolated from sediments collected at Bylot Sound, Greenland (Lind et al., in prep.): (a) Secondary Electron Imaging (SEI) mode image reflecting the morphological structure of the particle, (b) Backscattered Electron Imaging (BEI) mode image, where bright areas reflect high atomic number elements; (c) elemental spot analysis by XRMA, (d-f) X-ray mapping of elements (Fe, U and Pu) superimposed on a BEI mode image. Bar = 20 μm in all cases

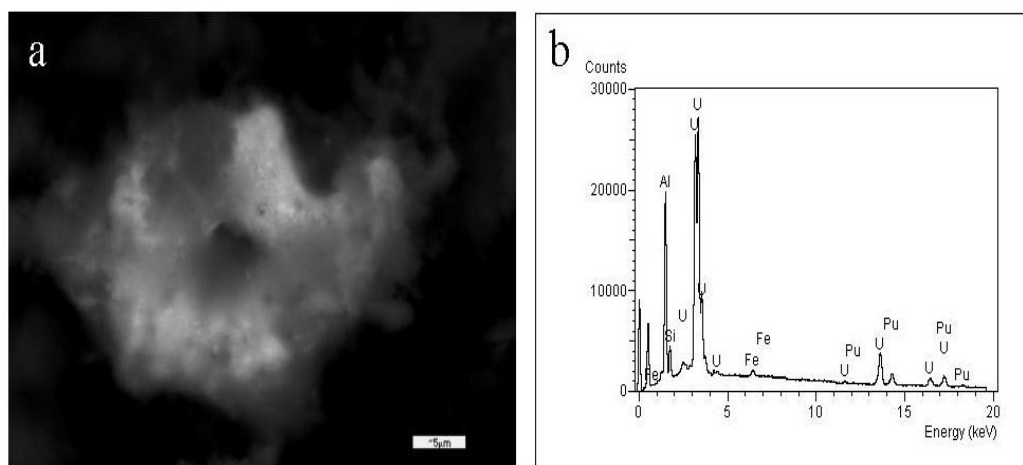


Figure 18. Scanning electron microscopy of particle #134 isolated from sediments collected at Bylot Sound, Greenland (Lind et al., in prep.): (a) BEI mode image; (b) Elemental spot analysis by XRMA. Bar = 5 μm

Oxidation state measurements by μ -XANES

The U L_{III} fluorescent XANES profiles of two Palomares particles are shown in Figure 19. The profile of particle #129 strongly resemble that of UO_2 , indicating that U imbedded in the particle is present as U(IV). In the other particle, partial oxidation of U is apparent indicating that U in the form of U_3O_8 is present in particle #130a (Figure 19). These data suggest all the U in the particles investigated were oxidized during the event (no U metal present).

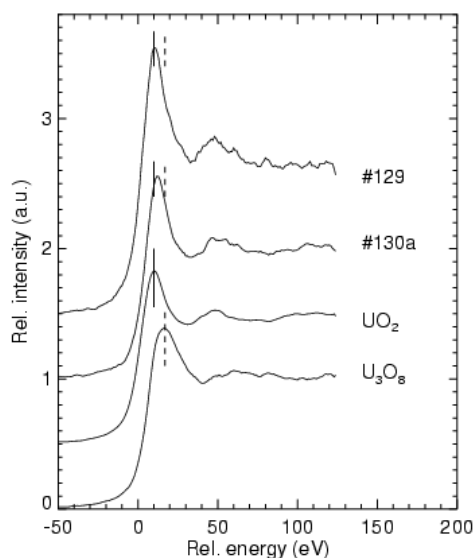


Figure 19. Fluorescent U μ -XANES profiles obtained from Palomares particles in comparison to UO_2 and U_3O_8 reference compounds

The U L_{III} fluorescent XANES profiles (uncorrected for self-absorption) of three Thule particles are shown in Figure 20. By comparison with the standards, uranium in the investigated particles was found to be present as UO_2 , with no uranium metal present. This, again, suggests that oxidation occurred during the accident. However, in contrast to observations in some particles from Palomares, no U_3O_8 was detected in the case of Thule.

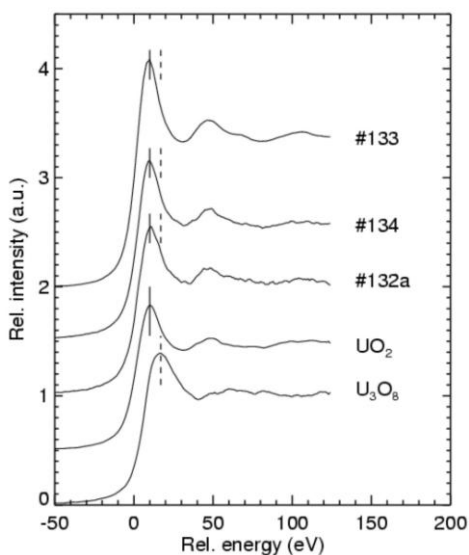


Figure 20. Fluorescent U L_{III} μ -XANES profiles obtained from Thule particles in comparison to UO_2 and U_3O_8 reference compounds

The L_{III} fluorescent XANES profiles for plutonium of three Palomares particles and three Thule particles are shown in Figures 21 and 22, respectively. Plutonium imbedded in all investigated particles is present as a mixture of Pu(III) and less soluble Pu(IV). Thus,

plutonium was also oxidized during these events. Most impact assessments concerning Pu contamination in Palomares and Thule are based on assumptions that plutonium is present as inert material or as the relatively inert Pu(IV). As Pu(III) also is present, impact assessments should be revised, taking into account particle weathering rates and remobilisation of uranium, americium and plutonium.

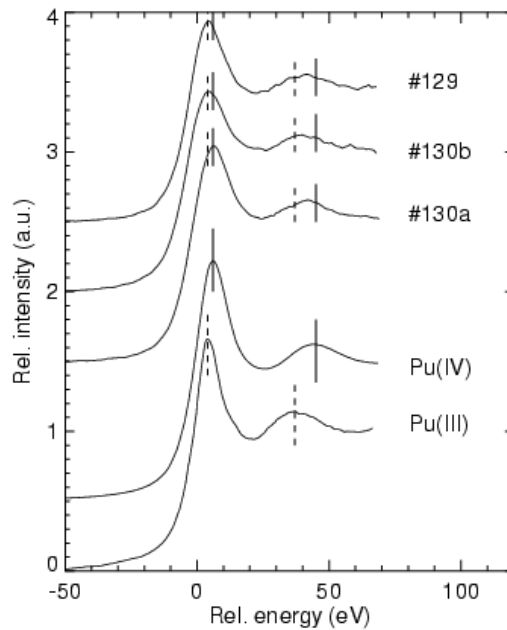


Figure 21. Fluorescent Pu μ -XANES profiles obtained from Palomares particles in comparison to published Pu(III) and Pu(IV) reference profiles

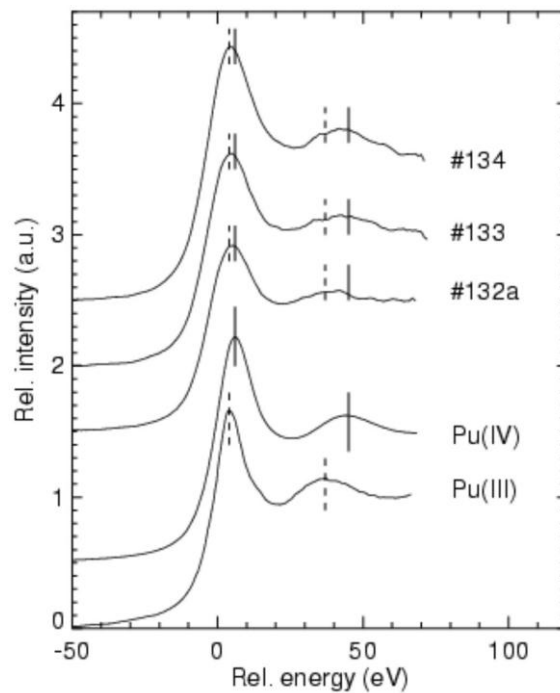


Figure 22. Fluorescent Pu L_{III} μ -XANES profiles obtained from Thule particles in comparison to published Pu(III) and Pu(IV) reference profiles

Nuclear reactor accidents: Chernobyl reactor (explosion and fire)

The accident at the Chernobyl nuclear power plant in April 1986 is the most serious accident to have occurred in the history of nuclear reactor operation. Severe violations of operating procedures in the course of an engineering test of the generator resulted in a prompt critical excursion of the 1 GW_e, graphite-moderated, light-water cooled reactor on April 26th, 1986.

The energy generated led to a series of explosions that destroyed the outer containment, exposing the core to the environment and injecting highly radioactive debris into the atmosphere. The releases continued in the following days due to the subsequent fire in the graphite moderator. However, the ‘blanketing’ of the core with boron, clay, lead, etc. led to increased temperatures and new releases from the 1st to the 5th of May. Emissions were terminated on May 6th upon cooling the reactor through tunnels constructed under the core (SCOPE, 1993).

As a result of the accident, about 6-8 tonnes of UO₂ fuel were released into the atmosphere (Victorova and Geiger, 1990). Large fuel particles with variable radionuclide composition deposited within a 30 km zone with respect to the plant, while small-sized particles were identified up to 2000 km from the site (Kuriny *et al.*, 1993; Kashparov *et al.*, 1999; Devell *et al.*, 1986). During the initial explosion on April 26th, mechanical destruction of the uranium dioxide fuel occurred at high temperature and under high pressure, and deposition of fuel particles took place to the west of the reactor.

In the period 26–30 April, volatile fission products and U fuel particles were released under high temperature and oxidising conditions due to the fire, and deposition of particles occurred to the north, northeast and south of the plant. From April 30th to May 6th the temperature was lowered and subsequently the emission of volatiles decreased (Kashparov *et al.*, 1999).

In the course of the ADVANCE project, information on surface structures and elemental distributions in individual particles from Chernobyl was obtained using SEM with XRMA. Radioactive particles were separated from soil and dust samples collected to the west and north of the Chernobyl reactor. Using SEM, a variety of sizes, shapes, structures and colours were observed, from compact small-sized crystalline single particles to large amorphous aggregates (e.g., see Figure 23). Gamma spectrometry measurements demonstrated that the particles contained several fission products. In addition, μ -XRF screening of particles, using the second generation synchrotron radiation source at *Hasylab* (Germany), demonstrated that the 2-D distributions of U and key fission products such as Zr and Sr were similar, and revealed the presence of white inclusions of Ru and Mo (Figure 24).

Using μ -XAS-tomography, information on the 3-D distribution of U in a fuel particle released during the explosion in the Chernobyl reactor was obtained (Figure 25). Tomographic reconstruction and computerised slicing of the 3-D image (Fig 25c) demonstrated the presence of channels or cavities within the particles, probably due to the formation of gaseous phases (e.g., volatile radionuclides) in the fuel during operation or during the accident. The cavity dimensions were similar to those observed on the particle surface. For U fuel particles released during the fire, the μ -tomographic reconstruction is depicted in Figure 26. The image reflects a heterogeneous structure and is very different from the crystallographic structure shown in Figure 25 for fuel particles released during the initial explosion.

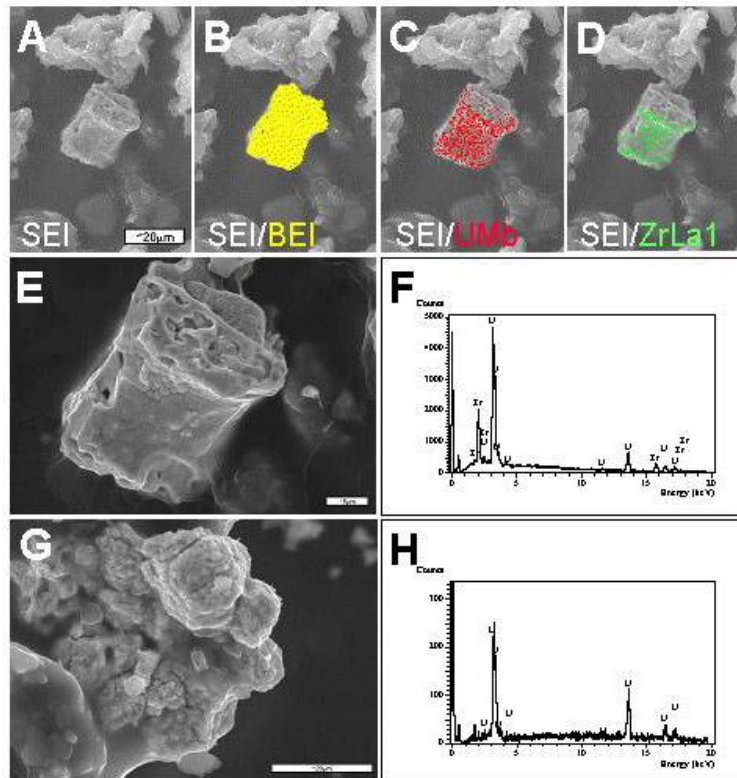


Figure 23. Electron microscopy of uranium fuel particles collected within the 30 km zone of Chernobyl. (a) Secondary Electron Imaging (SEI) of particles from the north of the reactor showing the surface structures, (b) Backscattered Electron Imaging (BEI) mode showing the distribution of high atomic number elements, (c) X-ray mapping of uranium (red), (d) X-ray mapping of zirconium (green), (e) SEI of particles from the west (higher magnification), (f) XRMA showing the presence of uranium and zirconium, (g) SEI of particles from the west, (h) XRMA showing the presence of U

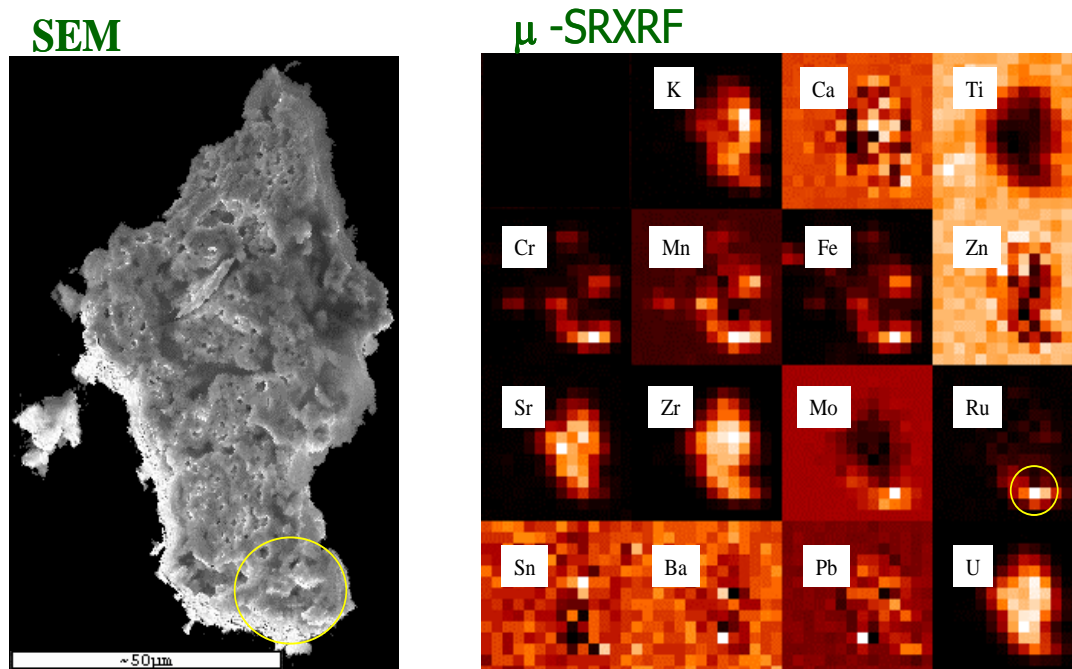


Figure 24. SEM (left, bar 50 μ m) and μ -SRXRF mapping (right) of a U fuel particle collected 1 km from the Chernobyl reactor

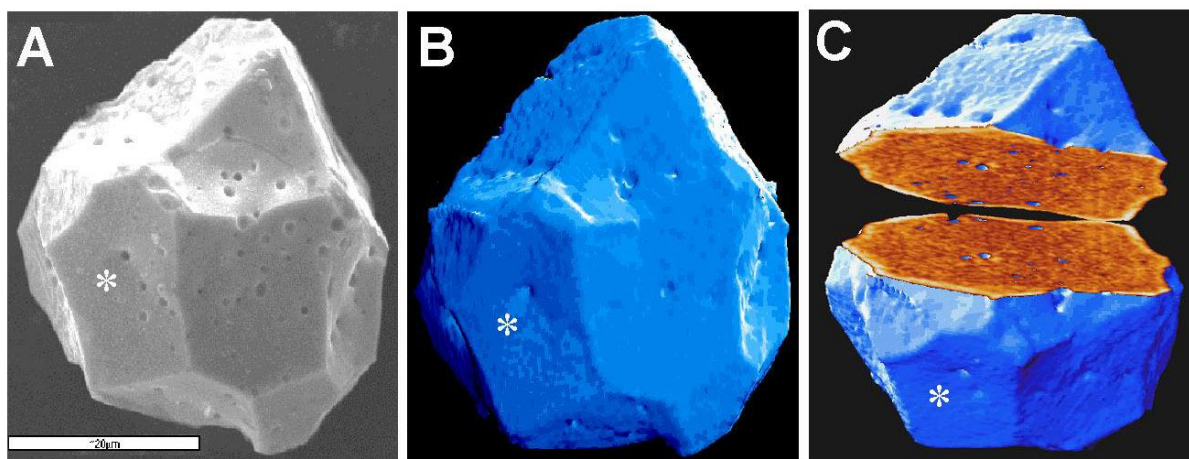


Figure 25. μ -tomography of a U fuel particle from Chernobyl. (a) Scanning electron microscopy image of the fuel particle containing non-oxidised U. Bar 20 μm . (b) 3-D rendering of 500 tomographic slices of the particle in (a) taken by rotating the sample 180° using 17 keV X-ray. Each projection image consisted of 1024×1024 pixels. (c) 3-D visualisation of the particle in (a). The data block has been cut and opened to show the inner structure of the particle. The * in figures a, b, and c indicates the same position at the particle surface

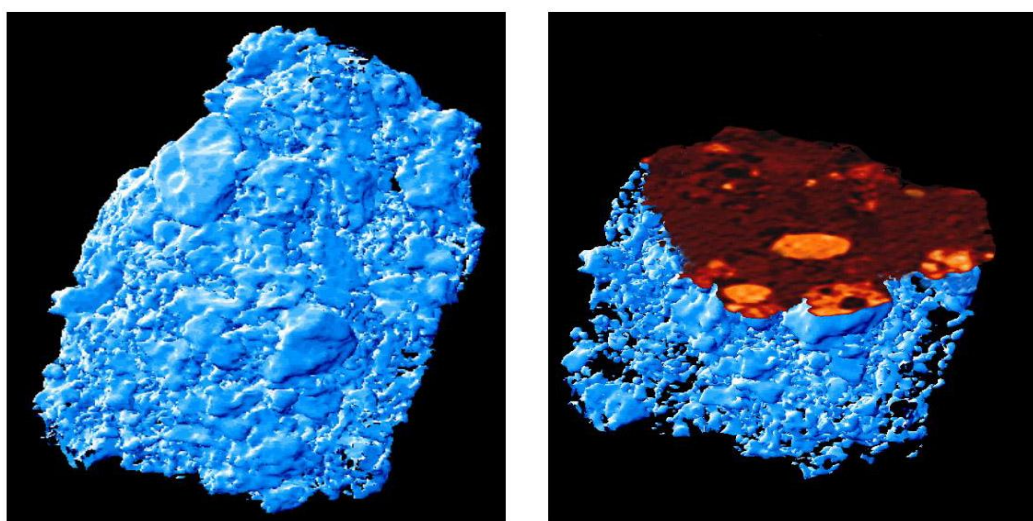


Figure 26. (a) μ -XAS-tomography of an oxidised fuel particle released during the fire in the Chernobyl reactor. (b) computerised slicing of the 3-D image of the oxidised fuel particle

The μ -XRD results demonstrated that U in the UO_2 fuel particles released during the reactor fire was oxidised to U_3O_8 or/and UO_5 . Crystalline fuel particles released during the explosion, however, were apparently reduced, as no sign of UO_2 and other oxidised forms could be observed, and weak signals of UO or U-carbides were indicated. Results from the μ -XANES imaging (Figure 27) demonstrated that particles released during the reactor fire (north of the reactor) were characterised by UO_2 cores surrounded by oxidised U ($\text{U}_2\text{O}_5/\text{U}_3\text{O}_8$ layers). The inflection point energy of U in fuel particles deposited to the west of the reactor was, however, significantly lower than for U in UO_2 . Thus, fuel particles released during the initial explosion contained apparently inert or reduced forms of U, probably due to interaction with carbon from the moderator.



Figure 27. μ -XANES imaging of a particle collected to the north of the Chernobyl reactor, released during the reactor fire. The particle has a UO_2 -core (U oxidation state 4) surrounded by an oxidised U_2O_5/U_3O_8 surface layer (U oxidation state 5)

Reprocessing facilities: Mayak PA (Russia) and Sellafield (UK)

Mayak PA

The Mayak Production Association (Mayak PA) in the southern Urals, which in the 1970s comprised seven nuclear reactors and two reprocessing plants, was established in the late 1940s in order to produce plutonium for the Soviet nuclear weapons programme (JNERG, 1997). Since its establishment, both routine discharges and accidental releases of radioactive waste have led to severe contamination of a significant area surrounding the plant, including rivers that have their catchments in the vicinity. The complex lies in the catchment basin of the Techa and Iset rivers, which are part of the hydrological system of the river Ob. A number of natural lakes on the Mayak site itself and in its surroundings have been used as reservoirs for radioactive waste disposal. These include Lake Kyzyltash (Reservoir 2), and Lake Karachay (Reservoir 9), and Reservoirs 3, 4, 10, 11 and 17. Reservoirs 3 and 4 are natural lakes in the upper reaches of the Techa river, with Reservoir 4 downstream from Reservoir 3. Although a significant proportion of the radionuclides discharged into Reservoir 3 were retained in the sediments of both Reservoirs 3 and 4, the Techa river was severely contaminated by the amount of radionuclides that passed through the reservoirs. In particular, the Asanov swamp, a broad flood plain 20-70 km downstream from Reservoir 3, was highly contaminated through sorption of radionuclides onto bottom sediments. In order to reduce further releases of radionuclides into the Techa river, two dams were built in the upper reaches of the Techa river to form Reservoirs 10 and 11, by flooding part of the river flood plain.

Actinide contamination has resulted mainly from (i) direct discharges from reactors and reprocessing plants to the Techa River over the period 1949–1956, (ii) direct discharges of intermediate-level liquid radioactive wastes into Lake Karachay from 1951 onwards, and (iii) discharges of low-level liquid radioactive wastes into Reservoir 3. It is estimated that about 100 PBq of radioactive liquid waste was released directly to the River Techa during

1949–1951, while about 20 EBq of radioactive liquid waste have been discharged into Lake Karachay, a small lake without outlet, since 1951. Additional minor sources include fallout from the waste tank explosion in 1957, which contaminated a terrestrial area up to 300 km from the site, the wind dispersion of Lake Karachay sediments in 1967, and airborne releases from the plant stacks since installation. Moreover, commencing in 1987, civil nuclear waste has been reprocessed at the Mayak plant. Based on recent investigations, the plutonium inventory in the reservoirs is at least 40 TBq. Analysis of isotopic ratios in sediments has demonstrated a change in discharge composition with time, from reprocessing of weapons-grade plutonium to reprocessing of civil nuclear fuel (Oughton *et al.*, 1999).

Sediment samples from Reservoir 10 and 11, as well as from the Asanov swamp along the Techa River, were screened for heterogeneities using digital phosphor imaging (autoradiography). Selected autoradiographic images from each of the three sites are given in Figures 28-30. The sediment screening using autoradiography showed the widespread presence of radioactive particles in Reservoir 10, both spatially (at different stations) and with depth in the sediment column (vertical distribution). Numerous radioactive particles were also present in Reservoir 11 (Figure 29) and in the Azanov swamp, along the Techa river (Figure 30). As mentioned above, Reservoirs 10 and 11 were built in the 1950s and 1960s to prevent contaminated water and sediments from draining into the Techa river. Our results clearly demonstrate that sediments contaminated by radioactive particles are (at least partially) retained in these reservoirs.

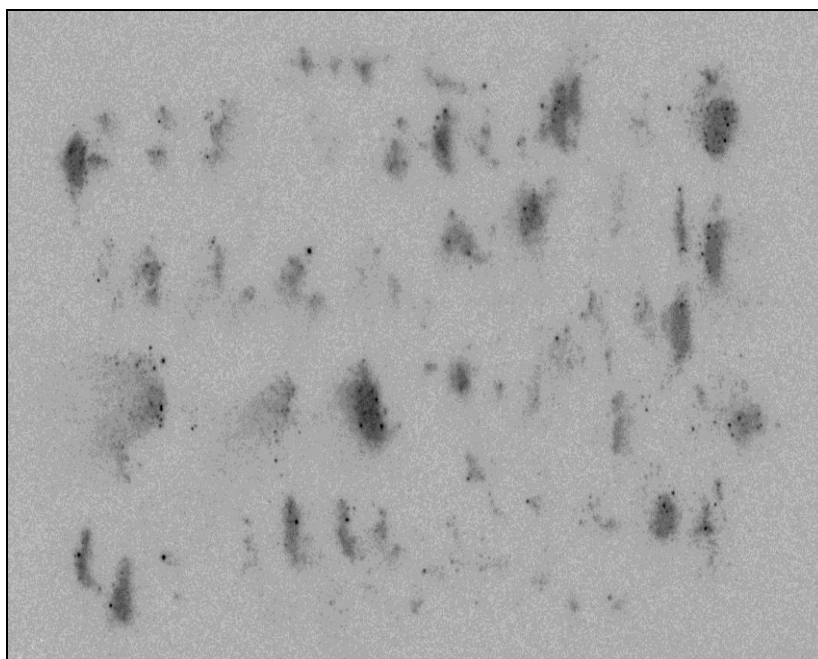


Figure 28. Digital phosphor imaging (autoradiography) of sediment from Reservoir 10 (Station 2, 0–10 cm) at Mayak Production Association

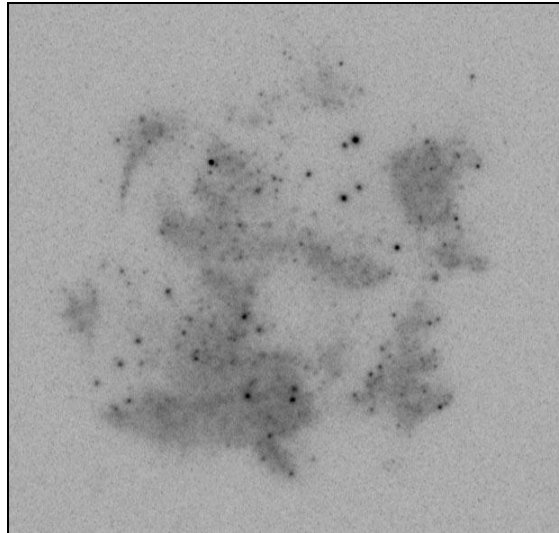


Figure 29. Digital phosphor imaging (autoradiography) of sediment from Reservoir 11 (Station 1, 0–10 cm) at Mayak PA

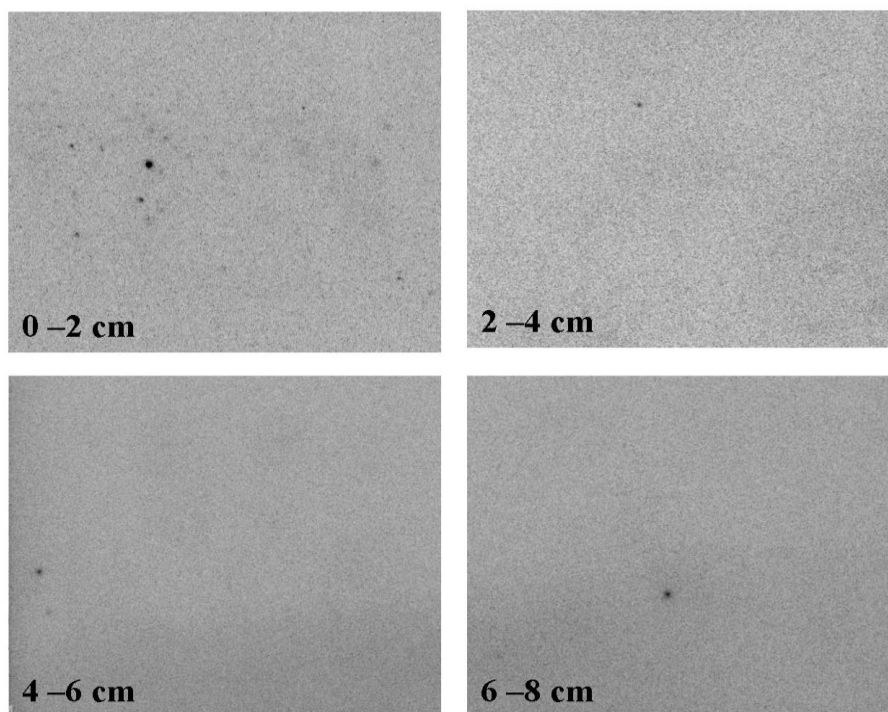


Figure 30. Digital phosphor imaging (autoradiography) of Amazova swamp soil, along the Techa River

SEM analysis of radioactive particles isolated from sediments collected in Reservoirs 10 and 11 showed that particles were embedded in residual sediment material. X-ray mapping revealed that Sr was a major component in the particle matrix and X-ray microanalysis spot measurement confirmed the presence of Sr, as well as Fe, Pb and Ti (Figure 31). Several heavy metals such as Ce, Mo and Pt were also associated with radioactive particles (Figure 32).

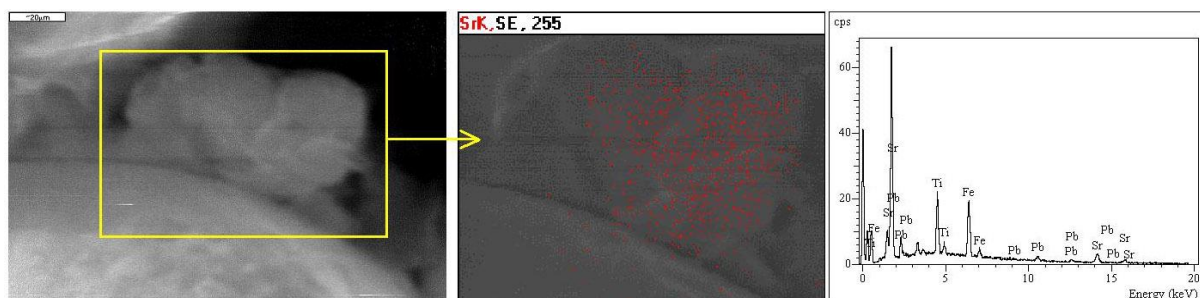


Figure 31. Scanning electron microscopy of a particle isolated from Mayak sediment sample # 2611 (Lind *et al.* in prep.). Secondary electron imaging mode shows the particle embedded in residual sediment material (left, bar 20 µm). X-ray mapping reveals that Sr is a major component of the particle matrix (middle) and X-ray microanalysis spot measurement confirms the presence of Sr, as well as Fe, Pb and Ti (right)

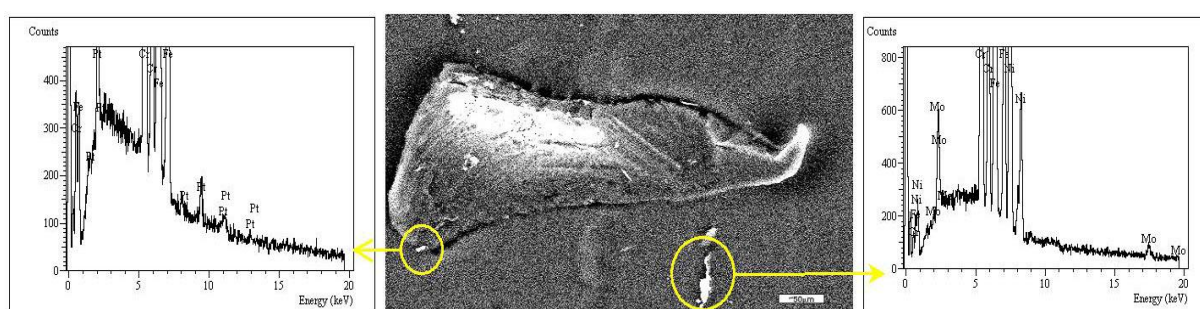


Figure 32. Scanning electron microscopy of particles isolated from Mayak sediment sample # 2611 (Lind *et al.*, in prep.). In Backscattered Electron Imaging (BEI) mode, bright areas reflect high atomic number elements (middle) and elemental analysis of the particles (in yellow circles) by XRMA (left and right, bar 50 µm) reveal the elemental composition (Mo, Cr, Fe, Pt, Ni, etc.)

Sellafield reprocessing plant

Of the three major reprocessing plants in Europe (Sellafield and Dounreay, UK, La Hague, France), Sellafield has been the major contributor of actinides to the North European seas. Overall, it has been estimated that approximately 0.12 PBq of ^{238}Pu , 0.61 PBq of $^{239,240}\text{Pu}$, 22 PBq of ^{241}Pu , 0.54 PBq of ^{241}Am and smaller quantities of other transuranium nuclides have been discharged to the Irish Sea during the period 1952–2000 (BNFL, 1980–2001; Gray *et al.*, 1995). Annual discharges of transuranium nuclides reached their peak in the early to mid-1970s and thereafter declined gradually as new effluent treatment and stricter discharge limits were introduced. Despite complications associated with continuous changes in the chemical composition of effluent discharges and methodological difficulties in the separation techniques employed, a number of studies have been carried out in order to characterise the different chemical and physico-chemical forms present in effluents from this reprocessing complex (Pentreath *et al.*, 1985; Salbu *et al.*, 1993; Leonard *et al.*, 1995). These studies demonstrated that a major fraction of the radionuclides was associated with particles and colloids upon discharge. Because of the physico-chemical speciation of transuranium nuclides in the effluent and the affinity of these radionuclides for particles (abundant in this shallow, coastal environment), much of the discharged transuranium inventories have become associated with fine-grained sediment, mainly in a strip of muddy sediments off the Cumbrian coast (Hetherington, 1978; Pentreath *et al.*, 1986; Mitchell *et al.*, 1996).

The offshore sediments in this 'mud patch' are mixed by the macrobenthos to depths of over 1.5 m (Kershaw *et al.*, 1988). This results in mixing of plutonium to depth and a very inhomogeneous distribution over small space scales. The relatively high concentration of plutonium in the subtidal sediments has allowed the determination of $^{239,240}\text{Pu}$ concentrations in pore-waters. Lovett and Nelson (1981) demonstrated that plutonium in eastern Irish Sea sediments was primarily in a reduced, Pu(IV), form. In some areas, however, the presence of burrowing brittle stars in large numbers [up to 400 per square metre; Swift (1993)] can result in the bio-irrigation of the upper few centimetres, allowing the maintenance of high levels of oxidised Pu(V) (Kershaw *et al.*, 1986).

Transuranium nuclides initially trapped in the mud patch are transported northwards, predominantly attached to sediment particles (MacKenzie, Scott & Williams, 1987) and undergo considerable mixing by physical and biological processes en route. The region is subject to frequent storms, and particle resuspension and transport is ubiquitous. The intertidal sediments along exposed beaches tend to be quite well mixed, to the depth of wave action, on a short time scale, while deposits in saltmarshes and floodplains such as those found along the Solway coast and the Esk Estuary are disturbed by channel migration on a scale of years or decades. As a result, the distribution and behaviour of plutonium in the estuaries bordering the eastern Irish Sea is complex. The migration of channels can lead to the re-exposure of relatively highly contaminated sediments, labelled with plutonium during the 1970s.

The geochemical conditions in which the sediment finds itself may also change during the transfer of sediment to intertidal and saltmarsh zones, with the transition from a well-oxygenated, alkaline marine environment to a terrestrial location with slightly acidic conditions, variable redox potential and an increasing influence of fresh water (Pulford, Allan, Cook & MacKenzie, 1998). In the Esk estuary, for example, the tidal circulation results in the transport of particle-associated plutonium to the upper reaches, where the low salinity and pH changes cause the rapid desorption of a labile form of plutonium (Hamilton-Taylor, Kelly, Mudge & Bradshaw, 1987).

Due to remobilisation, contaminated sediments in the north-eastern Irish Sea are now considered to be the predominant source-term of transuranium nuclides to the overlying water column within the Irish Sea and beyond (Mitchell *et al.*, 1999; Kershaw *et al.*, 1999).

In the course of the ADVANCE project, frozen sediment profiles collected from the eastern Irish Sea mud patch during the DIAPLU expedition (July 2002) were made available to the collaboration (courtesy of P. Kershaw, CEFAS and D. Boust, IRSN). The frozen profiles were sliced, air dried, homogenised and subjected to digital autoradiography. The autoradiographs in Figure 33 demonstrate the presence of radioactive particles throughout the profile collected at the mud patch.

In addition to offshore sediment, intertidal sediment material was collected from the Ravenglass Estuary, Cumbria. The surface sediment (0–5 cm) was dried, sieved (2 mm) and subjected to autoradiography. As in the offshore sediment, several hot particles could be identified. In this case, it proved possible to isolate two individual particles, approximately 5–20 μm in size, which were analysed by X-ray microanalysis. As illustrated in Figure 34, the matrix of these particles was found to be uranium. It is clear from this finding that uranium fuel particles originating from Sellafield have found their way to intertidal sites along the Cumbrian coast.

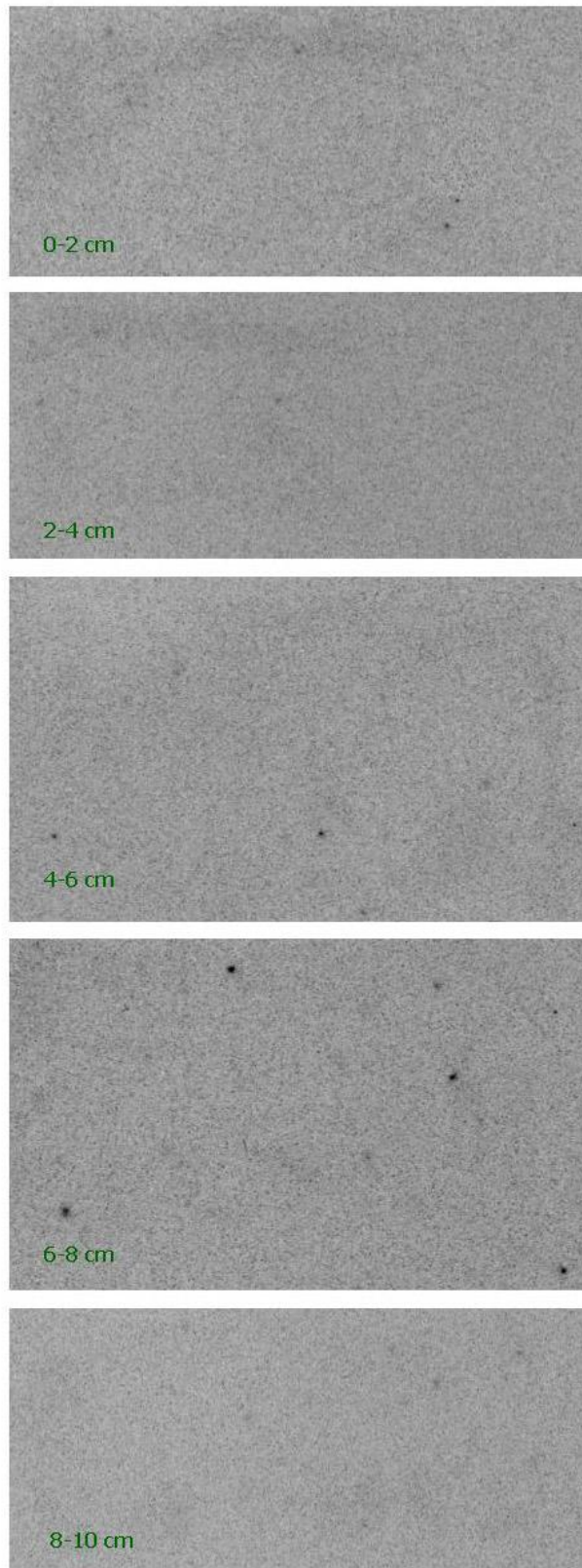


Figure 33. Digital autoradiography of dried Irish Sea mud patch sediment slices (0–10 cm) collected during the 2002 DIAPLU cruise

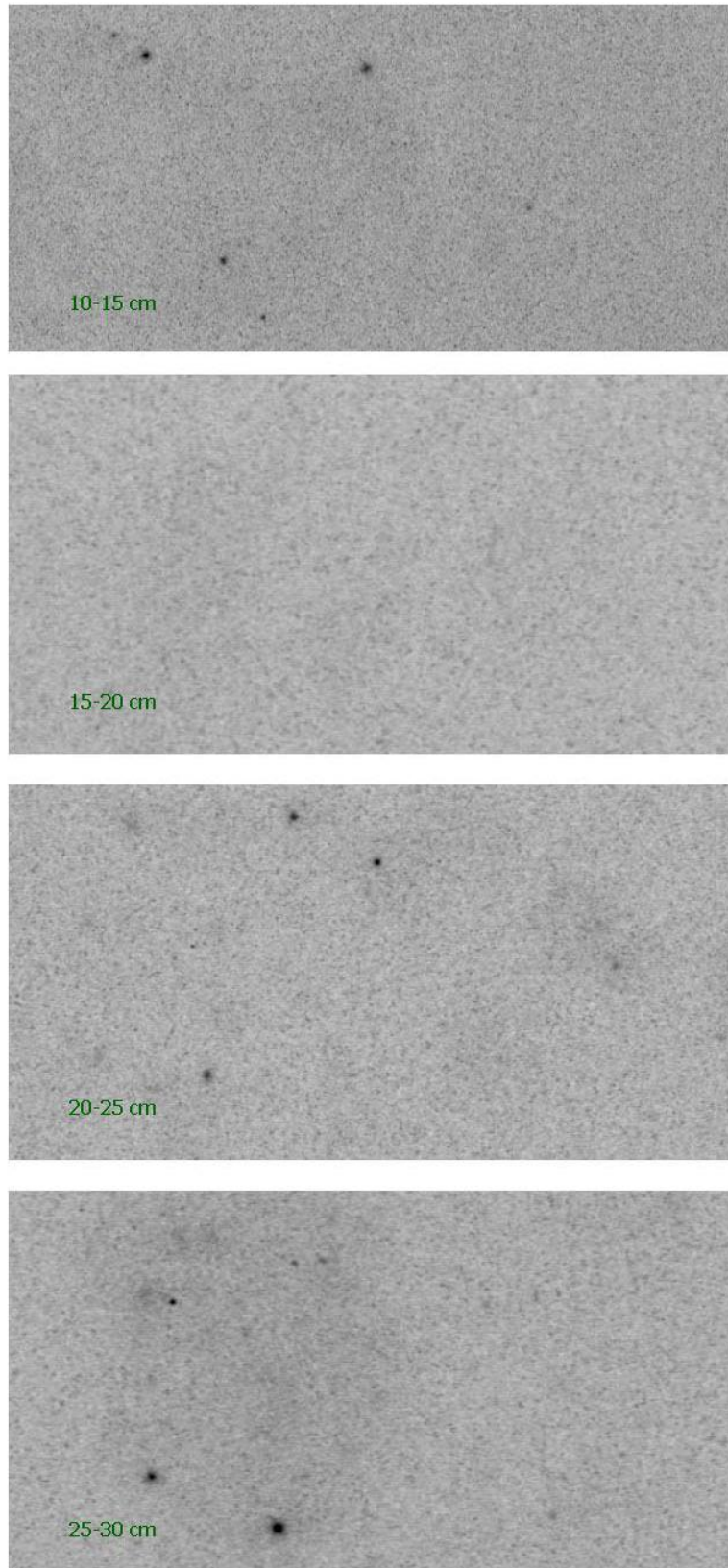


Figure 33 (cont.). Digital autoradiography of dried Irish Sea sediments sliced from a 30 cm profile collected at the mud patch during the 2002 DIAPLU cruise

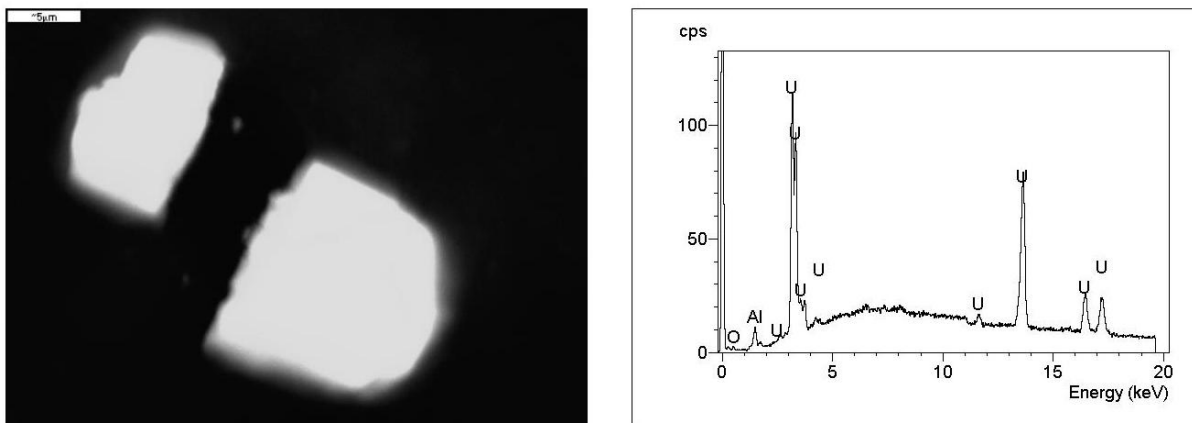


Figure 34. Electron micrograph (BEI mode; left) of two U fuel Ravenglass particles with X-ray microanalysis (right) confirming the presence of U. Bar = 5 μm

Depleted uranium (DU) munitions: Kosovo, Serbia and Kuwait

During the Gulf war and Balkan conflicts in the 1990s, armour-penetrating ammunition, containing conical depleted uranium (DU) ‘penetrators’, was extensively used. The fate of uranium metal in these penetrators is highly dependent on the hardness of the target. If the target is an armoured vehicle such as a tank, the impacting penetrator, made from metallic DU alloyed with small amounts of titanium, generates a cloud of DU dust (aerosol) that ignites spontaneously and creates a fire. If, on the other hand, the target is ‘soft’, the penetrator should be able to pierce the target and continue into the ground, where it will lie buried. ‘Unspent’ penetrators have been found to shatter fully or partially upon impact with ground, although, in some cases, they have remained intact. With time, the uranium metal in these buried penetrators will oxidise to form uranium oxides. The weathering of fragments and particles, and the subsequent mobilisation of uranium represents a potential exposure route to man. In addition, buried material can be directly transported to surface due to resuspension and agricultural practices.

In 1999, the International Atomic Energy Agency (IAEA) joined a UN mission to Kosovo and collected soil samples contaminated with DU. In 2002, the IAEA organised a field mission to collect samples at selected sites in Kuwait, where DU ammunition had been used. Soil and sand samples collected at a target site at Ceja Mountain in Kosovo and at four different sites in Kuwait were made available to the ADVANCE collaboration for the characterisation of particles.

DU in Kosovo

The collected soil samples from different sites were subjected to a variety of analytical measurements, including the determination of concentrations and isotopic ratios of uranium isotopes (Danesi *et al.*, 2003a; 2003b) using gamma spectrometry, inductively coupled plasma mass spectrometry (ICP-MS), accelerator mass spectrometry (AMS) and secondary ion mass spectrometry (SIMS). The particle size distribution obtained from SEM (BEI mode) ranged from submicrons to about 30 μm with an average size of 2 μm (Figure 35). This means that the particles were included in the respiratory fraction (Danesi *et al.*, 2003a; 2003b;

Salbu et al., 2003). Scanning electron microscopy in SEI mode (Figures 35 and 36) revealed the morphological structure of the particles, while X-ray mapping was used to determine the distribution of uranium within the particle.

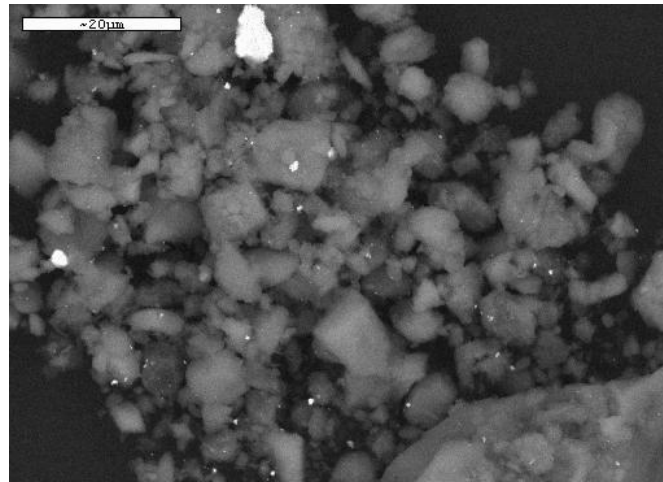


Figure 35. Scanning electron microscopy of DU-particle contaminated soil collected at Ceja Mountain, Kosovo. Backscattered Electron Imaging (BEI) with bright areas reflecting high atomic number elements are clearly visible. Bar = 20 μm .

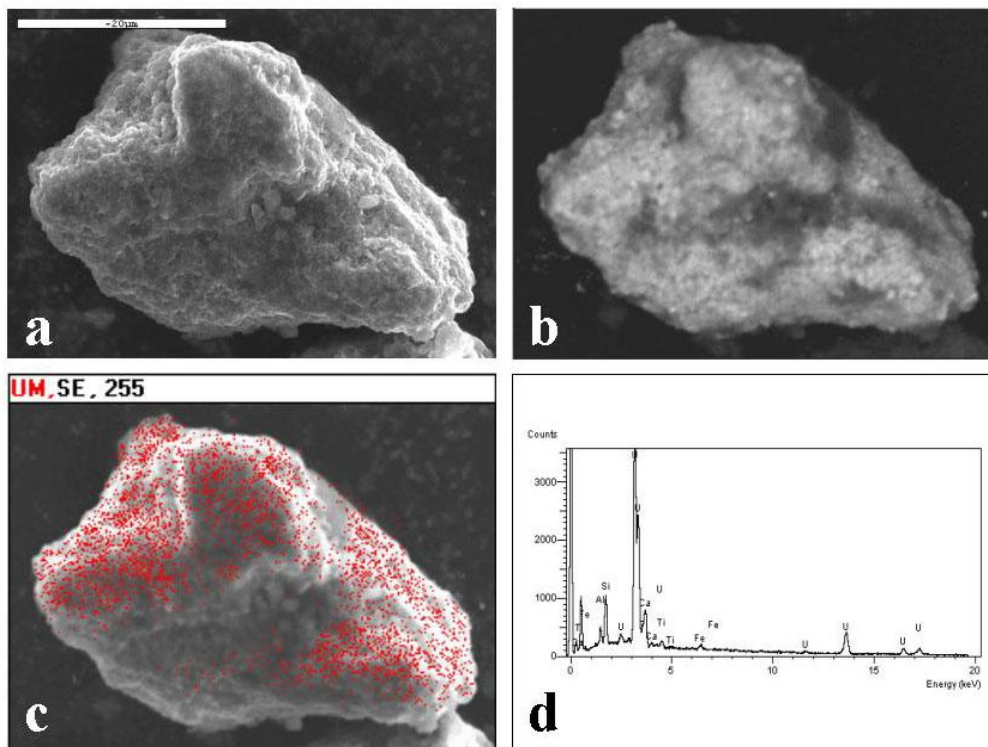


Figure 36. Scanning electron microscopy of a depleted uranium particle isolated from a soil sample collected at Ceja Mountain, Kosovo: (a) Secondary Electron Microscopy (SEI) mode reflecting the morphological structure of the particle; (b) Backscattered Electron Imaging (BEI) with bright areas reflecting high atomic number elements; (c) X-ray mapping of uranium in SEI mode; and (d) elemental analysis by XRMA. Bar = 10 μm .

Based on gamma spectrometry and ICP-MS, the concentration of uranium isotopes in the soil samples was found to be $4000 \pm 400 \text{ mg kg}^{-1}$, with a $^{235}\text{U}/^{238}\text{U}$ isotopic ratio of 0.0020 ± 0.0005 , in good agreement with previously reported results. The μ -XRF and XRMA analyses also demonstrated the presence of Ti within individual DU particles. The size distribution of DU particles, crystallographic structure, and the oxidation state of U were determined on selected samples using scanning electron microscopy with X-ray microanalysis (SEM-XRMA) and synchrotron radiation microscopic techniques (Salbu et al., 2003).

The oxidation states of uranium within these particles, as revealed by comparison with a well-defined standard using μ -XANES, showed that all the depleted uranium particles investigated were in an oxidised form (Figure 37). About 50 % of the depleted uranium particles (from Kosovo) were characterised as UO_2 , while the remainder were present as U_3O_8 or as a mixture of both oxidised forms (ca. $2/3 \text{ UO}_2$, $1/3 \text{ U}_3\text{O}_8$). No higher oxidation state for U was observed. In areas contaminated with DU particles, the particle weathering rates and the subsequent mobilization of U from DU particles depends on the oxidation state of U. As the weathering rate is higher for U_3O_8 than for UO_2 , the mobilization of U from U_3O_8 particles should be enhanced compared to UO_2 particles, when in contact with body fluids or present in soil-water systems.

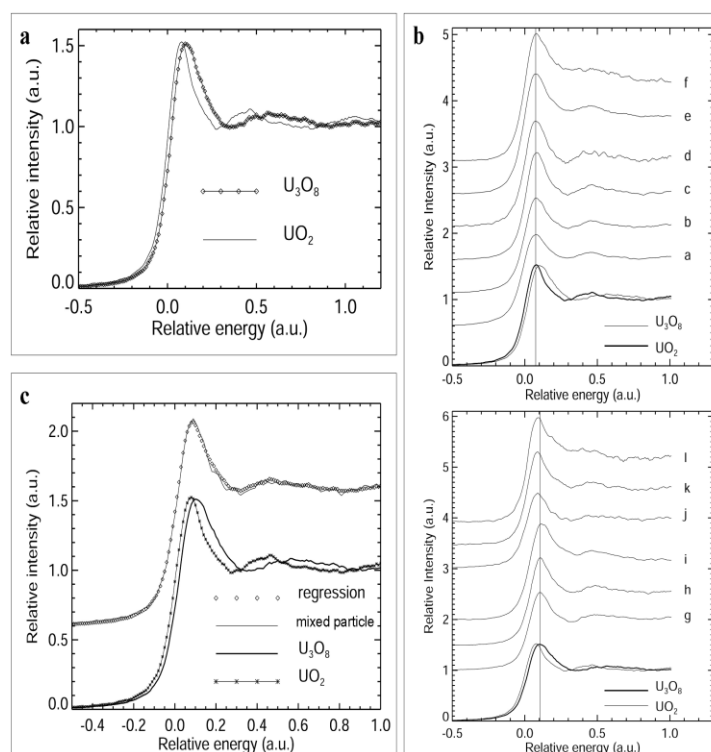


Figure 37. Oxidation states of uranium in DU particles. (a) μ -XANES analysis of UO_2 and U_3O_8 standards. (b) The μ -XANES spectra of uranium in the investigated DU particles. The solid lines indicate the peaks of UO_2 and U_3O_8 standards. (c) μ -XANES profile of a mixed U oxide particle compared to UO_2 and U_3O_8 standards using linear regression

DU in Serbia

Reports on the detection of traces of ^{236}U , a non-natural uranium isotope formed when uranium is used as fuel in nuclear reactors, triggered concerns about the possibility that other

nuclides from the nuclear fuel cycle and, in particular, transuranium nuclides, might be present in this type of ammunition. Indeed, analyses carried out by a number of laboratories on a small number of recovered penetrators, revealed the presence of $^{239,240}\text{Pu}$, with activity concentrations of up to 12 Bq kg^{-1} . To confirm this finding, analyses were also carried out in the course of the ADVANCE project on a DU penetrator recovered intact from a May 1999 target site in the southern Serbian community of Bratoselce, located 10 km northeast of Preševo. Our measurements, carried out using a combination of low-background, high resolution alpha spectrometry and multi-collector, inductively-coupled plasma mass spectrometry (MC-ICP-MS), confirmed the presence of ^{236}U (0.0028 % by weight) and plutonium isotopes in the DU ammunition used during the Balkan conflict. Although the activity concentration of $^{239,240}\text{Pu}$, at $45.4 \pm 0.7 \text{ Bq kg}^{-1}$, is the highest reported to date for any penetrator recovered from the Balkans, it is still below the values quoted for mean $^{239,240}\text{Pu}$ concentrations in DU armours used in tanks, at 85 Bq kg^{-1} (USA Army Material Command, 2000). From a radiological perspective, the amount of plutonium in the DU, at 0.019 ppb, is so low as to cause only a very small increase (<1%) in the dose received by persons exposed to this material.

DU in Kuwait

The concentration of uranium isotopes in sand samples collected in Kuwait (as determined by gamma spectrometry) varied from site to site due to the presence of varying amount of DU particles in the samples. XRMA analyses revealed the presence of Ti as well as traces of other metals within most of the DU particles, although for some DU particles Ti was found to be below the limits of detection. Based on ongoing ICP-MS and AMS work, the $^{235}\text{U}/^{238}\text{U}$ atom ratio in the DU particles analysed was rather constant, at approximately 0.002, while the $^{236}\text{U}/^{235}\text{U}$ isotope ratios varied according to the provenance of the DU particles analysed, ranging from $\sim 10^{-2}$ for DU particles associated with a fire in the DU ammunition storage facility to $\sim 10^{-3}$ in DU particles from swipes taken from the inside of DU penetrator holes in tanks (Table 2). It is clear, however, that as was the case for the Serbian penetrator, the DU in the munitions originated from reprocessed uranium fuel.

Table 2. Uranium atom ratios in individual DU particles and natural U (certified reference uranium mine ores) as determined by ICP-MS and AMS.

Sample description	n	Isotope atom ratio (± 1 S.D.)		
		$^{235}\text{U}/^{238}\text{U}^{\text{a}}$	$^{236}\text{U}/^{235}\text{U}^{\text{b}}$	$^{236}\text{U}/^{238}\text{U}^{\text{d}}$
DU munitions store fire	4	0.00198 ± 0.00006	$0.0097 \pm 0.0005^{\text{c}}$	$(2.0 \pm 0.1) \times 10^{-5}$
Swipe from inside damaged tank	4	0.0021 ± 0.0001	0.00097 ± 0.0004	$(2.1 \pm 0.9) \times 10^{-6}$
Uranium mine ores	2	0.0071 ± 0.0007	$(3.5 \pm 0.5) \cdot 10^{-7}$	$(2.5 \pm 0.5) \times 10^{-9}$

^a ICP-MS

^b AMS

^c Mean of one AMS and three ICP-MS measurements

^d Calculated by combining the ICP-MS and AMS data

The size distribution of isolated DU particles, as determined from SEM analyses, ranged from 2 to 64 μm (median 13 μm , $n = 36$) in samples taken either from penetrator holes in tanks hit by DU ammunition or in samples collected close to ‘unspent’ penetrators (Figure 38). On the other hand, DU particles originating from a fire in a DU ammunition store facility

showed a wider size distribution, ranging from 0.2 to 1500 μm (median 44 μm , $n = 43$). The large DU particles appeared with a strong yellow colour, typical of uranyl compounds, and a crystalline structure which was quite different from all DU particles observed in Kosovo and other sites in Kuwait (Figure 39), as well as from that of uranium particles released during the Chernobyl accident (see section on Chernobyl accident above).

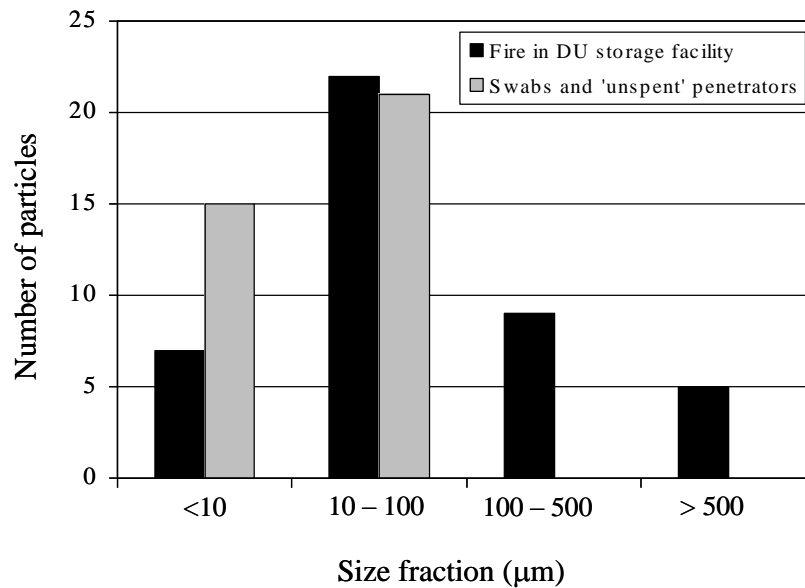


Figure 38. Size distribution of isolated DU particles observed in SEM.

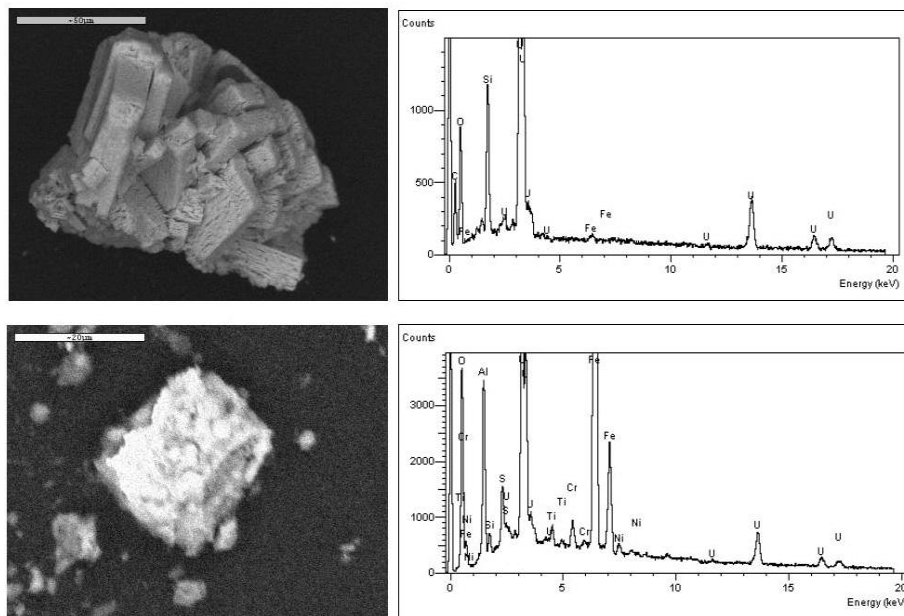


Figure 39. Scanning electron microscopy of depleted uranium particles . (Top) Large particle originating from fire in DU ammunition storage facility, collected from sand in Kuwait: Backscattered Electron Imaging (BEI) mode, with bright areas reflecting high atomic number elements (top left) and elemental analysis by XRMA (top right). Bar = 50 μm . (Bottom) Particle originating from the impact of DU munitions collected by swipe: Backscattered Electron Imaging (BEI) mode, with bright areas reflecting high atomic number elements (bottom left) and elemental analysis by XRMA (bottom right). Bar = 20 μm

The oxidation states of uranium in these particles were determined using μ -XANES. Based on well-defined standards, all the depleted uranium particles investigated were oxidised. Kuwaiti DU particles collected close to ‘unspent’ DU penetrators or inside attacked tanks (swipes) were characterized as UO_2 , U_3O_8 or a mixture of these oxidized forms, similar to that observed in DU affected areas in Kosovo. Uranium particles released during a fire in a DU ammunition facility were, however, present as oxidation states +5 and +6, with XANES spectra similar to the solid uranyl standards and μ -XRD data indicating the presence of carbonates. As the particle weathering rate is expected to be higher for U(V)/U(VI) and U_3O_8 than for UO_2 , the presence of respiratory $\text{U}_3\text{O}_8/\text{U}_2\text{O}_5$ /uranyl, their corresponding weathering rates and the subsequent remobilisation of uranium should be included in environmental impact assessments of areas contaminated with DU and in health implications assessments arising from the use of this type of ammunition.

WP3. Terrestrial ecosystems affected by actinide contamination

The main objectives of this work-package were to compare the transfer of actinides in different terrestrial ecosystems and to identify the main source- and ecosystem-related characteristics controlling their mobility and bioavailability within each of these environments. A site-by-site description of the field work and analyses undertaken during the project, together with the results of laboratory studies on the remobilisation potential for radionuclides associated with particles, and soil or sediment samples at each of the sites is given in the sections below.

Palomares (Spain)

A field expedition to Palomares was undertaken in October 2001 as part of the ADVANCE research activities. The measurement of ^{241}Am and plutonium inventories in soils collected in different areas within the vicinity of Palomares allowed an updated determination to be made of the spatial distribution of actinide contamination almost four decades after the accident. The sampling locations, shown in Figures 40 and 41, comprised three separate zones: Zone A, placed west of Palomares, where the chemical explosion of one of the bombs took place; and Zones B and C, south-east of Palomares, where the chemical explosion of the second bomb occurred and a third one was recovered intact. The ^{241}Am and $^{239,240}\text{Pu}$ inventories at these locations are given in Table 3.

The data shows that the highest levels of actinides are found in surface (0–5 cm) horizons of undisturbed soils within Zone A, particularly in sampling points close to the village of Palomares. The levels are lower in Zones B and C, where the agricultural use of the land has most likely contributed to the dilution of the signal as a result of ploughing. The data also suggest that contamination (particularly in Zone A) is quite heterogeneous, indicating the presence of numerous radioactive particles (some of which have been successfully isolated and subjected to further characterisation – see WP2 above) and variable inventories over a relatively small area.

Measurement of plutonium isotopic ratios in the most contaminated samples confirmed that the origin of the contamination can be attributed to weapons-grade plutonium dispersed during the accident (Table 4). Sequential extraction analyses carried out on these samples with a view to determine the bioavailability of plutonium for plant uptake, showed that up to 6% of the plutonium is now in a readily available form (operationally defined as the fraction

of plutonium extractable using a 1M solution of magnesium chloride; extraction time = 24 hours) (Table 5). The proportion of plutonium in an exchangeable form is higher than that previously reported by other workers, and could reflect a change in the geochemical association of the plutonium as a result of weathering. Additional work should be conducted to confirm this possible change in the bioavailability of the released plutonium.

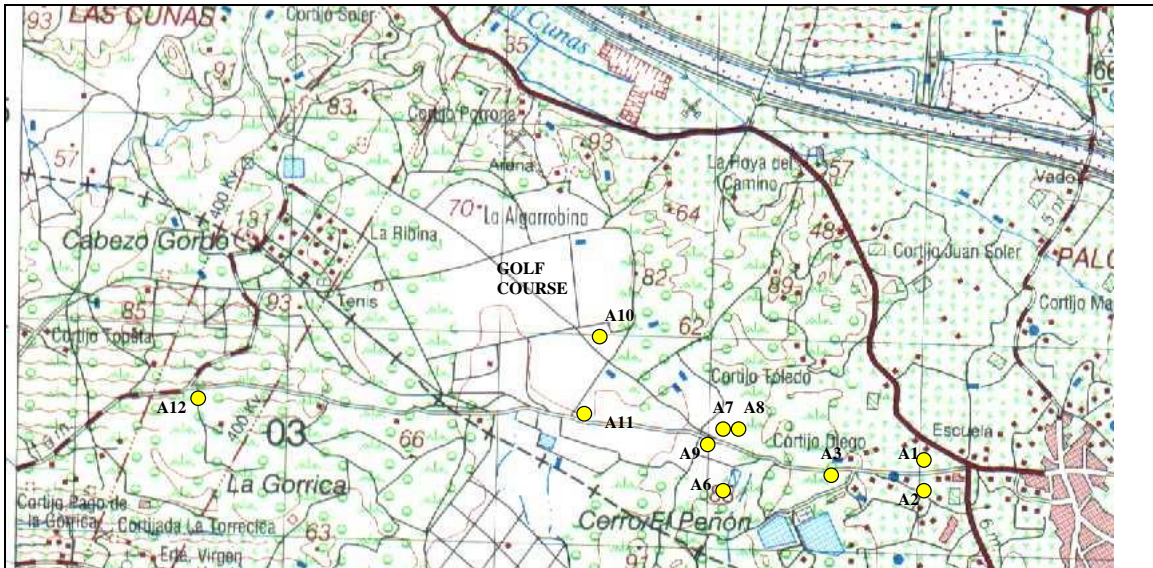


Figure 40. Map showing the sampling locations in Zone A, west of Palomares

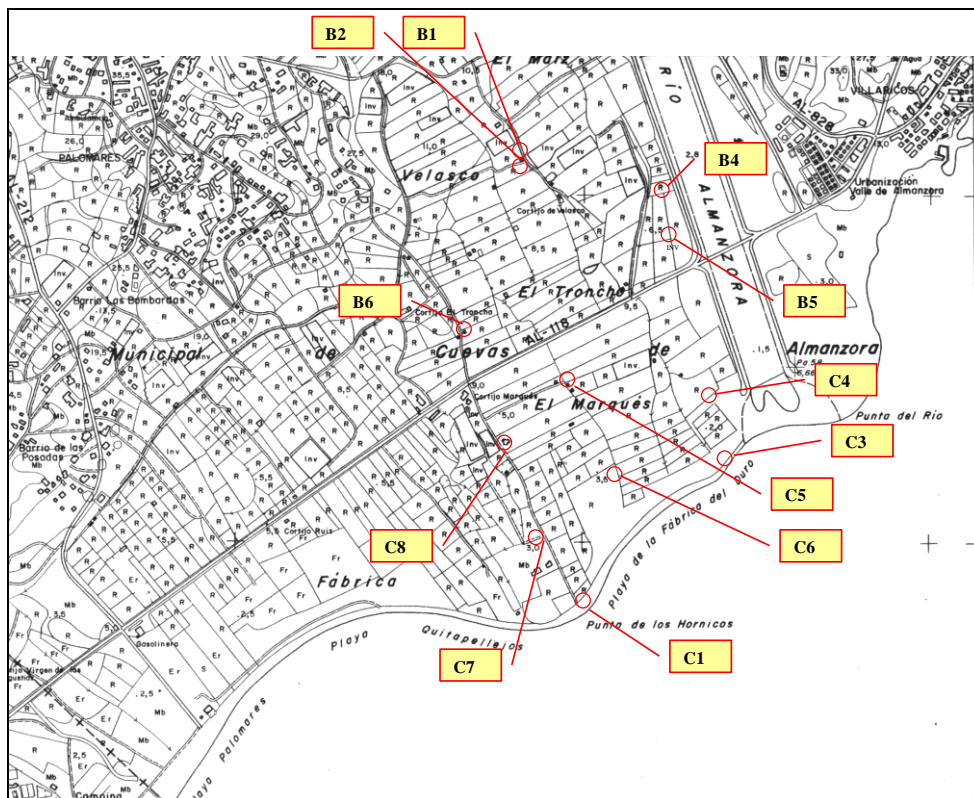


Figure 41. Map showing the sampling locations in Zones B and C, south-east of Palomares

Table 3. $^{239,240}\text{Pu}$ and ^{241}Am inventories in soils collected in Palomares (October 2001)

Location	Site	Inventory (Bq m^{-2})	
		$^{239,240}\text{Pu}$	^{241}Am
Zone A:	A1	21200 – 57900	720 – 27280
	A2	6450 – 56800	4350 – 157200
	A3	2070 – 21300	3050 – 23750
	A6	250 – 310	4700
	A7	110	
	A8	20	
	A9	8	
	A10	25	
	A12	40	
	Zone B:	B1	600 ± 25
B4		250 ± 13	
B5		84 ± 6	
B6		179 ± 12	
Zone C:	C1	80 ± 7	
	C3	72 ± 6	
	C4	349 ± 13	
	C5	262 ± 20	
	C7	71 ± 6	
	C8	25 ± 3	

Although the residual contamination of the Palomares accident area following the removal of the most contaminated soils was estimated to be around 0.1–0.2 TBq, more recent assessments carried out by CIEMAT (the scientific institution officially tasked with the monitoring of this area) suggest that the remaining inventories could be much higher than previously thought, with an estimated 2.9 TBq remaining in a 5.25 Ha area surrounding the point of impact of one of the bombs alone. A similar reassessment, taking into account the contribution of radioactive particles to the total inventory, has recently been reported for Thule, with the initially-estimated 1 TBq ($^{239,240}\text{Pu}$) being revised to a more realistic figure of 10 TBq (Ericsson, 2002). The above figures highlight the need to take into account the presence of radioactive particles when characterising the source-term in accident zones involving the fracture and dispersion of actinides in metallic form.

Table 4. $^{238}\text{Pu}/^{239,240}\text{Pu}$ activity ratios in some of the soils collected in Palomares (October 2001)

Sample code	$^{238}\text{Pu}/^{239,240}\text{Pu}$
A1-3	0.017 ± 0.002
A2-1	0.015 ± 0.002
A2-2	0.016 ± 0.001
A2-5	0.021 ± 0.004
A3-2	0.020 ± 0.005

Table 5. Percentage of plutonium extracted from Palomares soil samples using a 1M MgCl₂ solution (extraction time = 24 hours)

Sample code	% ^{239,240} Pu extracted
A2-1	5
A2-5	0.3
A3-2	3
D1-1	6
D2-4	4

Semipalatinsk nuclear test site (Kazakhstan)

In the course of the ADVANCE project, soil samples were collected at four localities within the Semipalatinsk nuclear test site, known to be heavily contaminated or identified as areas of potential radiological significance, namely Ground Zero, Balapan Lake and the Tel'kem 1 and Tel'kem 2 craters. Emphasis was given to the characterisation, in terms of radionuclide composition, of the activity levels and ratios at each of these sites. Measurements on samples collected at other locations within the STS, well removed from localised sources, were also carried out for the purpose of comparison. In addition, the association of plutonium with different geochemical phases at the above-mentioned four sites was investigated using the technique of sequential extraction analysis. Details of the precise sampling locations at each of the sites can be found in WP2 above.

Gamma spectrometry analyses carried out on soil samples from the four sites examined revealed the presence of fission and activation products such as ⁶⁰Co, ¹³⁷Cs, ¹⁵²Eu and ¹⁵⁴Eu. At Ground Zero, the fission and activation product gamma field was dominated by ¹³⁷Cs (61–72%), with a smaller contribution from ¹⁵²Eu (27–36%) and even smaller contributions from ⁶⁰Co (0.96–1.9%) and ¹⁵⁴Eu (<1.3%). Although no difference was observed between the ¹³⁷Cs/⁶⁰Co and ¹⁵²Eu/⁶⁰Co ratios measured in the <1 mm and >1 mm size fractions of the soil, these ratios differed significantly from those measured in the more active, vitrified material collected at the same location, which were significantly lower. The ¹⁵⁴Eu/¹⁵²Eu activity ratio, on the other hand, was found to be identical for both soil and vitrified material. The ¹⁵²Eu/⁶⁰Co and ¹⁵⁴Eu/¹⁵²Eu activity ratios measured in soil are in good agreement (once radioactive decay is taken into account) with those reported by Yamamoto *et al.* (1996a) for a soil collected near the hypocentre of the first nuclear detonation at Ground Zero. The ¹³⁷Cs/⁶⁰Co activity ratio for this soil sample, on the other hand, is about half of that measured in our sample. The observed large variability in the ¹³⁷Cs/⁶⁰Co ratio, however, is not unusual, and, as will be seen later, occurs even at locations affected mainly by a single nuclear explosion.

At Lake Balapan, the gamma field was not dominated by a single nuclide, but shared between ¹³⁷Cs (26–43%), ¹⁵²Eu (25–33%) and ⁶⁰Co (21–23%), with a smaller contribution from ¹⁵⁴Eu (12–18%). The measured ¹³⁷Cs/⁶⁰Co, ¹⁵²Eu/⁶⁰Co and ¹⁵⁴Eu/¹⁵²Eu ratios were distinctly different from the corresponding ratios at Ground Zero. Specifically, ¹⁵⁴Eu/¹⁵²Eu ratios at Lake Balapan were ~10–20 times higher than those measured at Ground Zero, while ¹³⁷Cs/⁶⁰Co and ¹⁵²Eu/⁶⁰Co ratios at Balapan were between one and two orders of magnitude

lower than those measured at Ground Zero. Although the $^{152}\text{Eu}/^{60}\text{Co}$ and $^{154}\text{Eu}/^{152}\text{Eu}$ activity ratios in the two size fractions considered were statistically indistinguishable, there appeared to be a difference in the $^{137}\text{Cs}/^{60}\text{Co}$ activity ratio, with lower ratios being observed for the <1 mm fraction, a result confirmed by the analysis of replicate samples.

At both Tel'kem 1 and Tel'kem 2 the measured gamma field was largely dominated by ^{137}Cs (86–99%). There were large variations in the measured $^{137}\text{Cs}/^{60}\text{Co}$ ratios, depending both on the sampling location and the size fraction analysed, with higher ratios being observed in the >1 mm size fraction. The $^{152}\text{Eu}/^{60}\text{Co}$ and $^{154}\text{Eu}/^{152}\text{Eu}$ ratios showed less variation, with values ranging between 0.8–4 and 0.11–0.21, respectively, for Tel'kem 1, and between 1.0–2.4 and 0.13–0.25, respectively, for Tel'kem 2.

For the samples collected well removed from any localised source, only ^{137}Cs could be detected. Measured concentrations were in the range 4–320 Bq kg⁻¹, dry wt. (equivalent to a deposition of 0.3–22 kBq m⁻² in the top 5 cm), with most data falling at the lower end of this range. The latter are typical of global fallout levels and are in good agreement with ^{137}Cs concentrations measured in soil from other villages and settlements situated outside of, but close to, the boundary of the STS (Hill *et al.*, 1996; IAEA, 1998).

Plutonium and americium concentrations in soil samples collected at each of the four areas studied are given in Table 6. In most cases, measured $^{239,240}\text{Pu}$ and ^{241}Am concentrations at these sites were 2 to 3 orders of magnitudes higher than those measured at the 'control' sites, well removed from localised sources, which showed levels in the range 0.6–360 mBq g⁻¹ (dry wt.) for $^{239,240}\text{Pu}$ and 2–10 mBq g⁻¹ (dry wt.) for ^{241}Am . Not unexpectedly, the highest $^{239,240}\text{Pu}$ concentration recorded, at 174 ± 10 Bq g⁻¹ (dry wt.), was in a sample of vitrified, 'tar-like' material, collected near Ground Zero. In all cases, plutonium and americium concentrations in the <1 mm fraction were found to be higher than those in the >1 mm fraction, indicating the predominant association of these nuclides with smaller particles.

$^{238}\text{Pu}/^{239,240}\text{Pu}$ activity ratios for most samples were in the range 0.012–0.07, and are consistent with those previously reported by other workers for the STS (Yamamoto *et al.*, 1996a; 1996b; Voigt *et al.*, 2001). However, an unusually high $^{238}\text{Pu}/^{239,240}\text{Pu}$ activity ratio was measured in samples from Lake Balapan, a result confirmed by the analysis of replicate samples. This seemingly anomalous ratio had previously been reported by Yamamoto *et al.* (1996a; 1996b), who suggested the $^{239}\text{Pu}(n, 2n)^{238}\text{Pu}$ reaction with fast neutrons as a likely explanation. Similar ratios have also been reported in samples contaminated by fallout from thermonuclear weapons tests (León Vitró *et al.*, 1996). The low $^{240}\text{Pu}/^{239}\text{Pu}$ atom ratio, measured by spectral deconvolution in these samples, at $0.072 \pm 0.004(2\sigma)$, and the similarly low $^{241}\text{Pu}/^{239,240}\text{Pu}$ activity ratio, at $0.87 \pm 0.16(2\sigma)$, indicate that the plutonium in this area is of weapons-grade quality. This suggests that the device was not a 'hydrogen' bomb, but rather a 'boosted' fission device, containing deuterium and tritium within the fissile material in order to augment the explosive yield. It is probable that the much enhanced flux of fast neutrons produced by such a device is responsible for the comparatively high ^{238}Pu activities present at Lake Balapan, though the use of ^{238}Pu as a neutron reflector cannot be excluded.

Measured $^{240}\text{Pu}/^{239}\text{Pu}$ atom ratios in soil samples from Tel'kem 1 and Tel'kem 2, at $0.051 \pm 0.003(2\sigma)$ and $0.054 \pm 0.003(2\sigma)$, respectively, also indicated that the main source of plutonium contamination at these sites is weapons-grade plutonium.

Table 6. Transuranium concentrations ($\pm 2\sigma$) and activity ratios ($\pm 2\sigma$) at selected sites on the STS (reference date: 1 July 2000).

Sample	Fraction	Concentration (Bq g ⁻¹ , dry wt.)			²³⁸ Pu/	²⁴¹ Am/
		²³⁸ Pu	^{239,240} Pu	²⁴¹ Am	^{239,240} Pu	^{239,240} Pu
Ground Zero:						
Soil	<1 mm	0.54 ± 0.08	8.4 ± 0.4	0.235 ± 0.008	0.07 ± 0.01	0.028 ± 0.002
	>1 mm	<i>NM</i>	<i>NM</i>	0.139 ± 0.004		
Vitrified material	Bulk	0.5 ± 0.1	174 ± 10	2.14 ± 0.04	0.0028 ± 0.0007	0.0123 ± 0.0007
Lake Balapan:						
Soil (shoreline)	Bulk	2.1 ± 0.1	4.9 ± 0.3	0.64 ± 0.02	0.42 ± 0.03	0.131 ± 0.009
Soil	<1 mm	2.6 ± 0.5	6.2 ± 0.3	1.05 ± 0.02	0.41 ± 0.08	0.168 ± 0.009
	>1 mm	4.3 ± 0.4	11.2 ± 0.8	1.21 ± 0.03	0.38 ± 0.05	0.109 ± 0.008
Tel'kem 1:						
Soil (centre of lake)	Bulk	0.34 ± 0.05	24.7 ± 0.6	2.32 ± 0.03	0.014 ± 0.002	0.094 ± 0.003
Soil North	<1 mm	0.26 ± 0.06	19 ± 1	3.08 ± 0.01	0.014 ± 0.003	0.165 ± 0.009
	>1 mm	<i>NM</i>	<i>NM</i>	0.66 ± 0.01		
Soil South	<1 mm	0.32 ± 0.07	23 ± 1	2.24 ± 0.01	0.014 ± 0.003	0.099 ± 0.006
	>1 mm	<i>NM</i>	<i>NM</i>	0.215 ± 0.003		
Soil East	<1 mm	0.008 ± 0.003	0.41 ± 0.04	0.447 ± 0.004	0.019 ± 0.008	1.1 ± 0.1
	>1 mm	<i>NM</i>	<i>NM</i>	0.108 ± 0.002		
Soil West	Bulk	0.11 ± 0.03	7.3 ± 0.4	1.91 ± 0.01	0.015 ± 0.004	0.26 ± 0.01
Tel'kem 2:						
Soil (centre of lake)	Bulk	0.35 ± 0.06	29.3 ± 0.8	3.67 ± 0.04	0.012 ± 0.002	0.125 ± 0.004
Soil South	<1 mm	0.39 ± 0.07	29 ± 2	6.80 ± 0.04	0.013 ± 0.003	0.24 ± 0.01
	>1 mm	0.12 ± 0.04	8.3 ± 0.5	0.80 ± 0.01	0.015 ± 0.005	0.097 ± 0.006
Soil West	Bulk	<i>ND</i>	0.08 ± 0.01	0.0042 ± 0.0008		0.05 ± 0.01
Soil North-East	<1 mm	<i>ND</i>	0.21 ± 0.03	0.144 ± 0.002		0.7 ± 0.1
	>1 mm	<i>NM</i>	<i>NM</i>	0.0085 ± 0.0007		
Soil North-West	<1 mm	2.8 ± 0.2	195 ± 10	20.90 ± 0.06	0.014 ± 0.001	0.107 ± 0.006
	>1 mm	<i>NM</i>	<i>NM</i>	2.93 ± 0.03		

This was further confirmed by the measured $^{241}\text{Pu}/^{239,240}\text{Pu}$ activity ratio at Tel'kem 1 which, at $0.84 \pm 0.20(2\sigma)$, is again typical of weapons-grade plutonium.

Measured $^{241}\text{Am}/^{239,240}\text{Pu}$ activity ratios varied from site to site and also in samples collected from a particular site. With two exceptions, the $^{241}\text{Am}/^{239,240}\text{Pu}$ activity ratios were lower than the value of 0.22 reported by Krey *et al.* (1976) for global fallout in the mid-1970s and the value of 0.37 reported for mid-latitude soils in the late 1980s by Ryan *et al.* (1995). Whilst differences in this ratio between sites are to be expected, variations at a given site are clearly not. Much (if not all) of the observed 'variability' at sites such as Tel'kem 1 or Tel'kem 2 is undoubtedly due to the presence of numerous hot particles in the samples analysed (a finding confirmed by replicate analysis, backed-up by autoradiography and passive track-etch detection), combined with the fact that the ^{241}Am content was measured by gamma counting bulk samples, whereas that of $^{239,240}\text{Pu}$ was determined by alpha counting small (~ 1 g) sub-samples.

The partitioning of plutonium in a small number of soil samples from Ground Zero, Lake Balapan, Tel'kem 2 and Tel'kem 1 was examined using a sequential extraction protocol, the details of which have been described elsewhere (Lucey, 2003). The protocol employed considers six fractions, namely exchangeable, acido-soluble, reducible, oxidisable, strongly bound and residual. The increasing strength of the extractants can be used to assess the potential for remobilisation and consequent bioavailability of the plutonium. The residual fraction, as defined in the protocol, is that remaining following extraction with 8M HNO_3 at 90°C for a period of 2 hours. The soils examined were collected close to the epicentre at Ground Zero, from the surrounding ring of spoil at Lake Balapan and Tel'kem 2, and from the centre of the lake at Tel'kem 1. The results, summarised in Figure 42, clearly show that, with the exception of Tel'kem 1, most of the plutonium in the soils analysed was in a highly refractory form; the proportion of plutonium in the residual phase was found to be $\sim 90\%$ at Ground Zero, $\sim 85\%$ at Lake Balapan, $\sim 60\%$ at Tel'kem 2 and $\sim 20\%$ at Tel'kem 1.

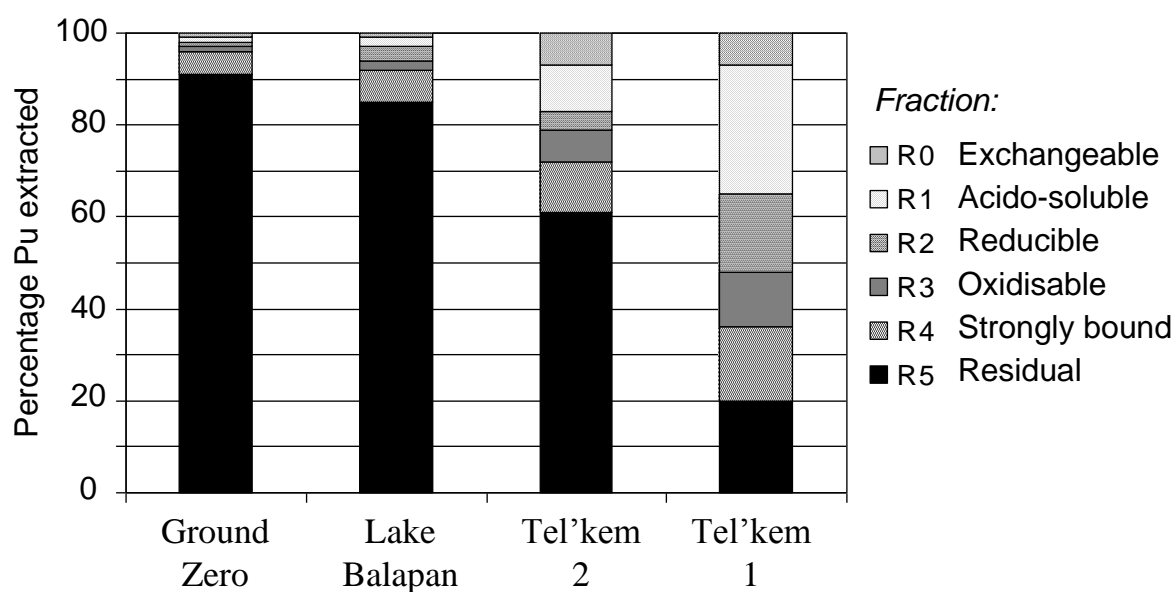


Figure 42. Sequential extraction of plutonium in soil samples from the STS

There is little doubt but that this pattern reflects differences in the temperature of the fireball which engulfed the soil following detonation at each of these sites, as well as differences in sampling location. In the case of Tel'kem 1 and Tel'kem 2, the latter is almost certainly the most relevant, as the explosive yields were both very low and quite similar. Again, with the exception of Tel'kem 1 (and perhaps Tel'kem 2), little plutonium was present in a readily exchangeable form (R0 + R1 fractions).

Mayak PA (Russia)

As part of the ADVANCE project, measurements were carried out in order to characterise the plutonium and uranium signatures in samples of soil, grass, water and aquatic biota collected from the Asanov swamp area and from Reservoir 11 during field work conducted in 1994 and 1996 by the Joint Norwegian Russian Expert Group (JNREG, 1997). The location of these areas within the Mayak site is shown in Figure 43. Measurements were carried out using accelerator mass spectrometry (AMS) at the 14UD tandem accelerator facility of the Australian National University (Canberra). Details of the samples analysed, selected from a sample bank of approximately 500 samples, are given in Table 7.



Figure 43. Map of the Mayak PA site showing the locations of Reservoir 11 (R-11) and the Asanov Swamp

Table 7. Mayak samples used for accelerator mass spectrometry measurement

Sample	Id. No.	Location	Matrix (family name)	Details
1	1532	Reservoir 11	Water	<0.45 μm
2	1500	Asanov Swamp	Water	<0.45 μm
3	3208	Asanov Swamp	Surface soil	0–5 cm
4	3209	Asanov Swamp	Surface soil	0–5 cm
5	4011	Asanov Swamp	Grass	Dried
6	4012	Asanov Swamp	Grass	Dried
7	7013	Asanov Swamp	Water plant (Apiaceae)	Dried
8	7014	Asanov Swamp	Water plant (Juncaceae)	Dried
9	6009	Reservoir 11	Mussel (Unionidae)	Ashed
10	6010	Reservoir 11	Pike bone (Esocidae)	Ashed
11	6011	Reservoir 11	Pike fillet (Esocidae)	Ashed
12	6014	Reservoir 11	5 Roach (Cyprinidae)	Ashed

In the terrestrial environment, two grass samples and representative samples of the underlying soil were collected from a 1 m² plot adjacent to the Techa River in the Asanov Swamp. Following radiochemical separation and purification, sources were prepared for AMS counting. Plutonium and uranium concentrations, and relevant atom ratios (i.e., ²⁴⁰Pu/²³⁹Pu, ²³⁵U/²³⁸U and ²³⁶U/²³⁵U) were determined at the AMS facility in Canberra. The ⁹⁹Tc content of the samples was also assayed using this technique. This information was used to calculate site-specific concentration factors (CFs) for the studied area.

The activity concentrations of plutonium, together with the corresponding ²⁴⁰Pu/²³⁹Pu atom ratios for the grass and soil samples analysed, are given in Table 8. The measured ²⁴⁰Pu/²³⁹Pu atom ratios in the soils, at ~0.02, are typical of weapons-grade plutonium and agree well with other published ratios in soils from the same area (Oughton *et al.*, 2000). The isotopic signature of the plutonium reflects the source-term of the contamination, which is due mainly to early discharges of intermediate level liquid waste between 1949 and 1951, when Mayak was dedicated to the production of military plutonium. The corresponding ratios in the grass samples were somewhat higher than those measured in the surface soil samples, perhaps reflecting the penetration of roots to deeper layers of soil containing a different ²⁴⁰Pu/²³⁹Pu ratio. The soil-to-grass (dry weight based) concentration factors calculated from these measurements, at ~10⁻⁴, are in good agreement with previously published values.

Table 8. Plutonium activity concentrations ($\pm 2\sigma$) and ²⁴⁰Pu/²³⁹Pu atom ratios ($\pm 2\sigma$) in terrestrial samples collected in the Asanov Swamp region, Mayak PA

Id. No.	Sample	Concentration (Bq kg ⁻¹)		²⁴⁰ Pu/ ²³⁹ Pu (atom ratio)
		²³⁹ Pu	²⁴⁰ Pu	
3208	Surface soil	2000 \pm 18	135 \pm 2	0.0228 \pm 0.0002
3209	Surface soil	1810 \pm 26	122 \pm 4	0.0205 \pm 0.0006
4011	Grass	0.163 \pm 0.019	0.023 \pm 0.012	0.040 \pm 0.016
4012	Grass	0.21 \pm 0.03	0.024 \pm 0.014	0.039 \pm 0.018

The activity concentrations of uranium, together with relevant atom ratios for the same soil and grass samples are given in Table 9. The $^{235}\text{U}/^{238}\text{U}$ atom ratios in the soils were found to be lower than the natural ratio of 0.00734 (extreme range: 0.00730–0.00737), possibly indicating the presence of reprocessed uranium. The measured $^{236}\text{U}/^{235}\text{U}$ atom ratios (in the range 0.0007 – 0.044), on the other hand, were significantly lower than those measured in other parts of the Mayak complex (see WP4), and are indicative of low nuclear-fuel burn-up times, reinforcing the view that the origin of contamination in the Asanov Swamp is mainly due to releases that took place when Mayak was dedicated to the manufacturing of nuclear weapons. The average uranium soil-to-grass (dry weight based) concentration factor derived from these measurements is 1.9×10^{-3} .

Table 9. Uranium activity concentrations and relevant atom ratios in terrestrial samples collected in the Asanov Swamp region, Mayak PA

Id.	Sample	Concentration (mBq kg ⁻¹)			Atom ratios	
		^{235}U	^{236}U	^{238}U	$^{235}\text{U}/^{238}\text{U}$	$^{236}\text{U}/^{235}\text{U}$
3208	Surface soil	945	126	22300	0.0067	0.0044
3209	Surface soil	932	104	21900	0.0067	0.0037
4011	Grass	1.52	0.062	NA	–	0.0014
4012	Grass	2.04	0.042	NA	–	0.0007

AMS measurements of ^{99}Tc allowed the determination of concentration factors for this radionuclide. A concentration factor of 6×10^{-2} was obtained based on single measurements of grass and soil samples. The ^{99}Tc concentration in the soil was found to be 2300 Bq kg⁻¹ (dry wt.), while that in the grass was 140 Bq kg⁻¹ (dry wt.).

Source-term characteristics and transfer in terrestrial ecosystems

It should be clear from the results presented in WP2, and those discussed in the previous sections of this work-package, that a significant proportion of the actinide contamination in all of the terrestrial ecosystems studied as part of the ADVANCE project is in the form of radioactive particles of varying composition and character. In order to evaluate differences in the bioavailability of actinides originating from different release scenarios, a series of laboratory experiments were conducted in which contaminated soils were subjected to leaching by a simulated stomach fluid.

Each sample (~2 g) was transferred to a centrifuge tube and extracted with 20 ml of 0.16 M HCl for 2, 24 and 168 hours. The supernatant was separated from the solid by high-speed centrifugation (10000 rpm), followed by filtration. The extracts, filters and residual material were then analysed for the actinide of interest.

In the case of Semipalatinsk, the nuclide investigated was ^{241}Am . The cumulative extracted percentages of ^{241}Am for soils collected at Tel'kem 1, Tel'kem 2 and Lake Balapan are shown in Figure 44. The extraction of ^{241}Am from the soils was very low, with 72–85 % of the ^{241}Am remaining unextracted, even after 168 hours of contact with the simulated

gastrointestinal fluid. As it will be shown in WP4, the percentages of ^{241}Am dissolved at the end of these experiments were much lower than, for example, those observed in contaminated sediments affected by releases from nuclear reprocessing, but similar to those obtained in the leaching of contaminated sediments from Thule. Clearly, differences in the source-term will have an important role in the bioavailability of actinides, and must be taken into account when assessing their transfer to biota and man.

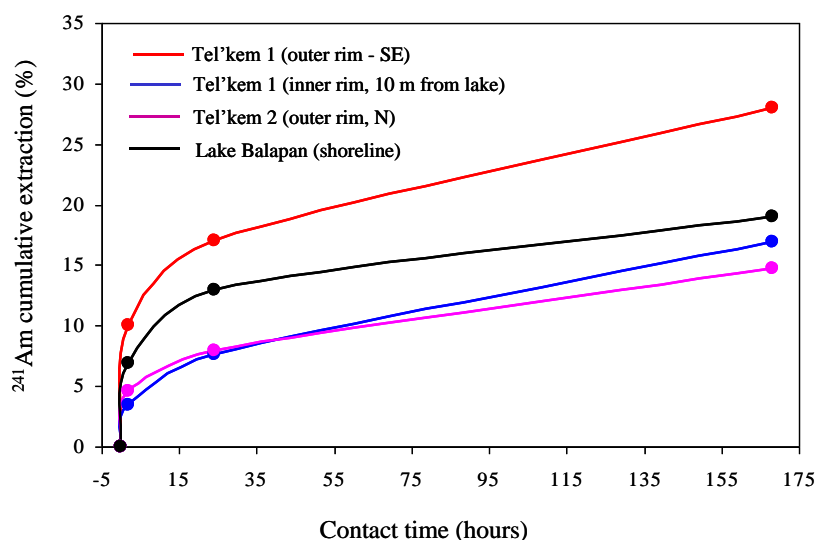


Figure 44. Cumulative extraction (%) of ^{241}Am from particle-contaminated soils collected at selected locations in the Semipalatinsk nuclear test site using simulated gastrointestinal fluid (0.16 M HCl)

Similar experiments were carried out in the case of soil/sand samples from Kosovo and Kuwait known to be contaminated with depleted uranium. The solubility of DU was found to vary significantly depending on the nature of the release scenario (Figure 45). Highly oxidised DU associated with particles originating from a fire in an ammunition storage facility (see WP2 above), was rapidly dissolved in 0.16 M HCl ($84 \pm 3\%$ after 2 hours of contact with the simulated gastrointestinal fluid, $n = 3$). In contrast, the initial kinetics of extraction of less oxidised DU particles, originating from the corrosion of ‘unspent’ DU penetrators or collected in tanks hit by DU ammunition, was significantly slower. In all cases, between 72–92% of the uranium was solubilised by the simulated gastrointestinal fluid after 168 hours of contact.

Further, experiments conducted using artificial seawater ($\text{pH} = 8$) instead of 0.16 M HCl showed that while seawater was able to dissolve the yellow, highly oxidised DU particles originating from the ammunition storage facility fire, particles collected from tanks hit by DU penetrators were relative inert.

The influence of the source-term in determining the weathering rate and bioavailability of radioactive particles is also clear from the analysis of samples contaminated by the Chernobyl release. In recent studies, the particle weathering rate (fraction dissolved per year), estimated from ^{90}Sr mobilisation measurements, was shown to vary from 0.02 to 0.7 y^{-1} (Kashparov *et al.*, 1999). The weathering rate constant was low for particles deposited to the west of the Chernobyl plant (affected by the initial explosion), and high for particles deposited to the north and south of the plant (affected by releases originating in the subsequent fire). Such

differences can now be understood on the basis of differences between the crystallographic structures and radionuclide speciation in particles from both zones. As demonstrated in the course of this project (see WP2), the crystallographic structure and the oxidation state distribution of uranium in fuel particles released from the Chernobyl reactor varied with the release conditions. Particles released during the initial explosion under high temperature and pressure conditions contained reduced uranium, while particles released during the subsequent fire, with lower temperatures and aerobic conditions, contained oxidised uranium (Figure 46). These source-term differences account (at least partly) for the observed differences in weathering kinetics, mobility and soil-to-plant transfer coefficients west and north of the Chernobyl reactor. Environmental factors, such as the soil pH, will also influence the weathering rate, with higher rates observed with increasing acidity.

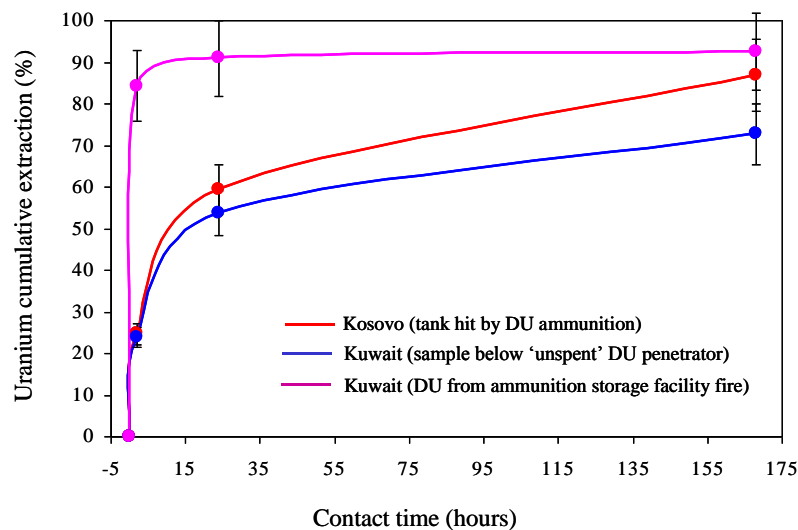


Figure 45. Cumulative extraction (%) of uranium from DU-contaminated soils/sands collected at locations in Kuwait and Kosovo using simulated gastrointestinal fluid (0.16 M HCl)

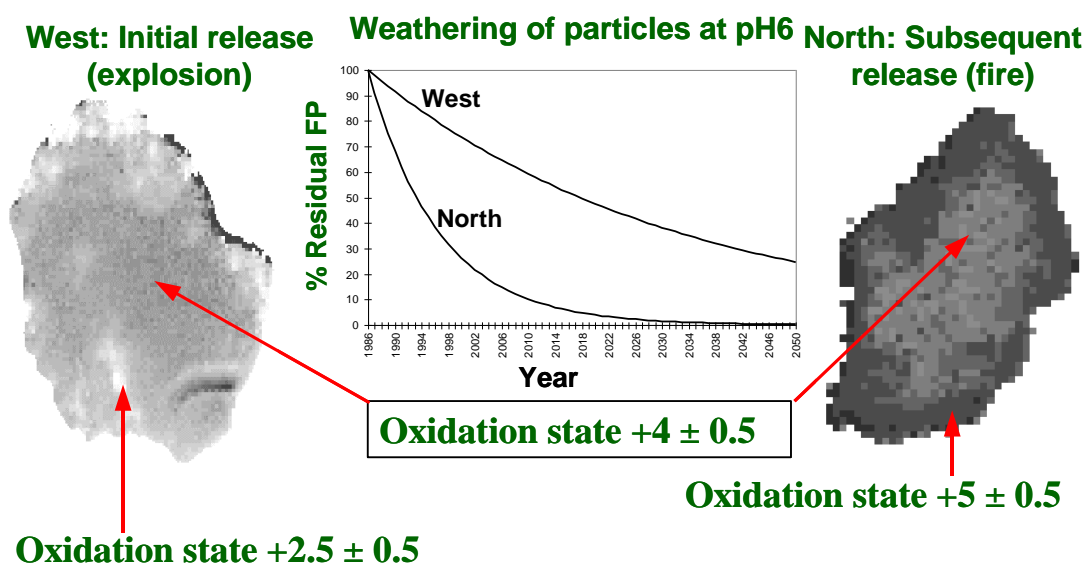


Figure 46. Weathering rate and oxidation state distribution of uranium particles released from Chernobyl during the initial explosion and in the subsequent fire

WP4. Mobility in fresh water systems

The main objectives of this work-package were to (i) identify factors influencing the transfer of actinides in groundwater and freshwater lakes by quantifying activity concentrations and isotopic ratios in water, sediments and biological endpoints; (ii) provide data on the speciation of transuranics in water and sediment; and (iii) refine models applied for migration of radionuclides in ground and surface waters from Mayak.

The study sites for this work-package included freshwater lakes and ground waters at the Semipalatinsk nuclear test site, and the freshwater system in the vicinity of Mayak PA. A combination of speciation techniques, including dual tracer coprecipitation and sequential extraction analysis, were used to provide data on transuranic speciation in water and sediments.

Semipalatinsk nuclear test site (Kazakhstan)

A large number of samples collected from wells, streams and atomic lakes within the Semipalatinsk nuclear test site during field campaigns in the summers of 2000, 2001 and 2002, were assayed for uranium, plutonium and americium content in the course of the project. The analyses included an evaluation, for the first time, of the oxidation state distribution of plutonium in these waters. The sampling locations are shown in Figure 47.

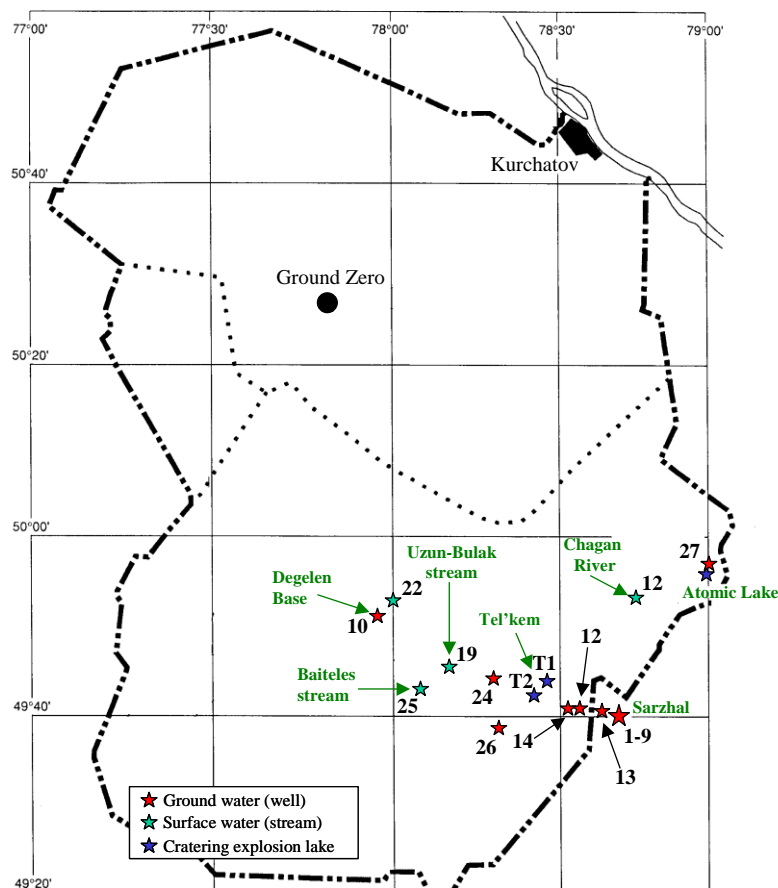


Figure 47. Map of the STS indicating the location of the sampling sites

Uranium levels and isotopic ratios in waters of the STS

Concentrations of ^{234}U , ^{235}U and ^{238}U , together with relevant isotopic ratios and total uranium concentrations in filtered water samples collected from wells in the village of Sarzhal, the Degelen military base, and the Tailan and Shurek farms, are given in Table 10.

With the exception of a well at the now derelict Degelen military base, concentrations of ^{234}U , ^{235}U and ^{238}U in all the wells analysed were in the range 177–412 mBq l^{-1} , 3.9–11 mBq l^{-1} and 74–213 mBq l^{-1} , respectively. In terms of total uranium concentration, these translate to a range of 6.0 to 17.3 $\mu\text{g(U) l}^{-1}$, which is at least an order of magnitude higher than the concentrations generally reported for treated drinking water in a number of developed countries (WHO, 2003). They are, however, comparable to the concentrations recorded by Gans (1985) in mineral waters in European countries such as France (0.6–77 $\mu\text{g(U) l}^{-1}$) and Germany (0.1–11 $\mu\text{g(U) l}^{-1}$). They are also within the US Environmental Protection Agency's maximum contaminant level for drinking water of 30 $\mu\text{g(U) l}^{-1}$ (USEPA, 2003), though the median concentration, at 11.4 $\mu\text{g(U) l}^{-1}$, marginally exceeds the World Health Organisation's more restrictive, proposed guideline of 9 $\mu\text{g(U) l}^{-1}$ (WHO, 2003), which is based on the latter's assessment of the chemical toxicity of uranium rather than on its radiological significance.

The fraction of uranium associated with suspended particulate matter in all of the well waters examined was very low (<2%), with virtually all of the uranium present in the micro-filtered fraction. This is consistent with observations reported by other researchers (e.g., Lee *et al.*, 2001) and suggest that most of the uranium in these groundwaters is present as dissolved species, most likely in the form of complexes with carbonate ions and/or dissolved organic matter, including humic substances (Gunter, 1972; Langmuir, 1978).

The $^{235}\text{U}/^{238}\text{U}$ activity ratio in most well waters (mean: 0.055; 95% confidence interval: 0.050–0.059), is slightly elevated above the 'best estimate' value of 0.0466 (extreme range: 0.04636–0.04681) reported for natural uranium world-wide (Holden, 1981), and almost certainly reflects the mixing of local fallout from some of the many diverse tests undertaken at the STS with naturally-occurring uranium. The $^{234}\text{U}/^{238}\text{U}$ ratio, with the exception of two outliers, shows even less variability (mean: 2.30; 95% confidence interval: 2.23–2.38), while the extreme range, at 1.44–3.96, is consistent with ratios reported for surface and groundwaters elsewhere (Hakam *et al.*, 2001; Lee *et al.*, 2001), and indicates that ^{234}U is not in equilibrium with its parent ^{238}U in any of the well waters examined. The main mechanisms which may contribute to the observed disequilibrium include α -particle recoil ejection of ^{234}Th into solution, preferential dissolution of ^{234}U due to radiation damage and the change of ^{234}U to more soluble U(VI) species in the associated rocks (Osmond *et al.*, 1983; Ivanovich *et al.*, 1991).

The well at the Degelen base is worthy of mention; clearly, the concentration of uranium in this well exceeds the US EPA recommended limit by almost a factor of five, though it would appear that in recent years the well has only been used for bathing and cleaning purposes by miners working at the open-cast coalmine in the Balapan region and specialists tasked with sealing both used and unused test bore-holes and tunnels in a joint project undertaken by Kazakhstan, the Russian Federation and the United States under a non-proliferation agreement to which the three parties are signatories.

Table 10. Uranium concentrations ($\pm 2\sigma$) in filtered ($<0.45 \mu\text{m}$) waters collected in wells from the Sarzhal region of the Semipalatinsk nuclear test site (July 2001)

Sample	Concentration (mBq l^{-1})			$^{234}\text{U}/$	$^{235}\text{U}/$	U ($\mu\text{g l}^{-1}$)	%U particulate
	^{234}U	^{235}U	^{238}U	^{238}U	^{238}U		
Sarzhal:							
Well #1	327 ± 12	6.8 ± 0.4	141 ± 5	2.32 ± 0.02	0.049 ± 0.002	11.5	–
Well #2	219 ± 9	4.8 ± 0.3	96 ± 4	2.28 ± 0.03	0.049 ± 0.002	7.8	–
Well #3	177 ± 13	4.3 ± 0.5	74 ± 6	2.38 ± 0.07	0.058 ± 0.006	6.0	–
Well #4	193 ± 27	3.9 ± 1.0	82 ± 12	2.36 ± 0.13	0.047 ± 0.010	6.7	–
Well #5	206 ± 8	4.3 ± 0.3	86 ± 4	2.39 ± 0.03	0.050 ± 0.002	7.0	0.19 ± 0.01
Well #7	330 ± 18	10.0 ± 0.9	145 ± 8	2.27 ± 0.02	0.069 ± 0.002	11.8	0.22 ± 0.04
Well #8	310 ± 56	9 ± 7	135 ± 6	2.3 ± 0.4	0.07 ± 0.05	11.0	0.24 ± 0.08
Well #9	412 ± 20	7.9 ± 0.8	167 ± 8	2.47 ± 0.03	0.048 ± 0.002	13.6	0.17 ± 0.05
Degelen Base:							
Well #10	4653 ± 210	63 ± 4	1175 ± 50	3.96 ± 0.02	0.054 ± 0.003	95.5	0.12 ± 0.02
Tailan:							
Well #12	309 ± 60	7 ± 3	146 ± 29	2.11 ± 0.13	0.047 ± 0.012	11.9	0.23 ± 0.06
Well #13	291 ± 11	6.6 ± 0.4	128 ± 5	2.27 ± 0.02	0.052 ± 0.002	10.4	0.15 ± 0.03
Shurek:							
Well #14	307 ± 31	11 ± 2	213 ± 22	1.44 ± 0.04	0.053 ± 0.005	17.3	1.9 ± 0.2
Well #24	310 ± 18	9.5 ± 1.2	150 ± 10	2.07 ± 0.05	0.064 ± 0.006	12.2	0.4 ± 0.1

Although only a few streams were analysed, total uranium concentrations in these surface waters (Table 11) were similar to those recorded in well waters, the sole exception, not unexpectedly, being a drainage stream flowing from a now ‘sealed’ test tunnel in the Degelen Mountains (Sample #22), where the recorded concentration was at least a factor of five higher. The lowest uranium concentration recorded, at $1.1 \mu\text{g(U) l}^{-1}$, was in a sample taken from the Irtysh River.

Uranium concentrations in natural surface waters has been show to vary widely over four orders of magnitude, from 0.01 to $100 \mu\text{g(U) l}^{-1}$ (Osmond and Ivanovich, 1992). This variation has been attributed, at least in part, to its varied chemical behaviour under different redox conditions. Under reducing conditions, uranium has a +4 valency and is virtually insoluble, while under oxidising conditions, it has a +6 valency and forms readily soluble anionic complexes. Most surface waters are oxidising, and therefore uranium behaves as a conservative constituent. The wide range of uranium concentrations observed are the result of the mixing of various source waters, some of which were originally reducing and barren (Osmond and Ivanovich, 1992).

$^{234}\text{U}/^{238}\text{U}$ activity ratios in natural surface waters are also variable, with values ranging from nearly 1.0 to about 2.0 (Figure 48). The observed variation, however, is considerably less than that found in groundwaters, where $^{234}\text{U}/^{238}\text{U}$ activity ratios as high as 29 have been reported (Osmond and Cowart, 1976). This is because most surface waters are mixtures of runoff and diverse groundwater sources. In the samples analysed, $^{234}\text{U}/^{238}\text{U}$ activity ratios for the Uzun-Bulak stream and the Chagan River, with values between 1.8 and 1.9 (Table 11), were in the upper part of this range, showing a considerable degree of disequilibrium. The departure from equilibrium is largely determined by the degree of soil weathering for the river in question. For rivers where intensive weathering takes place, the $^{234}\text{U}/^{238}\text{U}$ activity ratio of the leached uranium tends to the equilibrium value of unity, while in rivers where leaching is less dominant, such as in arid regions, the activity ratio generally shows higher values, reflecting the relative importance of recoil fractionation over gross leaching in less intensively weathered soils (Osmond and Ivanovich, 1992). Our measured ratios suggest that, for the rivers studied, recoil fractionation is dominant over leaching.

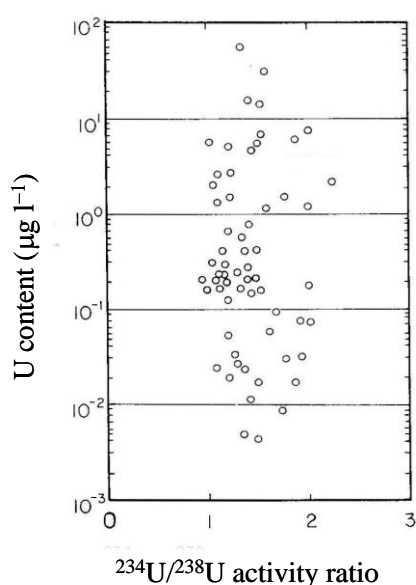


Figure 48. $^{234}\text{U}/^{238}\text{U}$ activity ratios in surface waters (Osmond and Ivanovich, 1992)

Table 11. Uranium concentrations ($\pm 2\sigma$) in filtered ($<0.45 \mu\text{m}$) waters collected in streams and lake craters from the Sarzhal region of the Semipalatinsk nuclear test site (July 2001)

Sample	Concentration (mBq l ⁻¹)			²³⁴ U/	²³⁵ U/	U ($\mu\text{g l}^{-1}$)	% U Particulate
	²³⁴ U	²³⁵ U	²³⁸ U	²³⁸ U	²³⁸ U		
Streams:							
Uzun-Bulak stream #19	215 ± 12	5.0 ± 0.7	118 ± 5	1.82 ± 0.07	0.042 ± 0.006	9.6	0.7 ± 0.1
Chagan River #20	266 ± 8	7.3 ± 0.3	140 ± 4	1.89 ± 0.01	0.052 ± 0.002	11.4	58 ± 2
Degelen Tunnel #22	1671 ± 80	32 ± 3	645 ± 32	2.59 ± 0.04	0.049 ± 0.003	52.4	–
Irtish River #11	39 ± 2	0.97 ± 0.16	13.0 ± 0.7	3.0 ± 0.1	0.074 ± 0.010	1.1	1.4 ± 0.6
Tel'kem 1:							
Bottom #15	923 ± 16	45.0 ± 1.4	744 ± 12	1.24 ± 0.01	0.061 ± 0.001	60.6	–
Surface #16	607 ± 26	30 ± 3	482 ± 22	1.26 ± 0.03	0.062 ± 0.006	39.2	–
Tel'kem 2:							
Bottom #17	2316 ± 70	85 ± 4	629 ± 18	3.68 ± 0.04	0.135 ± 0.004	51.8	–
Surface #18	2237 ± 95	82 ± 6	627 ± 28	3.56 ± 0.06	0.131 ± 0.008	51.6	–

In the drainage stream flowing from a tunnel in the Degelen Mountains (sample #22), a $^{234}\text{U}/^{238}\text{U}$ activity ratio of ~ 2.6 was recorded, which is similar to that found in wells from the Sarzhal region. The fact that the stream arises from a localised source, as opposed to being a combination of different sources, may account for this enhanced ratio. More difficult to explain is the even higher ratio measured for the Irtysh River water sample which, with a much larger flow than the Chagan River or the Uzun-Bulak stream, could be expected to display $^{234}\text{U}/^{238}\text{U}$ activity ratios closer to equilibrium than those measured in these two sources. A contribution of enriched uranium from one or more of the tests carried out at the STS, as evidenced by the enhanced $^{235}\text{U}/^{238}\text{U}$ activity ratio measured in this sample, could account for this higher-than-expected ratio.

Regarding the association to solid phases, while the percentage of uranium associated with suspended particulate was very small ($<1\%$) in the case of the Uzun-Bulak stream (sample #19), the corresponding figure for the Chagan River (sample #20) was much higher ($\sim 60\%$). This high percentage, however, is not unusual, as it has been reported that a significant proportion of uranium in rivers can be transported in association with suspended particles and colloids (Martin and Whitfield, 1983). Recent studies carried out in the Kalix River, northern Sweden, for example, have shown that uranium transport by this river into the Baltic is dominated by uranium sorbed to iron oxyhydroxides and biogenic particles which are $>0.45\ \mu\text{m}$ in size (Porcelli *et al.*, 1997; Andersson *et al.*, 1998).

Concentrations in waters sampled at the Tel'kem 1 and Tel'kem 2 atomic craters, at $39\text{--}61\ \mu\text{g}(\text{U})\ \text{I}^{-1}$, were also about five times higher than those recorded in well waters (Table 11). Significantly, the $^{235}\text{U}/^{238}\text{U}$ activity ratio at Tel'kem 2 was double that recorded elsewhere, suggesting that the plutonium-fuelled nuclear devices used to create the crater may also have contained considerable quantities of enriched uranium. The much higher (factor of three) $^{234}\text{U}/^{238}\text{U}$ activity ratio in Tel'kem 2 waters compared with Tel'kem 1 is consistent with this contention, as is the presence of uranium in some of the radioactive particles isolated from this site (WP2 – Figure 10). It would appear that the nature of the devices detonated there were not identical to the single device detonated at Tel'kem 1, contrary to what has been implied in the literature.

Transuranium levels and isotopic ratios in waters of the STS

Concentrations of ^{238}Pu , $^{239,240}\text{Pu}$ and ^{241}Am , together with relevant isotopic ratios, in filtered water samples collected from wells in the village of Sarzhal, the Degelen military base, and the Tailan and Shurek farms, are given in Table 12.

Concentrations of $^{239,240}\text{Pu}$ in the wells analysed were in the range $0.7\text{--}99\ \text{mBq}\ \text{I}^{-1}$, with a median concentration of $4.6\ \text{mBq}\ \text{I}^{-1}$. In radiological terms, these levels are very low, being well within the WHO's guideline level for ^{239}Pu or ^{240}Pu content in drinking water of $1000\ \text{mBq}\ \text{I}^{-1}$ (WHO, 2003); nevertheless, they are some two or three orders of magnitude higher than the levels in drinking water normally associated with global fallout in the Northern Hemisphere (ca. $10\text{--}50\ \mu\text{Bq}\ \text{I}^{-1}$). Suspended particulate $^{239,240}\text{Pu}$ concentrations were also very low, though they varied considerably (median: $0.08\ \text{mBq}\ \text{I}^{-1}$, 95% confidence interval: $0.05\text{--}0.52$). In percentage terms, the fraction of $^{239,240}\text{Pu}$ associated with particulate material represented between $0.2\text{--}36\%$ of the total $^{239,240}\text{Pu}$ concentration.

Table 12. Transuranium concentrations ($\pm 2\sigma$) in filtered ($<0.45 \mu\text{m}$) waters collected in wells from the Sarzhal region of the Semipalatinsk nuclear test site (July 2001)

Sample	Concentration (mBq l^{-1})			$^{238}\text{Pu}/$	$^{241}\text{Am}/$	%Pu(IV) in filtrate	%Pu Particulate	%Am Particulate
	^{238}Pu	$^{239,240}\text{Pu}$	^{241}Am	$^{239,240}\text{Pu}$	$^{239,240}\text{Pu}$			
Sarzhal:								
Well #1	0.11 ± 0.02	3.8 ± 0.2	0.15 ± 0.05	0.030 ± 0.004	0.039 ± 0.013	33	–	–
Well #2	0.10 ± 0.02	2.9 ± 0.2	0.04 ± 0.02	0.035 ± 0.007	0.014 ± 0.007	55	–	–
Well #3	2.0 ± 0.2	63 ± 4	10.3 ± 0.6	0.032 ± 0.003	0.163 ± 0.014	90	–	–
Well #4	3.8 ± 0.2	99 ± 5	87 ± 18	0.038 ± 0.001	0.9 ± 0.2	–	–	–
Well #5	0.14 ± 0.05	4.5 ± 0.4	<0.1	0.031 ± 0.010	<0.02	78	12.5 ± 1.5	–
Well #6	0.60 ± 0.04	46 ± 2	2.3 ± 0.1	0.0130 ± 0.0008	0.050 ± 0.003	–	0.18 ± 0.04	0.6 ± 0.2
Well #7	0.08 ± 0.01	3.0 ± 0.1	0.24 ± 0.03	0.027 ± 0.004	0.080 ± 0.010	–	36 ± 1	–
Well #8	0.37 ± 0.04	16.5 ± 0.6	0.84 ± 0.06	0.022 ± 0.002	0.051 ± 0.004	–	0.39 ± 0.09	<2
Well #9	–	0.7 ± 0.1	<0.3	–	–	–	1.8 ± 1.0	–
Degelen Base:								
Well #10	0.03 ± 0.01	0.67 ± 0.07	–	0.04 ± 0.02	–	–	7 ± 3	–
Tailan:								
Well #12	1.5 ± 0.1	98 ± 5	1.33 ± 0.08	0.015 ± 0.001	0.014 ± 0.001	97	–	25 ± 2
Well #13	0.21 ± 0.03	5.0 ± 0.3	0.16 ± 0.02	0.043 ± 0.006	0.032 ± 0.004	86	7.3 ± 0.8	<11
Shurek:								
Well #14	0.06 ± 0.02	1.1 ± 0.1	0.36 ± 0.04	0.05 ± 0.02	0.33 ± 0.05	53	24 ± 5	14 ± 2
Well #24	0.09 ± 0.04	4.6 ± 0.4	–	0.020 ± 0.008	–	–	1.1 ± 0.6	–

The mean $^{238}\text{Pu}/^{239,240}\text{Pu}$ activity ratio in filtered well waters, at 0.031, is similar to the ratio recorded for cumulative global fallout in the Northern Hemisphere; however, it shows considerable scatter (extreme range: 0.01–0.05), in contrast to the global fallout ratio, and is undoubtedly dominated by the influence of local sources, i.e., test site plutonium, as evidenced by the elevated levels of the latter in these waters. $^{238}\text{Pu}/^{239,240}\text{Pu}$ activity ratios in waters from wells in the village of Sarzhal are somewhat higher than those reported by Yamamoto *et al.* (1998) for soil samples collected within the village and its surroundings (mean: 0.009; extreme range: 0.005–0.013; $n = 7$), but are in good agreement with $^{238}\text{Pu}/^{239,240}\text{Pu}$ activity ratios measured by the same authors in soils from the Degelen Mountains and Balapan (mean: 0.025 ; extreme range: 0.016–0.037; $n = 6$).

In all the wells, ^{241}Am concentrations (Table 12) were lower, and in most cases much lower, than the corresponding $^{239,240}\text{Pu}$ concentrations. They were also some orders of magnitude inferior to the WHO's guideline level for ^{241}Am of 1000 mBq l^{-1} (WHO, 2003). The percentage of ^{241}Am in particulate form was similar to that observed for Pu, being between 0.6 and 25%. $^{241}\text{Am}/^{239,240}\text{Pu}$ activity ratio in filtered waters varied by more than one order of magnitude, with a median value of 0.05 (extreme range: 0.014–0.9).

Concentrations of ^{238}Pu , $^{239,240}\text{Pu}$ and ^{241}Am , together with relevant isotopic ratios, in filtered water samples collected from streams within the test site and from the Irtys River are given in Table 13. Measured $^{239,240}\text{Pu}$ concentrations (0.6–30 mBq l^{-1}) were broadly similar to those measured in well waters, with the highest level recorded in a sample collected from the Chagan River, some 15 km north of Sarzhal. In the Uzun-Bulak stream running eastwards from the Degelen Mountains onto the study area, the corresponding plutonium concentration was much lower, at 0.6 mBq l^{-1} . Similarly, and perhaps surprisingly, the concentration in the stream running out of the above-mentioned Degelen Mountains test tunnel was also low, at 2.0 mBq l^{-1} .

While the $^{238}\text{Pu}/^{239,240}\text{Pu}$ ratio in the Chagan River, at ~0.05, was close to those measured in wells from the Sarzhal region, higher values were found for the Uzun-Bulak stream and the drainage stream running out of the Degelen Mountains, possibly reflecting the ratios characterising underground tests carried out in this area. A relatively high $^{238}\text{Pu}/^{239,240}\text{Pu}$ ratio (~0.15) was also recorded for the sample of water originating in Area 10 of the Irtys River, indicating the presence of a source-term other than generalised global fallout.

$^{239,240}\text{Pu}$ concentrations in filtered water from the Tel'kem 1 and Tel'kem 2 atomic craters, in the range 59–135 mBq l^{-1} , were somewhat higher than those recorded in well and stream waters (Table 13). Some differentiation between plutonium (and uranium) levels in top waters at Tel'kem 1 was evident, though this was not apparent at Tel'kem 2. The $^{238}\text{Pu}/^{239,240}\text{Pu}$ activity ratios in the waters of both craters were indistinguishable statistically, being in the range 0.017–0.024; however, they were slightly higher than the ratios measured in ejected spoil (rubble) and sediment collected at both sites in the course of the same sampling campaign (mean: 0.014; 95% confidence interval: 0.013–0.015; $n = 8$) (see WP3). Although the reason for this difference remains unclear, it probably reflects the contribution of a separate source-term, characterised by a slightly higher $^{238}\text{Pu}/^{239,240}\text{Pu}$ ratio, and the insolubility of the plutonium in Tel'kem 2, which has been shown to be in a highly refractory form (see WP3).

Table 13. Transuranium concentrations ($\pm 2\sigma$) in filtered ($<0.45 \mu\text{m}$) waters collected in streams and lake craters from the Sarzhal region of the Semipalatinsk nuclear test site (July 2001)

Sample	Concentration (mBq l^{-1})			$^{238}\text{Pu}/$	$^{241}\text{Am}/$	%Pu(IV) in filtrate	%Pu Particulate	%Am Particulate
	^{238}Pu	$^{239,240}\text{Pu}$	^{241}Am	$^{239,240}\text{Pu}$	$^{239,240}\text{Pu}$			
Streams:								
Uzun-Bulak stream #19	0.06 ± 0.02	0.57 ± 0.05	0.056 ± 0.008	0.11 ± 0.03	0.10 ± 0.02	46	1.6 ± 0.7	–
Chagan River #20	1.46 ± 0.09	29.5 ± 1.4	0.86 ± 0.06	0.049 ± 0.003	0.029 ± 0.002	92	0.07 ± 0.03	4 ± 1
Degelen Tunnel #22	0.82 ± 0.13	2.0 ± 0.2	<0.1	0.42 ± 0.07	<0.05	62	–	–
Irtys River #11	0.31 ± 0.04	2.0 ± 0.2	–	0.15 ± 0.02	–	–	1.9 ± 0.5	–
Tel'kem 1:								
Bottom #15	2.5 ± 0.4	135 ± 6	0.56 ± 0.12	0.018 ± 0.003	0.0041 ± 0.0009	93	–	–
Surface #16	1.7 ± 0.2	100 ± 4	0.85 ± 0.14	0.017 ± 0.002	0.0085 ± 0.0014	98	–	–
Tel'kem 2:								
Bottom #17	1.4 ± 0.3	60 ± 3	0.49 ± 0.11	0.024 ± 0.005	0.008 ± 0.002	97	–	–
Surface #18	1.2 ± 0.2	59 ± 2	<0.1	0.020 ± 0.003	<0.002	89	–	–
Surface #A [†]	6.9 ± 0.4	510 ± 14	47 ± 2	0.0135 ± 0.0009	0.092 ± 0.005	–	–	–
Balapan Lake:								
Surface #D [†]	< 0.03	0.80 ± 0.08	–	–	–	–	–	–

[†] Unfiltered sample collected in July 2000

$^{241}\text{Am}/^{239,240}\text{Pu}$ activity ratios in filtered waters at the Tel'kem sites were <0.01 in all cases. These ratios are at least an order of magnitude lower than the ratios reported for spoil and sediment of about 0.1 by Jiménez Nápoles *et al.* (2004) and Priest *et al.* (2003), and reflect the lower soil-water distribution coefficient (K_d) of plutonium relative to americium.

Interestingly, the $^{238}\text{Pu}/^{239,240}\text{Pu}$ and $^{241}\text{Am}/^{239,240}\text{Pu}$ ratios recorded in a sample of unfiltered water collected at Tel'kem 2 in July 2000, which showed plutonium concentrations five times higher than those measured in filtered waters at the same location in July 2001 (Table 13), were identical to those measured in the soil and sediments, reflecting the contribution of resuspended particles to the total measured activity.

Although $^{239,240}\text{Pu}$ concentrations in Tel'kem 1 and Tel'kem 2 waters were relatively high, the corresponding concentration in a sample of unfiltered water collected from a borehole (Sample #B) located approximately 200 m from the Tel'kem 2 crater was much lower, at $0.80 \pm 0.04 \text{ mBq l}^{-1}$; this is at the lower end of the plutonium concentrations recorded in wells in the study area. If confirmed by further measurements, it would suggest that the influence of these craters on plutonium concentrations in the surrounding water table is rather limited.

The concentration of $^{239,240}\text{Pu}$ in a sample of unfiltered water collected from the shore of Lake Balapan (Atomic Lake) in July 2000, at 0.8 mBq l^{-1} , was much lower than in the samples from the Tel'kem sites. The $^{238}\text{Pu}/^{239,240}\text{Pu}$ ratio for this sample, at <0.04 , is at least an order of magnitude lower than that measured in soils and sediments from the lake, at ~ 0.4 (Yamamoto *et al.*, 1996a; 1996b; Jiménez Nápoles *et al.*, 2004 – see Table 6). The low plutonium concentration recorded in the water, together with the low activity ratio, again is likely to reflect the nature of the plutonium present in the ejected spoil (rubble), the bulk of which ($>95\%$) has been shown to be in a highly refractory, insoluble form (Figure 42).

Oxidation state distribution of plutonium in ground and surface waters of the STS

The percentages of oxidised plutonium in well, stream and lake waters from the Semipalatinsk nuclear test site are given in Tables 12 and 13. The results obtained for well and stream waters show considerable variation in the amount of $^{249,240}\text{Pu}$ in a reduced form, with values ranging from as much as 97% in a farm well (#12) at Tailan, situated between Tel'kem and Sarzhal, to as little as 33% in a well (#1) in Sarzhal, with an overall mean of 69% (95% confidence interval: 53–85%; $n = 10$). At both Tel'kem 1 and Tel'kem 2, the proportion in a reduced form was even higher, at 89–98%. It is likely that the reason for such large percentages of plutonium in a reduced form is the presence in most of the waters sampled of large amounts of dissolved and colloidal organic carbon, known to significantly increase the proportion of plutonium in reduced form in natural waters (Nelson *et al.*, 1987). A plot of the percentage of plutonium in an oxidised form versus $^{239,240}\text{Pu}$ concentrations (Figure 49) supports this contention, revealing a clear increase in the percentage of reduced plutonium with increasing concentrations. The occurrence of higher-than-normal dissolved plutonium concentrations in environments containing elevated dissolved organic matter, linked to the formation of Pu(III) organic complexes, is well documented. It is also noteworthy that the cratering explosions at Tel'kem took place in shallow boreholes drilled into sandstone containing large amounts of organic compounds (Izrael, 2002).

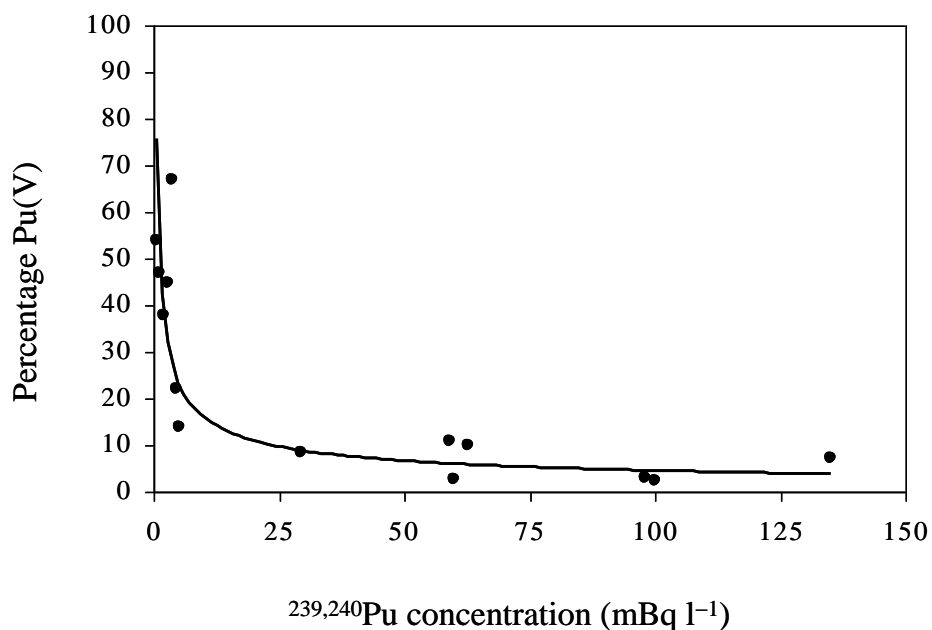


Figure 49. Percentage of oxidised plutonium versus $^{239,240}\text{Pu}$ concentrations in ground and surface waters from the STS

Mayak PA (Russia)

As discussed in WP3, a representative selection of samples collected in 1996 from Reservoir 11 and the Asanov Swamp in the vicinity of Mayak were taken from an extensive sample bank and, following radiochemical separation and purification, characterised in terms of actinide isotopic signatures using accelerator mass spectrometry. Details of the water and biota samples analysed are given in Table 7. The freshwater biota samples included pike (*Esox lucius*, order Esociformes, family Esocidae) and roach (*Rutilus sp.*, order Cypriniformes, family Cyprinidae). Pike are carnivorous fish that inhabit brackish and freshwaters in the northern hemisphere. They feed mainly on fish, but water voles and ducklings are also known to be potential prey. Pikes can grow to a relatively large size, with specimens measuring up to 150 cm in length and weighing 25 kg. The samples of pike fillet and bone analysed came from one fish caught in Reservoir 11 (weight 1.7 kg, length 65 cm). Roach inhabit slow flowing or still, muddy waters. They are abundant in rivers, lakes, canals and reservoirs, and can thrive in poor quality, even polluted water. Being omnivorous, they feed on insects, crustaceans, molluscs and plants, though adults prefer to feed on plants. Roach can grow to a length of about 50 cm and weigh 2 kg. Sample 6014 contained ash from five whole roach mixed into one sample. Sample 6009 was of thin-shelled freshwater mussel (*Anodonta sp.*, order Unionoida, family Unionidae). These filter-feeding freshwater bivalves inhabit rivers and lakes, preferring areas with low flow and soft sediments. The sample matrix analysed contained two ashed mussels mixed into one sample. Vegetation samples included water plants from the carrot family (Apiaceae) and from the rush family (Juncaceae).

The activity concentrations of plutonium, together with the corresponding $^{240}\text{Pu}/^{239}\text{Pu}$ atom ratios for the samples analysed are given in Table 14. The measured $^{240}\text{Pu}/^{239}\text{Pu}$ atom ratios in

the two water plants collected from the Asanov Swamp were in good agreement with the ratios obtained for grass and soil samples from the same location (Table 8), and are indicative of contamination by weapons-grade plutonium. The $^{240}\text{Pu}/^{239}\text{Pu}$ ratio in water from the swamp could not be determined, as ^{240}Pu was not detectable in the small sample available (~250 ml).

Table 14. Plutonium activity concentrations ($\pm 2\sigma$) and $^{240}\text{Pu}/^{239}\text{Pu}$ atom ratios ($\pm 2\sigma$) in aquatic samples collected in the Asanov Swamp region and in Reservoir 11, Mayak PA

Id. No.	Matrix	Location	Concentration (mBq kg ⁻¹)		$^{240}\text{Pu}/^{239}\text{Pu}$ (atom ratio)
			^{239}Pu	^{240}Pu	
1532	Water	Reservoir 11	0.31 ± 0.08	0.09 ± 0.08	0.08 ± 0.06
1500	Water	Asanov Swamp	0.13 ± 0.08	ND	–
7013	Water plant	Asanov Swamp	1700 ± 70	190 ± 35	0.031 ± 0.004
7014	Water plant	Asanov Swamp	362 ± 30	36 ± 15	0.030 ± 0.008
6009	Mussel	Reservoir 11	1010 ± 40	1150 ± 80	0.301 ± 0.018
6010	Pike bone	Reservoir 11	12 ± 2	4 ± 2	0.09 ± 0.04
6011	Pike fillet	Reservoir 11	95 ± 6	6 ± 2	0.015 ± 0.004
6014	Roach	Reservoir 11	119 ± 6	44 ± 6	0.075 ± 0.008

The $^{240}\text{Pu}/^{239}\text{Pu}$ atom ratio in water from Reservoir 11, at 0.08 ± 0.06 (2σ) is lower than the corresponding value previously reported for the northern part of the reservoir (0.17 ± 0.06 ; Oughton *et al.*, 2000), although both values overlap within the uncertainties of the measurement. Biota samples collected in Reservoir 11 showed $^{240}\text{Pu}/^{239}\text{Pu}$ atom ratios varying from 0.015 to 0.30. Earlier studies (Oughton *et al.*, 2000) had shown that the $^{240}\text{Pu}/^{239}\text{Pu}$ atom ratios in the reservoir vary both spatially and vertically in the sediments, reflecting the influence from civil reprocessing in addition to discharges from the production of weapons-grade plutonium. The results obtained during the ADVANCE project confirm this observation.

The activity concentrations of uranium, together with relevant atom ratios for the water and biota samples are given in Table 15. The average $^{235}\text{U}/^{238}\text{U}$ atom ratio, at 0.0075 ± 0.0006 (2σ) is statistically indistinguishable from the ‘best estimate’ value of 0.00734 (extreme range: 0.00730–0.00737) reported for natural uranium world-wide (Holden, 1981). Nevertheless, the measurable quantities of ^{236}U in all samples revealed the presence of reprocessed material. The $^{236}\text{U}/^{235}\text{U}$ atom ratios in water and plants from the Asanov Swamp varied between 0.0005 and 0.0014. These low ratios are similar to those measured in grass and soil samples from the same area (see Table 9), and again suggest the influence of low burn-up material due to early emission from the Mayak complex. In Reservoir 11, on the other hand, $^{236}\text{U}/^{235}\text{U}$ atom ratios varied between 0.002 and 0.015, possibly signifying a mixture of old, low burn-up, reprocessed material, with more modern, higher burn-up material from the reprocessing of civil fuel. Concentration factors derived from the data in Table 14 varied from a minimum of 5.6 ± 1.6 (2σ) for the rush (Juncaeeae) sample collected in the Asanov Swamp to a maximum of 106 ± 30 (2σ) for the roach sample collected in Reservoir 11, with the rest of the samples displaying values closer to the lower end of the range.

Table 15. Uranium activity concentrations and relevant atom ratios in aquatic samples collected in the Asanov Swamp region and Reservoir 11, Mayak PA

Id.	Sample	Location	Concentration (mBq kg ⁻¹)			Atom ratios	
			²³⁵ U	²³⁶ U	²³⁸ U	²³⁵ U/ ²³⁸ U	²³⁶ U/ ²³⁵ U
1532	Water	Reservoir 11	0.41	0.17	8.79	0.0079	0.0019
1500	Water	Asanov Swamp	0.38	0.022	7.56	0.0073	0.0014
7013	Water plant	Asanov Swamp	6.4	0.13	137	0.0074	0.0007
7014	Water plant	Asanov Swamp	2.10	0.031	<i>NM</i>	–	0.0005
6009	Mussel	Reservoir 11	19.8	9.1	390	0.0080	0.015
6010	Pike bone	Reservoir 11	5.2	2.0	10.7	0.0076	0.013
6011	Pike fillet	Reservoir 11	7.4	1.7	158	0.0074	0.007
6014	Roach	Reservoir 11	42.9	14.4	938	0.0072	0.011

AMS measurements for ⁹⁹Tc enabled the calculation of CFs values for this radionuclide. Measured ⁹⁹Tc activity concentrations ranged from 0.22 to 270 Bq kg⁻¹ (Table 16). The corresponding concentration factors varied between ~90 for the rush sample collected in the Asanov Swamp to ~400 for the roach sample collected in Reservoir 11 which, as in the case of uranium, showed the highest CF.

Table 16. ⁹⁹Tc activity concentrations ($\pm 2\sigma$) in aquatic samples collected in the Asanov Swamp region and Reservoir 11, Mayak PA

Id	Sample	Location	⁹⁹ Tc (Bq kg ⁻¹)
1532	Water	Reservoir 11	0.65 \pm 0.13
1500	Water	Asanov Swamp	0.22 \pm 0.04
7013	Water plant	Asanov Swamp	20 \pm 4
7014	Water plant	Asanov Swamp	42 \pm 8
6009	Mussel	Reservoir 11	70 \pm 15
6010	Pike bone	Reservoir 11	64 \pm 13
6011	Pike fillet	Reservoir 11	60 \pm 12
6014	Roach	Reservoir 11	270 \pm 50

Radionuclide concentrations in groundwater from Mayak had been determined in a previous study (Oughton *et al.*, 1999). Data obtained during field-work carried out in 1994 showed radionuclide concentrations in these waters ranged from 0.2–1.2 kBq l⁻¹ (⁹⁰Sr), 1–10 kBq l⁻¹ (⁹⁹Tc), 3–9 kBq l⁻¹ (⁶⁰Co), 20–400 Bq l⁻¹ (¹³⁷Cs) and 1–20 Bq l⁻¹ (α -emitting Pu). The fractionation of these radionuclides between the dissolved, colloidal and particulate phases was also examined using a combination of microfiltration and ultrafiltration techniques. The results showed that ~65% of the ^{239,240}Pu, 40% of the ¹³⁷Cs, and 10–15% of the ⁶⁰Co, ⁹⁰Sr and ⁹⁹Tc were present in the solid phase (defined as the sum of the colloidal and particulate fractions) (Figure 50). The observed colloidal association may play an important role in the transport of these radionuclides to groundwater. It is recommended that further attention to

the behaviour of colloiddally-bound radionuclides be paid in future studies of contaminated terrestrial ecosystems, especially in the case of plutonium.

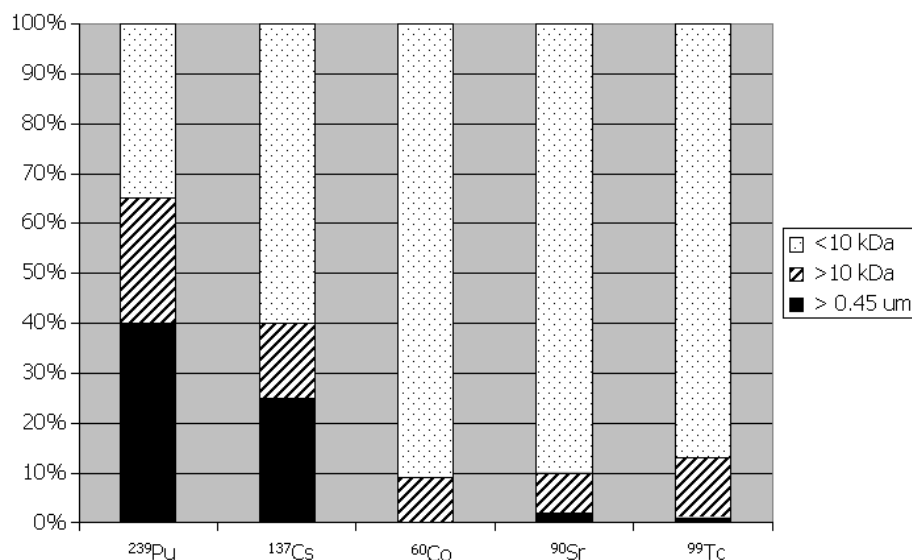


Figure 50. Size fractionation of plutonium, radiocaesium, cobalt, strontium and technetium in a sample of ground water collected at Mayak in 1994, some 5 km SE of Lake Karachay

To evaluate the remobilisation potential of radionuclides associated with particles, contaminated sediments from Mayak were extracted with different reagents. Plutonium isotopes were found to be strongly associated with sediments, although to a lesser extent than ¹³⁷Cs. The strong association of radiocaesium in comparison with plutonium has been reported for other environments, and explained on the basis of the different mechanisms of sorption operating for both elements. Although some evidence of association with organic phases was found, more extraction data is needed to confirm this.

Improvement of migration models (Mayak)

Mathematical models may be used to predict the concentration of radionuclides with time and location following a radioactive discharge to a river system such as that close to the Mayak PA complex. In the course of the ADVANCE project, a dynamic one-dimensional model for the Techa-Iset-Tobol-Irtysh-Ob river system was developed and used to predict the dispersion of radionuclides in this system under different (hypothetical) scenarios. The model includes a mass balance of contaminants and solids in the riverine system, and combines a continuous numerical technique with a simplified numerical model. The approach adopted takes into account sedimentation and resuspension of sorbed radionuclides due to sediment movement, advection and dispersion of both sorbed and dissolved radionuclides due to sediment transport and water movement, and sedimentation of particulate contaminants (Figure 51).

The programme TORT (Techa-Ob-River-Transport) was written in Microsoft Visual Basic 5TM and is operated in a Microsoft WindowsTM (Windows 95, 98, NT4) environment, with data being stored in and drawn from a Microsoft AccessTM database. The programme was designed to be user-friendly. Its starting window is shown in Figure 52.

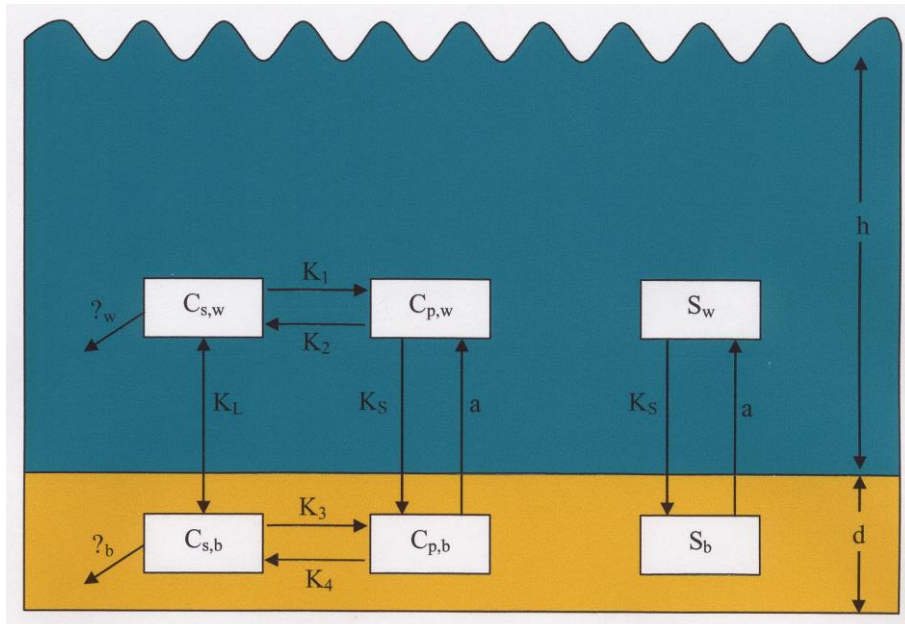


Figure 51. Schematic of reactions included in the TORT programme

The programme consists of three ‘blocks’, which can be described as follows:

1. Pre-processor: involving the interactive input of pre-formatted data or input from MS Access™ database (Figure 53).
2. Simulation: involving calculation of radionuclide transport within the river system. The results of the simulation are displayed on the screen in the dynamic mode as diagrams and output files on the hard disc. There is an option of pausing calculations for the assessment of intermediate results (Figures 54 and 55).
3. Post-processor: interactive post-processing of results in convenient tabular form or additional calculations on output data.



Figure 52. Start window of the programme

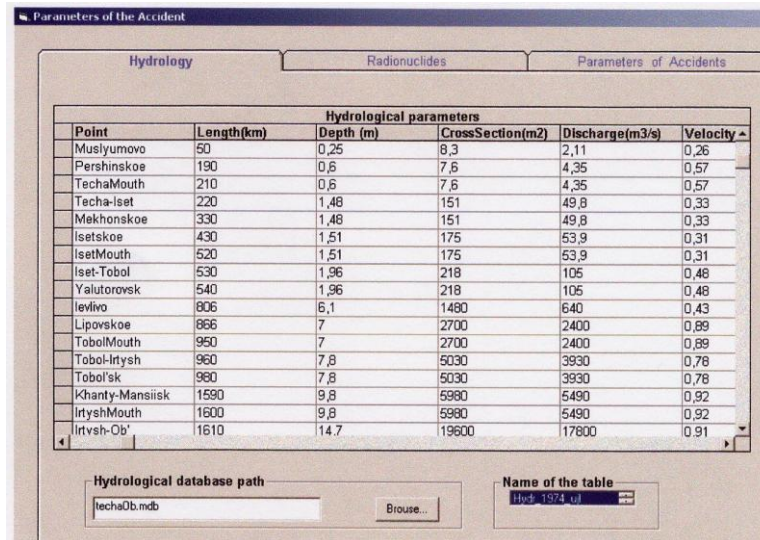


Figure 53. The interface for the input of hydrological parameters

Four different scenarios were considered in the programme's structure, namely (i) the controlled released of polluted waters from Reservoir 11 at Mayak as a measure to prevent the breakout of Dam 11 as a result of water rising above the maximum safe level; (ii) infiltration through Dam 11 and transport by bypass channels; (iii) accidental release of activity to the Asonov Swamp; and (iv) complete breakout of Dam 11.

A more detailed description of the environmental parameters specific to the Mayak site, the model development and its application to some of the above scenarios for specific radionuclides can be found in the document titled 'Influence of Site-Specific Information on Aquatic Modelling', submitted to the Commission as a deliverable of the project and appended at the end of this report.

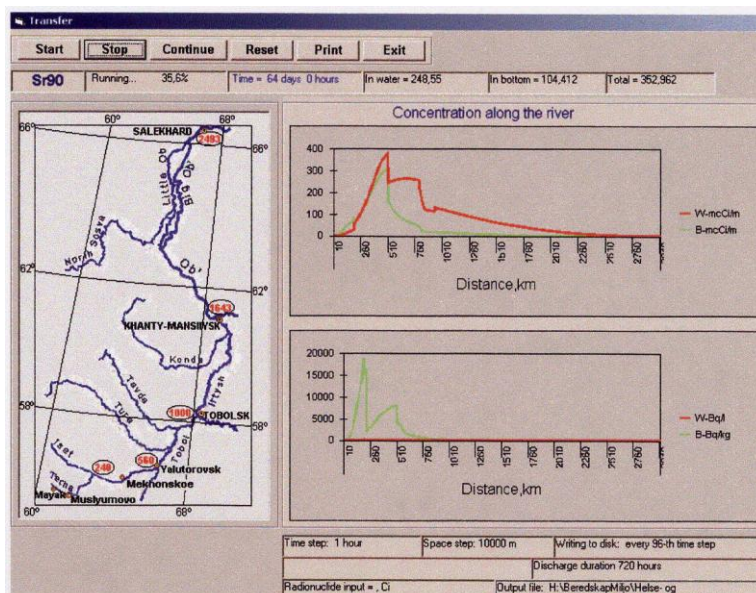


Figure 54. The simulation window.

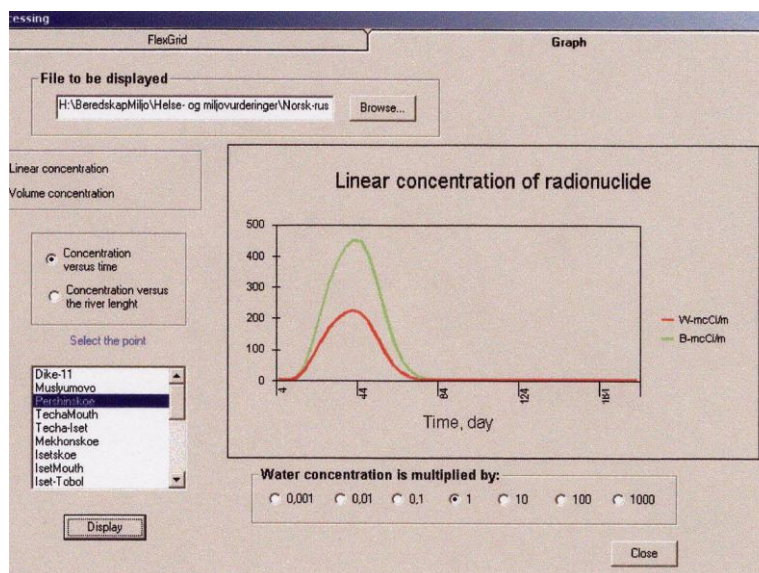


Figure 55. The results window showing the linear concentration of the Radionuclide considered for this particular simulation

As an illustration, model results obtained by running TORT in order to simulate the transport of ^{90}Sr along the Techa River system following a controlled discharge from Reservoir 11 are presented here. For the purposes of modelling, data on flow velocities, depths and other hydrological parameters for the Techa-Iset-Tobol-Irtysh-Ob river system, obtained in 1974, were used as input parameters. Although two different distribution coefficients are incorporated in the model, applicable to sediment-pore water and suspended particulate-water, respectively, the lack of data for the latter forced us to use a single value for the distribution coefficient in each section of the river system, based on sediment-water measurements carried out in the course of the Joint Norwegian-Russian Expedition (Table 17).

Table 17. Summary of distribution coefficient values for ^{90}Sr in the Techa-Ob river system (JNRG, 2004)

Section of the river system (period of measurement)	Range of values
Muslyumovo and upstream (1990–94)	165 – 310
Muslyumovo and upstream (1953)	360
Muslyumovo – Salekhard (1970–94)	8 – 250

The most sensitive parameters in determining radionuclide concentrations along the river system were found to be the thickness of the active sediment layer, d (see Figure 51), the sediment – water distribution coefficient, and the mass transfer coefficient between sediment and water, K_L (Figure 51). As no direct measurement of these parameters were available, simulation using values from partial databases (such as that in Table 17) or from data obtained in other river systems were employed to obtain a range of possible radionuclide concentrations in the different compartments. By taking into consideration the data of Table 17, concentration factors ranging from 100 to 350 were used for locations upstream of Muslyumovo (50 km from Reservoir 11), while values in the range 5 – 250 were used from

locations downstream of Muslyumovo, e.g. Pershinskoe (190 km from Reservoir 11), Techa mouth (210 km from Reservoir 11) and Mekhonskoe (330 km from Reservoir 11). Figure 56 shows the linear concentration of ^{90}Sr in sediments from the Techa mouth and Mekhonskoe as a function of the values used for the distribution coefficients (K_d) upstream of Muslyumovo and the location under consideration.

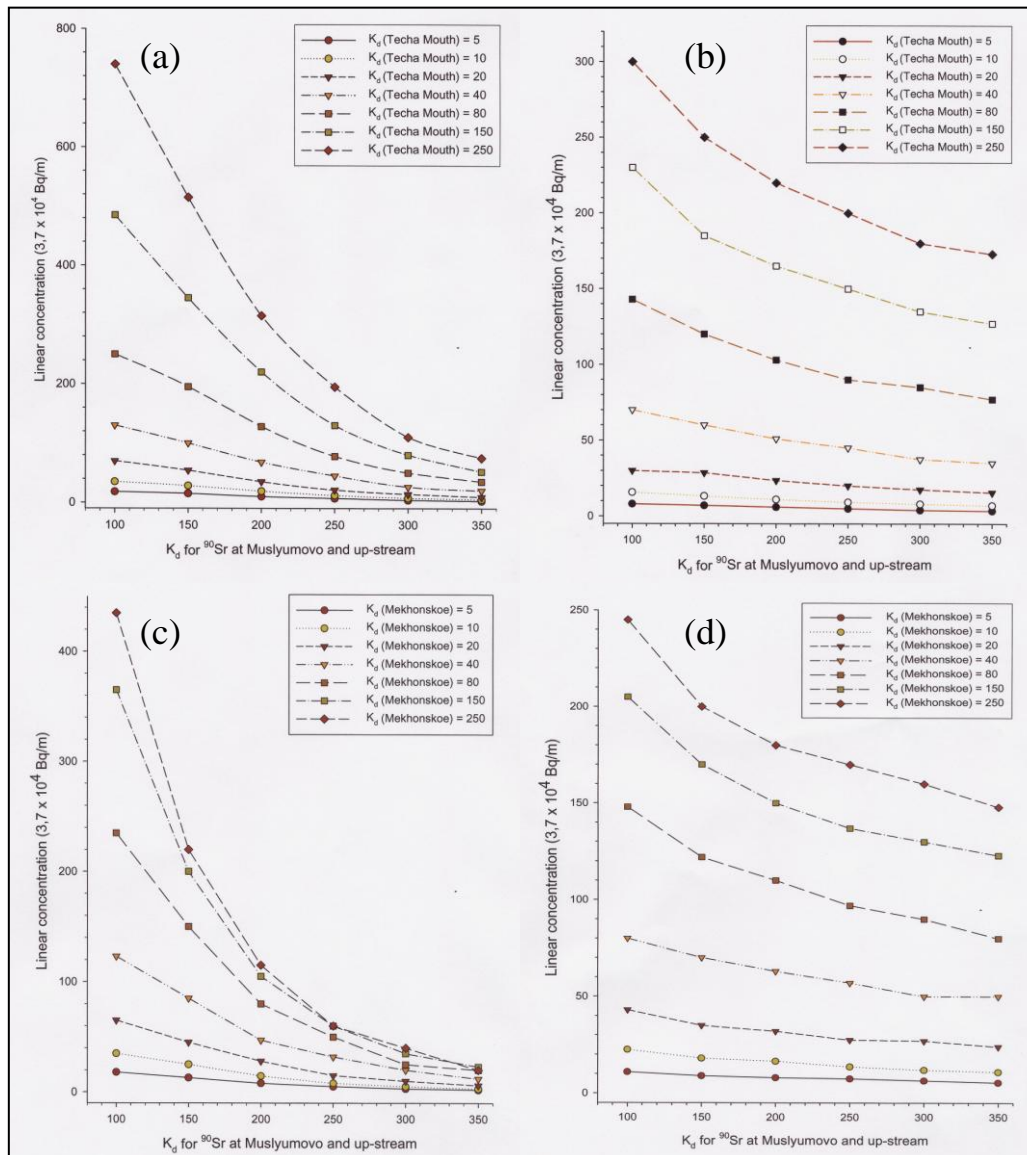


Figure 56. Simulated ^{90}Sr concentrations in bottom sediments of the Techa mouth and Mekhonskoe as a function of K_d upstream of the sampling location for different values of K_d at the two sampling locations. Plots (a) and (c) are calculated for a mass transfer coefficient (K_L) value of $10^{-5} \text{ m day}^{-1}$, while (b) and (d) are calculated for a K_L value of $10^{-6} \text{ m day}^{-1}$

The plots above clearly illustrate that the ^{90}Sr concentration in bottom sediments at any given location depends not only on the K_d value at that location, but also on those in previous sections of the river. In particular, it is shown that as the K_d value at the location is increased, concentrations in bottom sediments also increase, although in a non-linear manner. The opposite effect is observed with respect to the K_d in sections upstream of the location point,

with concentrations decreasing as the K_d value at locations upstream increases. For each location, two plots, each with a different value of the mass transfer coefficient, K_L , are given. The effect of this parameter, however, is not straightforward, and is closely linked to that of the K_d .

Figure 57 illustrates the profound effect that the mass transfer coefficient has on the radionuclide concentration sorbed to the sediments and on the time the radionuclide will remain in the sediment. If the mass transfer between the seabed sediment and the water column is rapid ($10^{-5} \text{ m day}^{-1}$), the shape of the radionuclide concentration in sediment in time is very similar to that of radionuclide concentrations in the water column (Figure 57a). The sediment is quickly affected by the contaminated water, but it also cleanses itself very rapidly by desorption/diffusion processes. On the other hand, if the mass transfer is slower ($10^{-7} \text{ m day}^{-1}$), then the sediment becomes contaminated quickly, but desorption/diffusion back to the water column is relatively slow (Figure 57b)

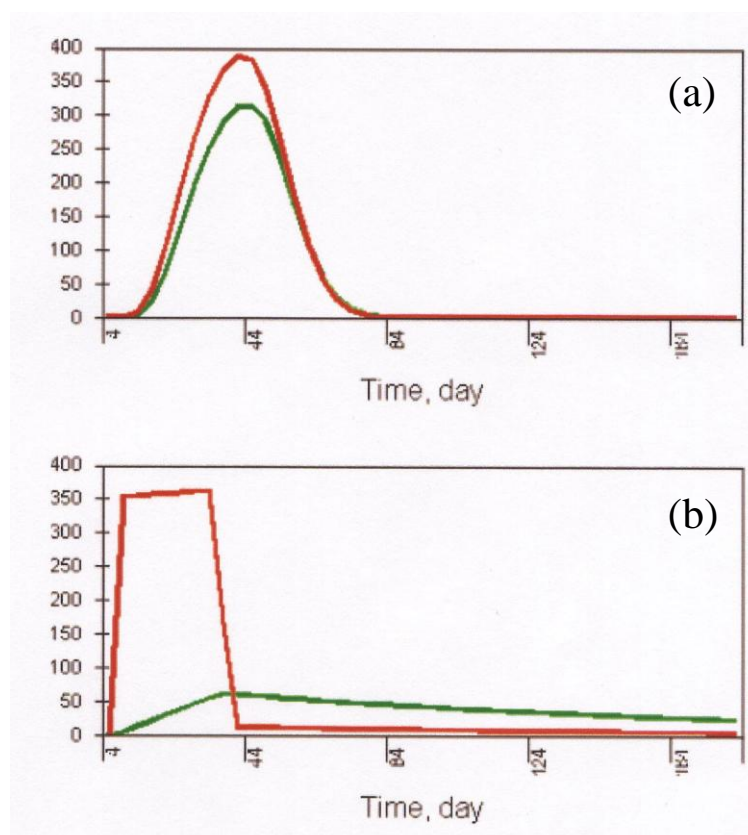


Figure 57. Linear concentration ($3.7 \times 10^4 \text{ Bq m}^{-1}$) of ^{90}Sr in sediments from the Techa mouth as a function of time, following a controlled discharge of contaminated water from Reservoir 11. (a) $K_L = 10^{-5} \text{ m day}^{-1}$; (b) $K_L = 10^{-7} \text{ m day}^{-1}$ (note: green line: water; red line: sediment)

The effect of the depth of the active sediment layer on simulated concentrations in seabed sediments is shown in Figure 58. It is clear from this figure that an increase in the depth of the active layer from 1 to 5 cm is accompanied by a decrease in sediment concentrations by a factor of almost exactly four.

The simulation runs, using the improved model describing the river system developed during the ADVANCE project, highlight the need to obtain site-specific parameters to reduce

uncertainties in the predictions. Clearly, model outputs will only be as good as the input parameters. The latter, in turn, have been shown in previous work-packages to vary with both source-term and environmental parameters. Model simulations should, therefore, be treated with caution, and efforts should be made, for a given scenario, to obtain site-specific information applicable to that particular case.

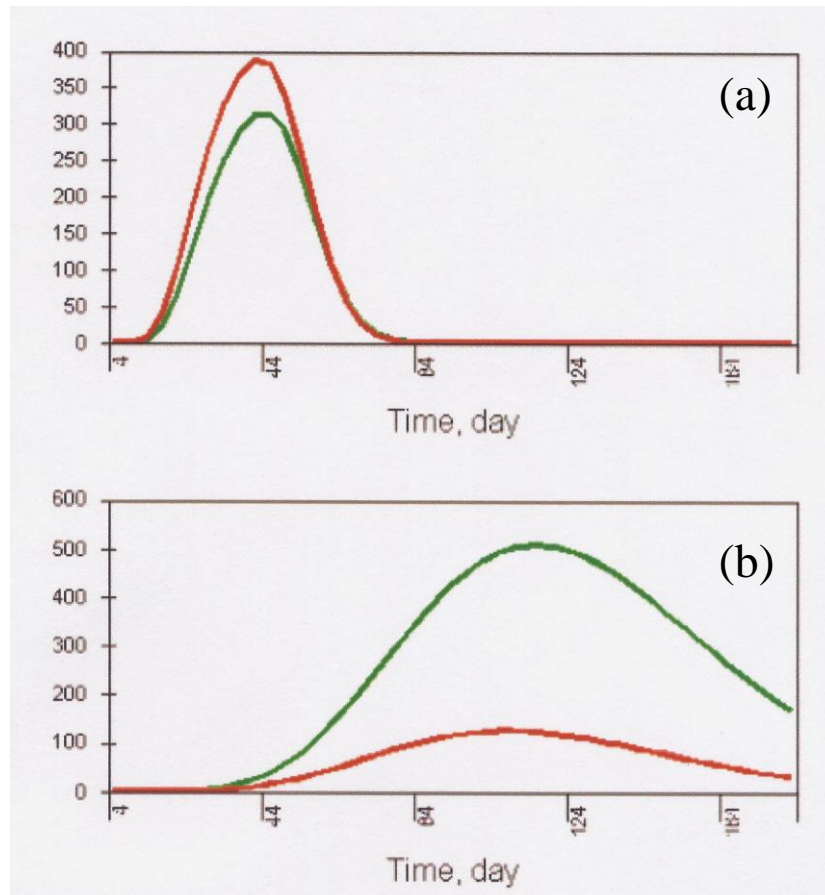


Figure 58. Linear concentration ($3.7 \times 10^4 \text{ Bq m}^{-1}$) of ^{90}Sr in sediments from the Techa mouth as a function of time, following a controlled discharge of contaminated water from Reservoir 11. (a) active sediment layer $d = 1 \text{ cm}$; (b) $d = 5 \text{ cm}$ (note: green line: water; red line: sediment)

WP5. Transfer processes in marine (saline) ecosystems

The main objective of this work-package was to identify factors influencing the transfer of actinides within marine ecosystems. This was achieved by the actinide analyses of environmental materials from different compartments in conjunction with a detailed programme of speciation analyses aimed at determining the key mechanisms governing the transfer between the different compartments. The main study site selected for this work-package was the vicinity of the Sellafield reprocessing plant in Cumbria (UK), where levels are sufficiently high to carry out this type of analyses. Work was also carried out in the Mediterranean Sea zone close to the Palomares area in order to assess the transfer of actinides from the accident area to the surrounding sea.

A significant effort in this work package was devoted during the first year of the project to the development of a meaningful, well-tested, sequential extraction analysis protocol for the

determination of the solid partitioning of actinides in sediments (both oxic and anoxic). The protocol adopted is based on the procedure proposed by Tessier *et al.* (1979) and partitions radionuclides into five operationally-defined geochemical fractions: exchangeable; acid-soluble; reducible; oxidisable and residual. The protocol was specifically modified to allow controlled dissolution of oxygen sensitive sulphide species in the first extraction step while preserving the reductive nature of the sediment during subsequent extractions (prior to the oxidisable extraction step). In addition, a complexing agent (sodium citrate) was employed to inhibit post extraction resorption, and stringent precautions were taken throughout to preserve the natural geochemical conditions of the sediment column.

A rigorous evaluation of the selectivity of the proposed scheme was undertaken to validate the efficacy of the protocol. The results of these experiments indicated that post-extraction resorption of plutonium in the course of sequential extraction analysis is greatly reduced by the addition of sodium citrate to each extractant. While no significant dissolution of any non-targeted geochemical phases was observed, it was clear, however, that plutonium bound to carbonate minerals can be solubilised during the exchangeable extraction due to ligand competition with sodium citrate. Nevertheless, although the data showed that the addition of sodium citrate does modify the selectivity of the protocol, on balance its use is to be recommended if resorption and redistribution are to be minimised.

The decision as to whether a chelating agent is used in a sequential extraction protocol should be governed by the objectives of the study. If the primary question concerns the determination of precise geochemical associations, rather than the simulation of actual environmental processes, the inclusion of such an agent is indicated as it facilitates the identification of those sediment phases with which plutonium is predominantly associated.

The development of the sequential extraction protocol and its application to Irish Sea sediments was done in close collaboration with another EC-funded programme (REMOTRANS). In the course of this programme, a sampling campaign, organised by the Institute de Radioprotection et de Surete Nucleaire (IRSN), was undertaken to the eastern Irish Sea (DIAPLU). The objectives of this sampling campaign were to (i) determine the solid partitioning of plutonium originally discharged to the northern-eastern Irish Sea from the Sellafield reprocessing plant in tidal and subtidal sediments from the Cumbrian area, and (ii) investigate the influence of pore-water chemistry and the development of anoxic conditions on the remobilisation of this element from sediments to the overlying water column. The main challenges faced by the participating laboratories were the recovery of high-quality sediment and pore-water samples, and the maintenance of anoxic conditions throughout the analytical processes employed. Sub-tidal sediment cores were retrieved using a modified FLUCHA box-corer from aboard the French research vessel *Côtes de la Manche* (INSU/CNRS). Sediment description and pH-EH profiling were performed onboard immediately after retrieval, and sub-cores taken for sedimentological and diagenetic studies. In the intertidal zones, cores were retrieved by driving PVC tubes into the sediment and excavating the surrounding sediment. Back in the (field) laboratory, sediment core extrusion and sectioning was carried out in an oxygen-free atmosphere under nitrogen, within a glove box specially designed for the purpose. The cores were sectioned at 2 cm intervals, an outer rind of sediment was removed to eliminate smear contamination, and the sediment placed in pore water squeezing pots. The pots were placed in a pneumatic squeezing rig, where porewater from each section was extruded and collected in 50 ml disposable plastic syringes. The pore water was then transferred to a separate nitrogen-filled glove box, where it was filtered (0.45 µm) in an inert (N₂) atmosphere and subdivided into aliquots prior to the

determination of the various pore water parameters referred to above. The squeezing pots were disassembled and the sediment immediately frozen inside heavy-duty plastic bags purged with nitrogen, for storage until further analysis by sequential extraction.

A number of parameters were determined for water samples (major and trace elements, sulphides, sulphates and dissolved organic carbon) as well as for sediments (some major and trace elements, particulate organic carbon, carbonate content, grain-size distribution, gamma-emitting radionuclides). Special attention was paid to the determination of acid-volatile sulphides (AVS) and chromium reducible sulphides (CRS), and to the solid partitioning of plutonium.

To illustrate, the results for a sediment core taken from a site (Stn. INT-010; 54° 20.35'N, 03° 24.09'W) in the intertidal reaches of the Esk Estuary, some 10 km south of Sellafield, are presented in this report. The sampling site was a non-vegetated area, located in the mid-region of a saltmarsh, away from any major edge features or creeks. Previous studies have shown that this site is geomorphologically stable, at least over periods of decades.

Grain size analysis indicated that the sediment was predominantly composed of silt (64–83%), with smaller quantities of sand (16–41%) and clay (8–11%). Although little variation in particle size was observed in the top 20 cm of the core, a layer containing an increased proportion of sand was evident between 20 and 34 cm. Loss on ignition data showed that the organic carbon content of these sediments was very low (<1.4% in all strata), though the uppermost layers exhibited the highest levels. On the other hand, the calcimetry data showed little variation in carbonate content (~ 6%) down the profile.

Field measurements of the redox potential in the interstitial pore water showed a rapid decrease in Eh with depth, with values changing from +45 mV at 1 cm to –350 mV at 24 cm and below, clearly reflecting the anoxic character of the subsurface sediment. A similar trend was observed for the pH profile, which relaxed smoothly from 7.3 at 1.0 cm to about 6.7 at 15 cm. Both Eh and pH measurements were carried out using well-calibrated microelectrodes.

A characteristic vertical and time-related redox reaction sequence was evident in the concentration profiles of dissolved Fe, Mn, SO_4^{2-} and alkalinity. Clear evidence of diagenetic redox cycling was apparent, with sulphate reduction accompanied by the production of large pore water concentration gradients of alkalinity and the formation of subsurface maxima in Mn and Fe. Moreover, the fall in sulphate concentration by at least a factor of 3 in the first few centimetres of the profile clearly reflects the anoxic character of the sub-surface sediment.

The concentration profiles of ^{137}Cs , ^{241}Am , ^{99}Tc and $^{239,240}\text{Pu}$ for the core are shown in Figure 59. In the case of ^{137}Cs and ^{241}Am , pronounced sub-surface maxima were observed at depths of approximately 26 and 36 cm, respectively. The $^{239,240}\text{Pu}$ profile also peaked at about 30 cm. Similar sub-surface maxima had previously been observed at shallower depths (~10 cm) in cores taken during the late 1970s in the same general area. The change in the depth of these peaks reflects the progressive burial of the Sellafield signal in a zone of active sediment accretion. Clearly, these sub-surface maxima in ^{137}Cs , $^{239,240}\text{Pu}$ and ^{241}Am concentrations correspond to the periods of maximum discharges of these nuclides from nearby Sellafield, and imply a sedimentation rate of approximately 1.2 cm yr^{-1} , which is consistent with sedimentation rates previously reported for this zone. It is also consistent with the

sedimentation rate determined from the ^{99}Tc concentration profile, which displays a clear sub-surface maximum at around 6 cm. The discharge history of technetium is very different to those of ^{137}Cs , $^{239,240}\text{Pu}$ and ^{241}Am , and is characterised by relatively low discharges during the 1980s and early 1990s, followed by a pronounced peak in 1994–98. These trends were clearly reflected in the core. Furthermore, the presence of well-defined maxima in these profiles, decades after input, indicated that relatively little post-depositional mixing of sediment has occurred during this period.

Data on the solid partitioning of plutonium at progressively increasing depths are presented in graphical form in Figure 60. At all depths, a substantial proportion of the plutonium was found to be associated with the R0 exchangeable/readily-oxidisable (mean: $29 \pm 8\%$; range: 13–45%) and R1 acido-soluble (mean: $45 \pm 6\%$; range: 30–54%) phases. Smaller amounts were associated with the R2 reducible (mean: $5 \pm 2\%$; range: 3–10%), R3 oxidisable (mean: $10 \pm 3\%$; range: 6–15%), R4 strongly bound (mean: $8 \pm 4\%$; range: 3–14%) and residual (mean: $4 \pm 2\%$; range: 2–11%) phases.

The small amount of plutonium associated with the exchangeable/readily-oxidisable phase in the oxygenated surface layer compared to that associated with this phase in the deeper anoxic layers, would suggest that some, at least, of the latter is associated with readily-oxidisable geochemical species developed under reducing conditions (e.g. acid volatile sulphides), a result confirmed by measurement of AVS concentrations (carried out by IRSN as part of the REMOTRANS project) in the sediment core (Figure 61).

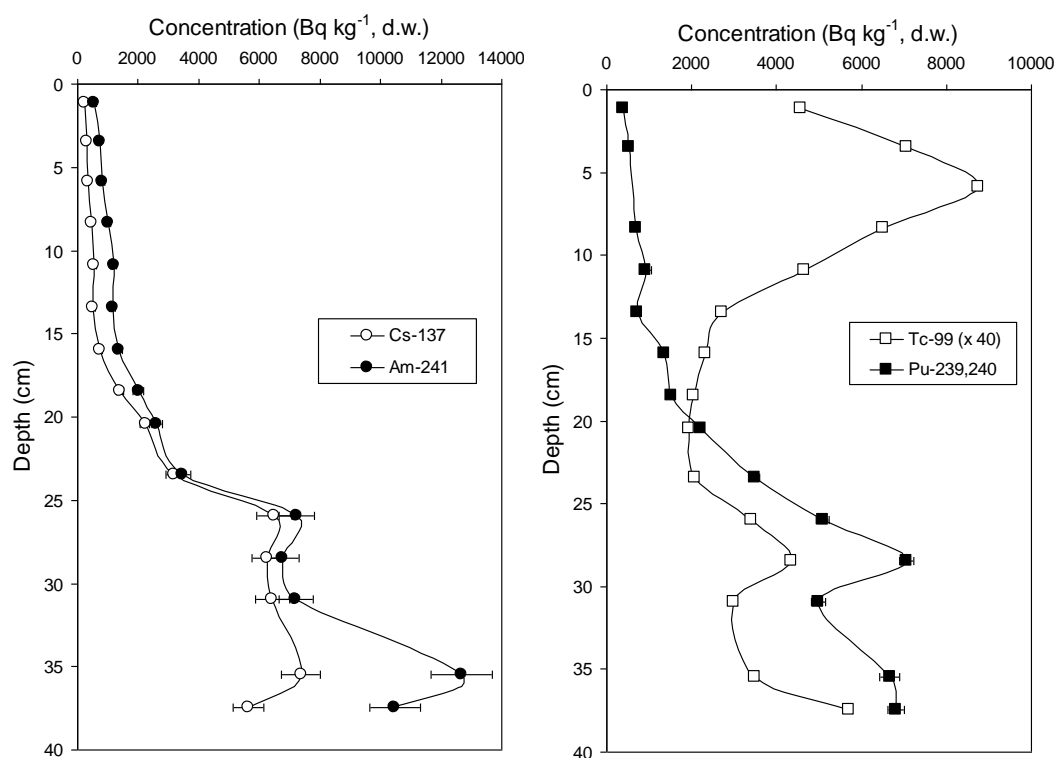


Figure 59. ^{137}Cs , ^{241}Am , ^{99}Tc and $^{239,240}\text{Pu}$ concentration profiles (Bq kg^{-1} , dry weight) in sediment (core INT-010). In some cases, measured uncertainties ($\pm 2\sigma$) are masked by the data points

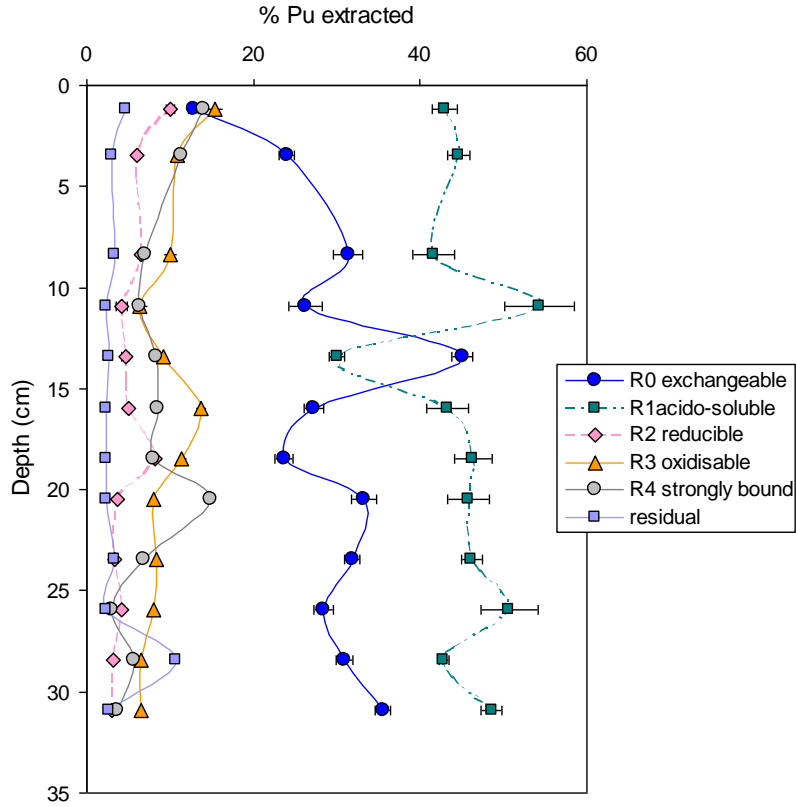


Figure 60. Sequential extraction of $^{239,240}\text{Pu}$ from successive sediment horizons (core INT-010). Uncertainties are given to $\pm 2\sigma$

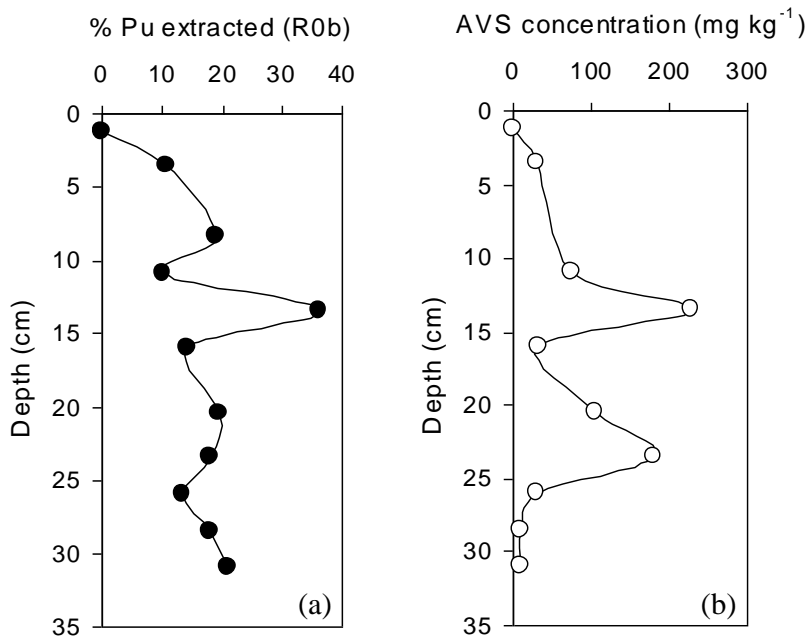


Figure 61. Profiles of (a) fraction of Pu in an easily-exchangeable / readily-oxidisable form, and (b) the concentrations of AVS (mg kg^{-1} of dried sediment) in successive sediment horizons of the Ravensglass Estuary core

More plutonium was found to be associated with the reducible phase in the surface layer compared to deeper sediments, reflecting the geochemical behaviour of iron and manganese. A similar pattern was evident in the case of the oxidisable phase, more than likely reflecting the somewhat higher concentrations of organic matter in the surface layer. It is interesting that the portion of plutonium associated with the oxidisable (R3) extraction, which is designed to target organic matter, amongst other phases, closely agreed with the organic content of the sediment.

Overall, the results showed that the plutonium is predominantly bound to geochemical phases targeted by the acido-soluble and exchangeable phases, indicating that a significant proportion of the plutonium in these and similar sediments is associated with relatively mobile geochemical phases. Similar results were obtained for intertidal sediments from the Solway Firth, and have also been reported by other partners within the REMOTRANS collaboration for sediment samples collected in the 'mud path' off the Cumbrian coast near Sellafield (Gouzy *et al.*, submitted). The results are consistent with the relatively high levels of plutonium remobilisation now known to be taking place throughout the north-eastern Irish Sea.

The combined data clearly indicate that diagenetic reactions taking place during the development of anoxic conditions influence the partitioning of plutonium in the solid phase. Plutonium is known to behave non-conservatively in the Ravenglass Estuary, with low salinity water and changes in pH causing the rapid desorption of a labile form of plutonium. The present work supports this observation, and indicates that this labile fraction is rather large. Although the results of this work contradict previous sequential extraction studies, which have reported that little of the plutonium in Irish Sea sediments is in a readily available form (most publications identifying primary associations with oxide and organic sediment phases) some, at least, of the disparity is almost certainly attributable to failure to take account of the resorption of plutonium in the course of sequential extraction. In addition, many researchers have not taken the necessary precautions to preserve the anoxic integrity of the sediment during sampling, storing and extraction, an omission which undoubtedly leads to unwanted, non-quantifiable phase changes in the course of analysis.

Interestingly, the measured $^{238}\text{Pu}/^{239,240}\text{Pu}$ activity ratios in the residual fractions were consistently lower than those in the previous extraction. This observation is best illustrated in Figure 62, showing the $^{238}\text{Pu}/^{239,240}\text{Pu}$ ratios measured in each fraction (R0, R1, R2, R3, R4 and residual) in six separate samples from a subtidal sediment core collected in the eastern Irish Sea (Stn 64E), and eleven sections of an intertidal core collected in the Ravenglass Estuary (Stn. INT-010). The $^{238}\text{Pu}/^{239,240}\text{Pu}$ ratios measured in the first five extractants for both sets of samples are entirely consistent with those previously reported for eastern Irish Sea sediments (Mitchell *et al.*, 1991a; 1995; 1999) and clearly reflect the time integrated discharge signal from Sellafield. However, many of the $^{238}\text{Pu}/^{239,240}\text{Pu}$ isotopic ratio measurements recorded for the residual fraction were significantly lower than expected (mean: 0.12 ± 0.05 ; range: 0.068–0.19), being characteristic of earlier discharges in the 1960s. Although the 'origin' of this difference is not clear, it could relate to the presence in the integrated signal of 'hot particles' from early releases, characterised by a much lower isotopic ratio. Evidence of these particles in sediment samples collected in the course of the same sampling campaign has been provided in an earlier work package (see WP2). If confirmed, this could indicate the presence of relatively unreactive hot particles, which could remain undissolved for longer time periods than previously believed (Hamilton, 1981; Kershaw *et al.*, 1986).

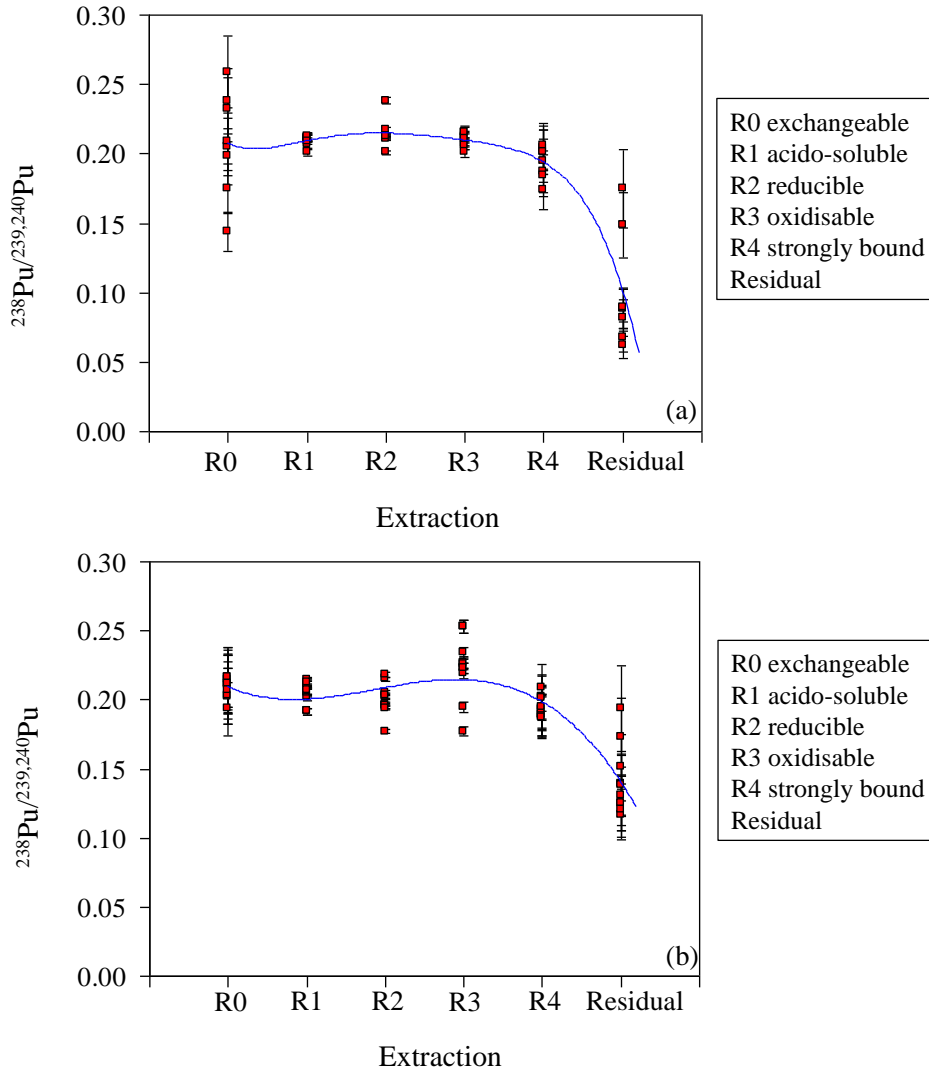


Figure 62. Isotopic ratios measured in each extractant from (a) subtidal sediment collected in the eastern Irish Sea (Stn 64E), and (b) intertidal sediment from the Ravenglass Estuary (Stn INT-010)

In addition to the solid partitioning studies, a number of pore water samples extracted from intertidal and subtidal sediment cores were also analysed for plutonium content. The oxidation state distribution of plutonium in some of these samples was also examined using sequential coprecipitation of reduced and oxidised species with iron hydroxide. Owing to the low concentrations expected, measurements were carried out by accelerator mass spectrometry, again using the 14D tandem accelerator facility at the Australian National University, in Canberra. The measured profiles are shown in Figure 63. As in previous studies, plutonium concentrations in the pore waters showed a consistent (qualitative) relationship with the solid phase profiles, with a distribution coefficient (K_d) of $\sim 10^6$ describing the behaviour of plutonium below the redoxcline. Reduced plutonium was found to be predominant, except in the top-most layers, where the apparent K_d was $\sim 10^5$. The bulk of the plutonium, therefore, remains associated with settled sediments, although the sequential extraction data suggest that the association is with relatively mobile geochemical phases. This finding is important, particularly with regard to biological bioavailability, and should be the subject of further study.

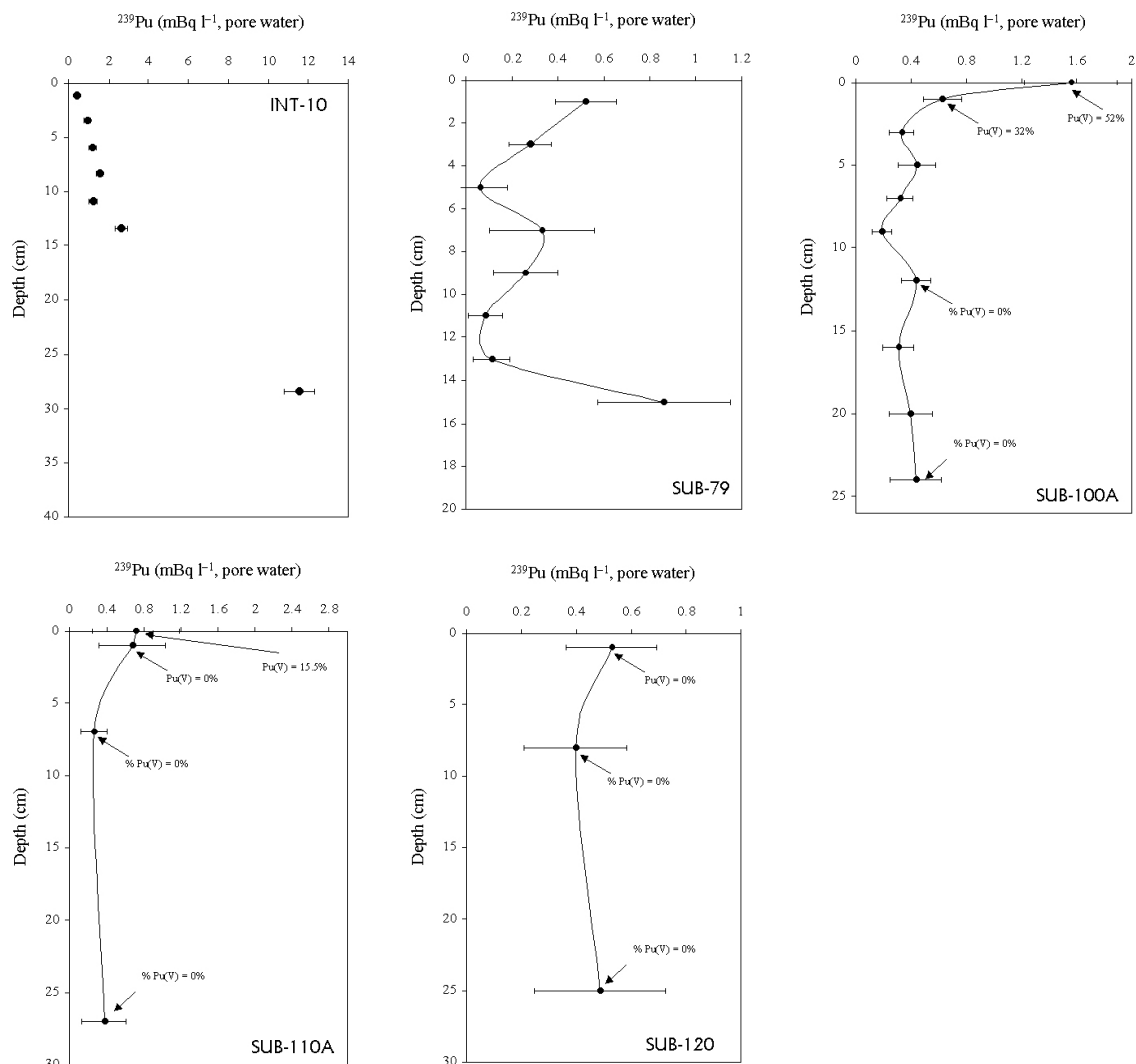


Figure 63. ^{239}Pu concentration profiles in pore waters from eastern Irish Sea intertidal and subtidal sites (DIAPLU campaign, Summer 2002). Uncertainties given are $\pm 2\sigma$

The marine environment in the vicinity of Palomares

Although the accident at Palomares mainly affected the terrestrial environment surrounding the point of impact of the fragmented weapons, past studies have unequivocally demonstrated that some of the actinide contamination has found its way to the marine coastal environment in the proximity of Palomares (Romero, 1992; Gascó *et al.*, 1992; Gascó and Antón, 1997). The main mechanism for the transfer of transuranium nuclides from Palomares to the Mediterranean shelf has been identified as the transport of contaminated terrigenous material from the Palomares area to neighbouring coastal waters via run-off during intense flood events, not unusual in this zone. Surveys conducted in the period 1985–1991 have shown the presence of enhanced $^{239,240}\text{Pu}$ inventories in the continental shelf close to Palomares (Gascó *et al.*, 1992). The inventories, in the range $200\text{--}1500 \text{ Bq m}^{-2}$, are typically an order of magnitude higher than those measured at locations well removed from the accident site along the Spanish continental shelf ($25\text{--}120 \text{ Bq m}^{-2}$), and are characterised by $^{238}\text{Pu}/^{239,240}\text{Pu}$ activity ratios consistent with those measured in contaminated soils from Palomares.

Perturbations in the $^{137}\text{Cs}/^{239,240}\text{Pu}$ ratio at these locations provide further confirmation of the influence of the Palomares accident on the nearby marine environment.

For many years, it was assumed that the impact of the Palomares accident on local marine waters was restricted to the sediment compartment. Indeed, sequential extraction experiments in sediments collected south-east of the Almanzora river mouth, close to Palomares, showed that the plutonium in these sediments was essentially present in an insoluble form, associated with residual phases (Antón *et al.*, 1995), while measurements conducted in coastal waters from the Palomares region in the early 1990s showed no evidence of enhanced levels of plutonium or perturbation of plutonium isotopic ratios attributable to the accident (Mitchell *et al.*, 1995). The refractory nature of the dispersed plutonium, together with the rapid scavenging of particles upon entry to the sea accounted for these observations. Nevertheless, recent evidence (see Table 5) suggests an increase in the availability of plutonium, which could result in the remobilisation, over time, of at least part of the deposited inventory back to the overlying sea water.

The presence of plutonium originating from the Palomares accident in biological compartments was first confirmed by one of the ADVANCE partners in the late 1980s. Measurements carried out in seaweeds (*Fucus vesiculosus*) collected along the southern Spanish Mediterranean coast showed enhanced levels of plutonium in samples collected in the proximity of Palomares (Table 18; Manjón *et al.*, 1995). Further confirmation of this observation was obtained in the course of the ADVANCE project by the analysis of seaweed samples collected along the Palomares coastline in 2002 (Table 19). The plutonium levels in the seaweeds analysed were consistent with those measured 14 years earlier in the same zone, reflecting the continued impact of the Palomares accident on the surrounding marine environment. Carefully determined $^{238}\text{Pu}/^{239,240}\text{Pu}$ activity ratios confirmed the origin of the contamination, with measured values in Palomares (mean = 0.024 ± 0.002) identical to those reported for contaminated soils from the accident area (Mitchell *et al.*, 1997), and lower than those at locations away from the accident site (mean = 0.047 ± 0.013). The presence of plutonium originating from the accident has also been reported in plankton samples from the Palomares coast (Sánchez Cabeza *et al.*, 2003). It is clear from these studies that plutonium from the accident is now not only present in the sediment compartment, but can also be found in biota from the vicinity of Palomares. Whether this is in the form of small sediment particles remobilised from the seabed or in the form of dissolved species remains uncertain at the present time.

Table 18. Transuranium activity concentrations in *Fucus vesiculosus* samples collected along the southern Spanish coast in the late 1980s (Manjón *et al.*, 1995)

Location	Sampling date	Concentration (mBq kg ⁻¹ , dry wt.)			Activity ratios	
		²³⁸ Pu	^{239,240} Pu	²⁴¹ Am	²³⁸ Pu/ ^{239,240} Pu	²⁴¹ Am/ ^{239,240} Pu
Palomares	1988	26 ± 13	1080 ± 60	170 ± 20	0.024 ± 0.013	0.15 ± 0.08
Palomares	1989	49 ± 5	2020 ± 20	420 ± 50	0.024 ± 0.020	0.21 ± 0.02
P. Palomas	1998	3 ± 2	120 ± 20	21 ± 4	0.028 ± 0.014	0.17 ± 0.04
I. Cristina	1999	2 ± 1	51 ± 9	9 ± 2	0.041 ± 0.024	0.18 ± 0.05
Ayamonte	1988	7 ± 2	94 ± 15	13 ± 3	0.072 ± 0.002	0.14 ± 0.04

Table 19. Plutonium activity concentrations and isotopic ratios in *Fucus vesiculosus* samples collected in the vicinity of Palomares during a field campaign in 2002

Location	Sampling date	Concentration (mBq kg ⁻¹ , dry wt.)		Activity ratios
		²³⁸ Pu	^{239,240} Pu	²³⁸ Pu/ ^{239,240} Pu
Palomares	2002	21 ± 4	946 ± 38	0.022 ± 0.005
Palomares	2002	20 ± 4	824 ± 33	0.025 ± 0.005

Source-term characteristics and transfer in marine ecosystems

As in the case of terrestrial samples (WP3), the bioavailability of radionuclides associated with contaminated marine sediments for different release scenarios was investigated by subjecting the samples to leaching with a simulated gastrointestinal fluid (0.16M HCl). The samples selected for this type of analyses included intertidal and subtidal sediments from the north-eastern Irish Sea (affected by discharges from the Sellafield reprocessing plant), and sediments from Bylot Sound (Greenland), contaminated as a result of the Thule weapons accident.

Irish Sea

The cumulative extracted percentages of ²⁴¹Am from sediments collected in the Ravenglass Estuary and the ‘mud patch’ off the Sellafield after different contact times are shown in Figure 64. Only 14–20% of the ²⁴¹Am was left in the residual material after 168 hours of extraction. These results are consistent with plutonium sequential extraction data in the same type of sediments (see Figure 60), and confirm that a large proportion of the transuranics is associated with relatively mobile geochemical phases.

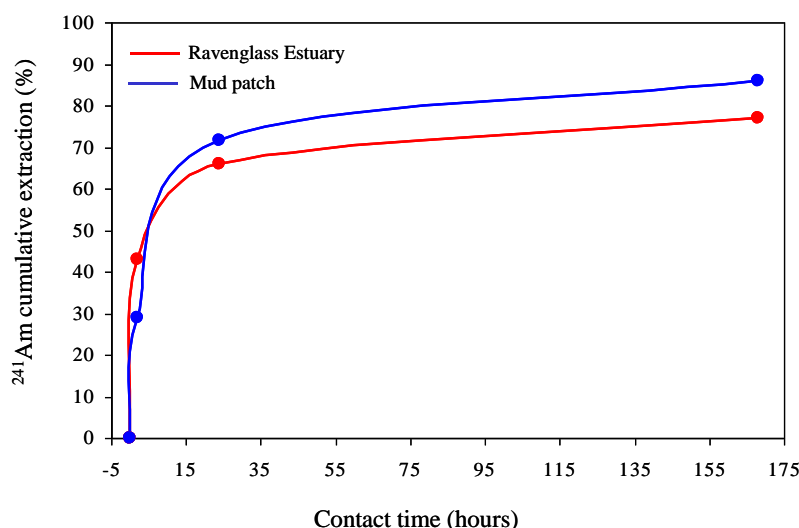


Figure 64. Cumulative extraction (%) of ²⁴¹Am from contaminated sediments collected in the Ravenglass Estuary and the Sellafield ‘mud patch’ using simulated gastrointestinal fluid (0.16M HCl) Thule

In contrast to Irish Sea sediment, little ²⁴¹Am was extracted from a sample of contaminated sediment collected in Bylot Sound (Greenland), even after 168 hours of extraction (Figure

65). This confirms the observation (WP1) that contamination resulting from the Thule accident is mainly in the form of dissolution resistant, inert radioactive particles.

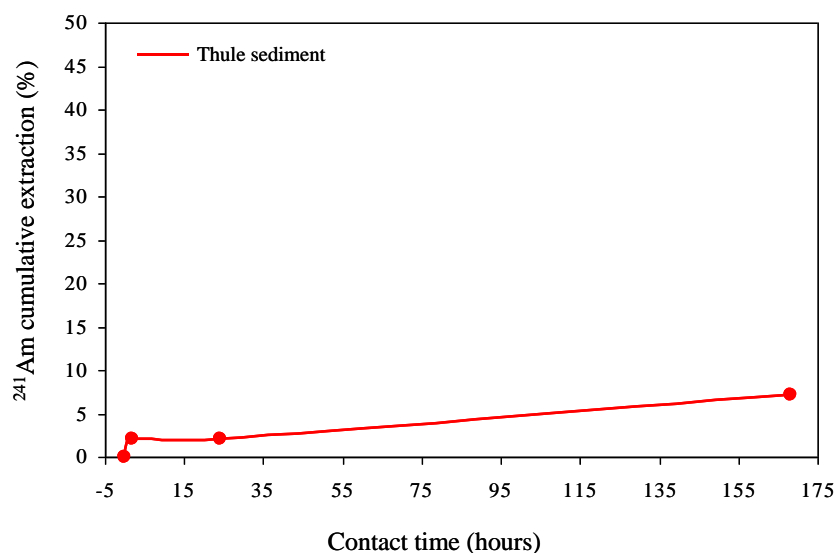


Figure 65. Cumulative extraction (%) of ^{241}Am from contaminated sediments collected in Bylot Sound (Greenland) using simulated gastrointestinal fluid (0.16M HCl)

WP6. Comparative assessment of source-specific and ecosystem-specific characteristics

The objectives of this work-package were to (i) identify source-specific and environment-specific factors influencing the mobility and bioavailability of actinides within different ecosystems, and (ii) provide a set of recommendations on analytical techniques applicable to the characterisation of source-terms.

As described in WP2, heterogeneities in activity concentrations, reflecting the presence of radioactive ‘hot’ particles, were identified at all the study sites with the aid of autoradiography techniques. More detailed information on the particle characteristics for each of the source-terms was obtained using a combination of advanced analytical tools, applied either to bulk samples (e.g., sequential extraction, solubility tests) or to individual isolated particles (e.g. XRMA, XANES). The combination of scanning electron microscopy with X-ray microanalysis and synchrotron radiation X-ray micro-techniques, provided valuable information on key particle characteristics, such as particle size, structure, elemental distribution, and actinide oxidation state distribution. As shown in WP3-WP5, these characteristics have a profound influence on particle weathering rates and, consequently, on the mobility of the actinides and their transfer to living species. In the next sections, the source-term and environment-specific factors influencing the mobility and bioavailability of actinides at each of the study sites considered in the ADVANCE project are briefly summarised

Semipalatinsk (Kazakhstan)

Source-term: Nuclear weapons tests

Analyses carried out on soil samples from Ground Zero, Lake Balapan and the Tel'kem experimental sites within the Semipalatinsk NTS showed that these sites are contaminated with significant amounts of transuranium nuclides, as well as fission and activation products. Analyses of plutonium isotopic ratios showed that the plutonium contamination in these areas is mainly due to weapons-grade plutonium. However, considerable differences were observed in the composition of the artificial radioactivity labelling each of the sites.

Radioactive particles with sizes ranging from micrometres to millimetres were identified in soil sampled at each location. Individual particles, especially from Ground Zero, appeared to be vitrified (fused), probably due to the extremely high temperatures involved. The distributions of uranium and plutonium in these particles were well correlated, although no correlation was observed with other major constituents within the particles (e.g., Ca, Fe).

Measurements on the solid partitioning of plutonium at each of the sites showed that a significant proportion of the plutonium contamination is in a highly refractory, non-labile form at the present time. Experimental tests on the availability of ^{241}Am using simulated gastrointestinal fluid on contaminated soils yielded a similar conclusion, with ~70–80% of this radionuclide remaining unextracted even after 168 hours.

Palomares (Spain) and Thule (Greenland)

Source term: Nuclear weapons disintegration

Isolated particles from the Palomares accident ranged in size from 1–50 μm , whereas those at Thule were in the range 20–40 μm . As in the case of Semipalatinsk, the distributions of uranium and plutonium within the particles were well correlated. Uranium in Palomares particles was found to be present as UO_2 and U_3O_8 . The absence of metallic uranium suggests the oxidation of uranium during the accident. A similar observation was made in the case of Thule particles. However, here, all the uranium was found to be in the form of UO_2 , with no metallic uranium or U_3O_8 present in any of the particles analysed. It seems that although the oxidation of uranium occurred following both accidents, the degree of oxidation was higher in the case of Palomares.

Plutonium in Palomares and Thule particles was present as a mixture of the relatively soluble Pu(III) and the less soluble Pu(IV). Most impact assessments concerning plutonium contamination at these two sites have been based on the assumption that plutonium is present exclusively in a rather inert form, either as metallic plutonium or as Pu(IV). As Pu(III) is also present, impact assessments should be revised to take into account particle weathering rates and potential remobilisation of Pu(III).

Indeed, evidence obtained using sequential extraction in the course of ADVANCE suggests a change in the geochemical association of plutonium in Palomares soils as a result of weathering, with a higher proportion of the plutonium present in readily available phases in comparison with previous results. Solubility studies carried out on Thule sediments using

simulated gastrointestinal fluid, on the other hand, suggest that actinides in this area remain rather insoluble, with ~90% of the ^{241}Am un-extracted after 1689 hours.

Chernobyl (Ukraine)

Source-term: Nuclear reactor accident

The temperature, pressure and redox conditions under which particles were released during the Chernobyl accident changed in the course of the event. During the initial explosion on April 26th 1986, mechanical destruction of the uranium dioxide fuel occurred at high temperature and pressure, and deposition of fuel particles (Figure 66) took place in a 100 km \times 10 km trace to the west of the reactor (Kashparov *et al.*, 1999). Large particles having high deposition velocities and a composition of radionuclides close to the estimated fuel burnup, deposited within 2–5 km of the site (Loschilov *et al.* 1991; 1992; Kuriny *et al.*, 1993; Kashparov *et al.*, 1999). Subsequent releases took place as a result of the graphite fire which followed the initial explosion. During this period, volatile fission products and uranium fuel particles were released under high temperature and oxidising conditions during April 26th-30th, and deposition of particles occurred along a trace to the northwest, and to the north and northeast of the plant (Kashparov *et al.*, 1999). From April 30th to May 6th the temperature and subsequently the emission of volatiles decreased, and uranium fuel particles deposited along a trace to the south of the reactor.

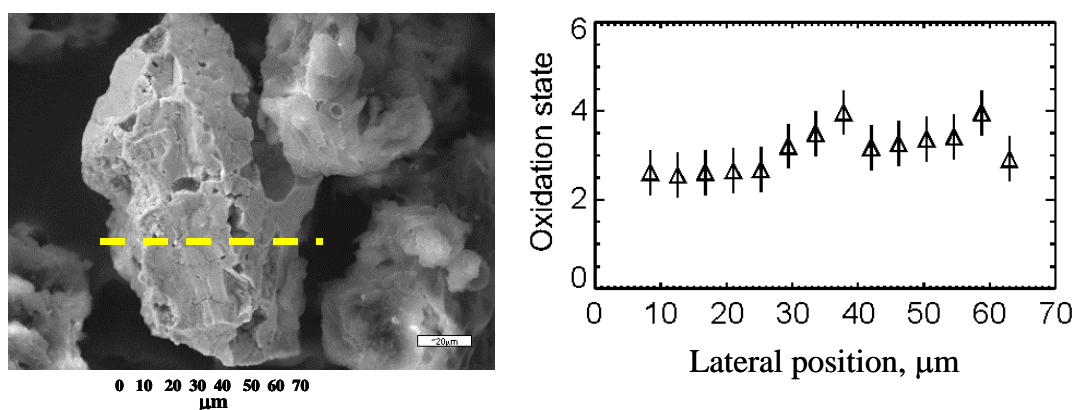


Figure 66. SEM image of a west particle (left) and horizontal line scan of U-oxidation state across this particle (right). Scan path is indicated as a dashed line. Bar = 20 μm

In the course of the ADVANCE project, particles with a variety of sizes, shapes, structures and colours were isolated, from compact small-sized crystalline single particles to large amorphous aggregates. Synchrotron radiation X-ray microtechniques demonstrated that crystalline, inert fuel particles were released during the initial explosion. These particles were characterised by UO_2 -cores surrounded by reduced forms of U (+2), probably due to interactions with carbon from the moderator. In contrast, uranium in the UO_2 fuel particles released during the reactor fire was oxidised to U_3O_8 or/and U_2O_5 . These particles were characterised by UO_2 -cores surrounded by a layer of oxidised uranium (in the form of U_2O_5 and U_3O_8).

As illustrated in Figure 67b (Kashparov *et al.*, 1999), the weathering rate of fuel particles released during the initial explosion and deposited to the west of the Chernobyl reactor was low (0.04 year^{-1}) compared to that of fuel particles released to the north and south during the subsequent fire (0.4 y^{-1}). The low weathering rates of fuel particles to the west of Chernobyl

can be attributed to the inert crystalline structures and the presence of reduced forms of uranium, formed during high temperature and pressure conditions, without the influence of oxygen (Figure 66). In contrast, the increased weathering rates for particles to the north and south is attributed to the presence of oxidised fuel particles, having UO_2 cores with oxidized U_3O_8 and U_2O_5 layers (Figure 67a) formed during the subsequent fire.

Although the source term (UO_2 fuel) was the same in both cases, the different release scenarios influenced the characteristics of the uranium particles ejected. Uranium particles released during the initial explosion were inert with low weathering rates and low soil-to-plant transfer, while uranium particles released during the subsequent fire were oxidised with high weathering rates and high soil-to-plant transfer. Thus, differences in crystallographic structures and oxidation states of uranium in fuel particles explain the observed differences in weathering kinetics, mobility and soil-to-vegetation transfer coefficients of radionuclides associated with particles located west and north of the Chernobyl reactor.

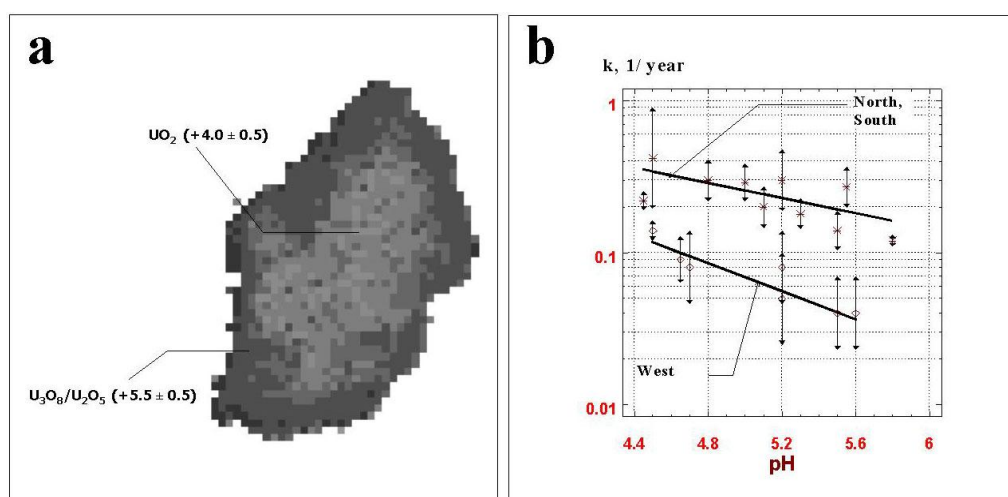


Figure 67. Particles released from the Chernobyl reactor and associated weathering rates. (a) Oxidised fuel particle (UO_2 core with oxidised U_3O_8 and U_2O_5 layers) released during the reactor fire and obtained from 2-D micro-XANES (Salbu *et al.*, 2000; Salbu *et al.*, 2001), (b) weathering rate constants as functions of pH for fuel particles released during the explosion (lower) and during the fire (upper) (Kashparov *et al.*, 1999).

It should, however, be noted that ecosystem-related characteristics can also influence the weathering rate constants for deposited fuel particles. Indeed, Kashparov *et al.* (1999) showed that weathering rates were dependent on soil pH, with increased rates occurring with increasing acidity of the soil.

Sellafield (UK) and Mayak PA (Russia)

Source-term: Reprocessing discharges

Previous studies had shown that a major fraction of the actinide discharge in effluents from reprocessing operations is associated with particles and colloids. In the course of the ADVANCE project, the persistence of these particle and colloidal forms in the terrestrial and

freshwater environments surrounding the Mayak PA reprocessing plant, and the marine environment close to the Sellafield reprocessing plant, were thoroughly examined.

In contaminated ground waters from Mayak, about 65% of the plutonium was found to be associated with particles and colloids. Autoradiography of sediments from Reservoirs 10 and 11 clearly revealed the presence of radioactive particles. However, all attempts to isolate particles containing plutonium or uranium were unsuccessful. Instead, the particles analysed appeared to contain a mixture of other radionuclides as well as heavy metals. Nevertheless, sequential extraction experiments showed that plutonium in these sediments is rather inert, with little (if any) present in a readily available form.

Radioactive particles were also identified throughout a sediment core taken in the muddy sediments close to the Sellafield outfall. Uranium fuel particles originating from Sellafield were also isolated from intertidal sediments collected in the Ravenglass Estuary. Sequential extraction analyses, however, revealed that, in contrast to the plutonium in the Mayak reservoirs, ~75% of the plutonium in these sediments was associated with relatively mobile phases (including exchangeable, easily oxidisable and acido-soluble phases). The relatively high mobility and bioavailability of actinide species in contaminated sediments from Sellafield was confirmed in leaching experiments with simulated gastrointestinal fluid. The fraction of ^{241}Am extracted after 168 hours of contact, at ~80%, was much higher than that obtained for samples collected at Thule and Semipalatinsk. Certainly, the remobilisation potential of actinides from contaminated sediments in the Irish Sea should be taken into account in any impact assessment (and modelling) of this particular area. Indeed, a number of studies have shown that it is remobilisation of actinide radionuclides from historically-contaminated sediments, rather than direct contemporary discharges, that now constitute the main source of actinides to the waters of the Irish Sea.

Kosovo and Kuwait

Source-term: Depleted uranium (DU) ammunition

In the course of the ADVANCE project, radioactive particles were isolated from sites in Kosovo and Kuwait contaminated by depleted uranium. The particle-size distribution of the particles was found to differ depending on the release scenario.

In Kosovo, particles isolated from contaminated soils ranged from submicrometers to ~30 μm , with an average size of 2 μm . In Kuwait, particles collected from holes in tanks hit by DU ammunition or from the vicinity of intact DU penetrators ranged from 2–64 μm (median = 13 μm , $n = 36$). Larger particles, in the range 0.2–1500 μm (median = 44 μm , $n = 43$) were isolated from samples collected at the site of a DU ammunition storage facility destroyed by a fire. These DU particles appeared with a strong yellow colour (typical of uranyl compounds), and were distinctly different to those observed in Kosovo and at target sites within Kuwait. They also differed from uranium particles released during nuclear weapons tests (Semipalatinsk) or following nuclear reactor accidents (Chernobyl).

Measurements carried out on particles from Kosovo and Kuwait yielded a rather constant $^{235}\text{U}/^{238}\text{U}$ atom ratio (0.0020 ± 0.0005), which was in good agreement with previously reported values. In contrast, the $^{236}\text{U}/^{235}\text{U}$ atom ratio measured in DU particles from Kuwait varied depending on the sampling site, with values of $\sim 10^{-2}$ measured in particles associated

with the DU ammunition storage facility fire, and values of $\sim 10^{-3}$ measured in particles collected inside disabled tanks. The presence of ^{236}U can only be due either to the use of uranium recycled from spent fuel or to the handling of natural uranium with equipment previously contaminated in the course of recycling operations in the enrichment plants. Variations in the $^{236}\text{U}/^{235}\text{U}$ ratio are thus readily attributable to differences in the nature of the nuclear fuel employed or the history of the enrichment plant producing a particular DU batch.

Speciation experiments conducted on selected, isolated DU particles showed that, in all cases, DU was in an oxidised form. About 50% of the DU particles from Kosovo were characterised as UO_2 , while the remainder were present as U_3O_8 or a mixture of both oxidised forms (with *ca.* 2/3 UO_2 and 1/3 U_3O_8). Kuwaiti DU particles collected close to DU penetrators or inside disabled tanks (swipes) were similarly characterized as UO_2 , U_3O_8 or a mixture of these oxidized forms. In contrast, DU particles released during a fire in a DU ammunition facility were found to be present in oxidation states +5 and +6, similar to solid uranyl standards.

It is clear that, despite having the same origin (DU ammunition), particles formed during the fire were very different from those formed during impact with hard targets, with large, highly oxidised particles characterising the former, and small, less oxidised particles characterising the latter. The weathering behaviour of the two types of particles was also found to differ. Highly oxidised DU associated with particles originating from the fire in the ammunition storage was rapidly dissolved in 0.16 M HCl ($84 \pm 3\%$ after 2 hrs contact time, $n = 3$). The kinetics of the extraction was much slower for less oxidised DU particles originating from DU penetrators impacting with tanks or corrosion of DU penetrators. Furthermore, artificial seawater (pH 8) was able to dissolve large, yellow, highly oxidised DU particles originating from the ammunition storage fire, while DU particles originating from impact on tanks appeared to be relatively inert.

As the particle weathering rate is expected to be higher for U(V)/U(VI) and U_3O_8 than for metallic U or UO_2 , the presence of respiratory $\text{U}_3\text{O}_8/\text{U}_2\text{O}_5/\text{UO}_3$ /uranyl, their corresponding weathering rates and the subsequent remobilisation of uranium should be included in environmental impact assessments of areas contaminated with DU.

Recommendations regarding the characterisation of samples containing radioactive particles

It should be clear from the results presented in this report that radioactive particles and fragments varying in size, shape, structure, morphology, density, oxidation state distribution, and charge are often present in events involving the release of actinide radionuclides to the environment. As demonstrated by bioavailability and sequential extraction experiments conducted in the course of the project, failure to recognise the presence of these particles and their weathering characteristics may lead to analytical inconsistencies, irreproducible results and, ultimately, to erroneous conclusions regarding the mobility of these radionuclides in a given ecosystem.

To assess the impact of radioactive particles on a particular ecosystem, and in order to implement effective cost-efficient measures, information on the physical and chemical characteristics of the particles is essential, as is kinetic information on processes influencing particle weathering, mobility and bioavailability of released radionuclide species associated with these particles. Characterisation of source-terms, including radioactive particles in the

submicrometer to micrometer range, certainly represents an analytical challenge. However, as demonstrated in the course of the ADVANCE project, application of emerging, state-of-the-art, advanced technologies in conjunction with more traditional techniques, can greatly help in gaining much of the needed information. It is, thus, proposed that any future assessment of a site contaminated by actinide releases should include, in addition to a programme to evaluate the radionuclide distribution in the ecosystem's compartments, a suitable strategy to identify, isolate and characterise radioactive particles present at the site. This strategy should include:

- Screening of samples to identify radioactive heterogeneities;
- Isolation of individual particles;
- Determination of size distribution;
- Determination of element distribution within individual particles;
- Determination of element or isotopic ratios;
- Determination of crystallographic structures;
- Determination of oxidation states;
- Determination of weathering rates.

The recommended techniques to be used for each of the above steps are briefly discussed below.

Identification of heterogeneities

Heterogeneities containing localised radioactivity (i.e., hot spots) can be observed in the near field using portable Geiger-Muller tubes or NaI detectors (Salbu *et al.*, 1994; 1994b). To avoid altering the physico-chemical forms of radionuclides in a sample during storage, fractionation techniques should be applied *in situ*, at site or shortly after sampling at the laboratory. When screening solid material such as contaminated soil or sediment samples for heterogeneities, the samples should be dried at room temperature. Autoradiography using digital phosphor imaging is a very convenient way of screening samples for radioactive heterogeneities. This technique allows the production of digital autoradiographs using a reusable image sensor with 10-100 times higher sensitivity than conventional X-ray or alpha radiation sensitive film. The preparation is usually the same for both techniques, i.e. spreading the dried samples (soil, sediment, vegetation) on paper or plastic foils which are placed in close contact with the sensitive film or image plate.

For radionuclides associated with colloids and particles in water, tangential-flow systems applied in the field have proved to be most useful (Salbu, 2000; Mitchell *et al.*, 2002; Smith *et al.*, 2004).

Isolation of individual particles

Hot spots identified by autoradiography using digital phosphor imaging can be sub-sampled directly from the sample foils, which have been placed in close contact with the sensitive image plate. Thus, the sample volume is efficiently reduced, and microscopic tools can be utilised for isolation of particles in the obtained sub-sample. Alternatively, splitting a sample in numerous sub-samples followed by gamma measurements has proved to be an efficient mean for detecting and isolating particles, provided that the particles contain gamma emitters (Lind *et al.*, 2002; in prep.).

One of the latest developments within microscopic tools and, in particular, within electron microscopy, is the environmental scanning electron microscope (ESEM), which enables soft, moist and/or electrically insulating materials to be viewed without any pre-treatment. A major advantage of ESEM for the isolation of radioactive particles is the possibility to introduce relatively large samples of soil, sediment or dust, which are spread out on a large diameter substrate (e.g., sticky double-faced carbon tabs) in the specimen chamber. Radioactive particle identification can then be achieved using X-ray microanalysis (XRMA). Whereas conventional scanning electron microscopy requires a relatively high vacuum in the specimen chamber to prevent atmospheric interference with primary or secondary electrons, an ESEM may be operated with a poor vacuum (up to 10 Torr of vapour pressure, or one seventy-sixth of an atmosphere) in the specimen chamber.

Activity concentrations and elemental isotopic ratios

Due to the high sensitivity in comparison with alpha-spectrometry, mass spectrometry techniques such as inductively coupled plasma mass spectrometry (ICP-MS), thermal ionisation mass spectrometry (TIMS) and AMS have been utilised to determine the activity concentrations and the isotopic ratios of uranium and transuranic elements such as plutonium in radioactive particles. However, the full dissolution of particles is necessary prior to analysis (Oughton *et al.*, 1993).

Characterisation of colloidal species by transmission electron microscopy (TEM) with X-ray microanalysis (XRMA)

For colloidal radioactive material in water, transmission electron microscopy (TEM) with XRMA can be utilised for structure and element analysis. When droplets of water are transferred to coated grids and carefully dried under an UV-lamp prior to analysis, electron dense structures can be recognised, when compared to the blank (distilled water). Using this method, colloidal material with particle sizes close to 20 nm and pseudocolloids in the range of 100 nm has been identified in Sellafield effluents (Salbu *et al.*, 2001). XRMA provides information on the element composition, while the distribution of elements is obtained from X-ray mapping.

Determination of particle size distributions, elemental surface distributions and surface structures by SEM with XRMA

Particles isolated using microscopic tools can be further subjected to scanning electron microscopy (SEM) using an instrument interfaced with surface sensitive XRMA (X-ray microanalysis). This technique has proved most useful for obtaining information on particle size distributions, elemental distributions and structures in particles of different origin (Salbu *et al.*, 1998; Salbu *et al.*, 2003; Salbu *et al.*, in press). Sub-samples containing particles are mounted on stubs with carbon sticky tape and analysed at different magnification. Carbon coating is usually avoided, since C may interact with radionuclide species on particle surfaces. Using Backscattered Electron Imaging (BEI) mode, bright areas reflect the presence of high atomic number elements, while the distribution of elements in the upper particle surface layer is obtained using X-ray mapping. XRMA measurements provide information on elemental composition. The structure of particles is characterised from images acquired in Secondary Electron Imaging mode. SEM also serves as a screening technique prior to further detailed studies using Synchrotron Radiation (SR) based X-ray microbeam techniques.

Alternatively, ESEM combined with XRMA can be used for the determination of particle sizes, elemental distributions and structures of particles imbedded in soft, moist and/or electrically insulating materials without any pre-treatment, thus avoiding the pre-treatment required in conventional scanning electron microscopy.

Determination of elemental distributions within particles by SIMS and PIXE

In Secondary Ion Mass Spectrometry (SIMS), an energetic beam of focused ions is directed at the sample surface in a high vacuum environment. The transfer of momentum from the impinging primary ions to the sample causes sputtering of the surface atoms and molecules. Sputtered ions are analysed by an imaging mass spectrometer equipped with a position sensitive detector. The technique has been applied to measure the isotopic composition of several thousand μm -sized depleted uranium particles present in an area of several mm^2 in about 4–5 h (Danesi *et al.*, 2003).

In Particle Induced X-Ray Emission (PIXE), radiation with charged particles ionise the inner shells of atoms and characteristic X-rays are detected. Using energy-dispersive detectors, the X-ray spectrum at each beam position (pixel) is recorded, while the sample is moved in front of the beam. The 2D elemental maps have detection limits within the range 1-100 ppm and inferior spatial resolution within 0.5-10 μm . PIXE has been used to provide elemental contents and elemental distribution maps of elements at the surface of Pu contaminated particles at the former British test sites, Maralinga and Emu, Australia (Burns *et al.*, 1995). Only a small fraction of the larger particles could be analysed. Major components of the particles from the most contaminated area were Fe and in some cases Pu, U and Pb.

Determination of 2D and 3D element distributions within individual particles, 2D crystallographic structures and oxidation states by synchrotron radiation based μ -X-ray techniques

Recent development within synchrotron based X-ray microtechniques have proved to be very promising for the determination of 2D and 3D elemental distributions, crystallographic structures and oxidation state for matrix elements. Potential applications of sensitive X-ray microprobe techniques for solid surface analysis have been reviewed by several authors (Bertsch *et al.*, 1994; Nitsche *et al.*, 1995; Adams *et al.*, 1998). Using monochromatic X-ray microbeams, microscopic X-ray fluorescence analysis (μ -XRF) and microscopic X-ray absorption (μ -XAS) provide information on the elemental distribution on the particle. Micro-X-ray diffraction (μ -XRD), on the other hand, gives information on the crystallographic structures on microscopic areas of solid particles.

By tuning the energy of the microbeam source and scanning the energy over an absorption edge of an element of interest, extended X-ray absorption fine structure analysis (EXAFS) provides information on the number of atoms, the atomic number and the distance to neighbouring atoms and co-ordination in the surface of the solid, while X-ray absorption near edge structure spectrometry (XANES) can provide information on the oxidation state.

In the laboratory, efficient μ -X-ray sources based on rotating anode tubes equipped with capillary X-ray optics can be applied (Adams *et al.*, 1998). However, the third generation synchrotron radiation sources, yielding high intensity and highly monochromatic X-ray microbeams, have significantly increased the sensitivity and applicability of X-ray microprobe techniques. Using synchrotron (SR) based XANES, the oxidation states of

uranium associated with components in soils and sediments have been well documented (Nitsche *et al.*, 1995; Bertsch *et al.*, 1994).

As shown in previous work-packages, different SR-microprobe techniques have been combined by utilising the μ -X-ray beam at the European Synchrotron Radiation Facility (ESRF), France, to study uranium species in μ m-sized radioactive particles released from the Chernobyl reactor (Salbu *et al.*, 2000; 2001). In this work, carried out during the ADVANCE project, μ -XAS tomography (3D), μ -XRF, μ -XRD and 2D μ -XANES were utilised to obtain information on distributions, structures and oxidation states. From μ -XRD different crystalline forms could be identified, while μ -XANES clearly demonstrated differences in oxidation states of U in released UO_2 fuel (apparently reduced U fuel particles were released during the initial explosion and oxidised U_3O_8 particles were released during the fire). Using μ -tomography (Raven *et al.*, 1996), internal cavities and channels due to formation of volatiles during normal operations could be observed (Salbu *et al.*, 2000; 2001).

Not only the third generation synchrotrons are useful for solid speciation of radioactive particles; SR based μ -X-ray Fluorescence (μ -SRXRF) screening of particles using a second generation SR source (e.g. HASYLAB, Germany) has proved useful, as subsurface hot spot areas of elements of interest can be identified. Furthermore, the μ -XANES technique for uranium particles was developed at ID22, ESRF, though recently a similar approach with lower resolution has become available at beamline L, HASYLAB (Salbu *et al.*, 2003; in press).

Determination of particle weathering rates

High activity particles can act as a point source when inhaled, ingested, or if deposited on skin (skin dose). Alternatively, radionuclides are mobilised from particles (due to particle weathering) and can be transferred to man via ecosystem transport. As earlier demonstrated, particle weathering constants will depend on particle size, crystallographic structure, and on the oxidation state of the carrying matrix.

To evaluate the mobilisation potential of radionuclides from particles, several leaching procedures have been described in the literature. Sequential extraction procedures have extensively been used to extract radionuclides from contaminated soils and sediments (Kennedy *et al.*, 1997; Oughton *et al.*, 1992). However, rather few papers deal with leaching of radionuclides from individual well-characterised particles (Lind *et al.*, in prep).

When sequential leaching is applied, it is essential that the first step (i.e. the first extractant), is relevant, and does not interfere with the subsequent steps. Thus, site-specific waters (e.g., soil water, sediment pore water, sea water) reflecting the conditions where particles are deposited should be applied, rather than strong electrolytes (e.g., artificial Ca-solutions), which may aggregate colloidal systems. By gradually decreasing the pH of the extractant solutions, information on pH sensitive phases can be obtained.

Previous studies have demonstrated that weak oxidising reagents (H_2O_2 in HNO_3) are efficient for dissolving oxidised fuel particles from Chernobyl, and associated radionuclides (Salbu, 2000). However, to evaluate the potential for uptake via the gastrointestinal tract, rumen liquid (e.g., domestic animals) or simulated stomach juice (e.g., man, 0.16 M HCl) is particularly relevant. In the course of the ADVANCE project, the extraction yield obtained by extraction with simulated stomach juice (0.16 M HCl) varied

with particle characteristics, being high for highly oxidised uranium (V, VI) and low for U metal or UO₂ (Lind *et al.*, in prep).

2.3. Conclusions

Heterogeneities in activity concentrations, reflecting the presence of radioactive particles, have been identified at all our study sites using autoradiography techniques. More detailed information of the particle characteristics for each of the source-terms has been obtained using a combination of advanced analytical tools, applied either to bulk samples (e.g., sequential extraction, solubility tests) or to individual isolated particles (XRMA, XANES). The combination of scanning electron microscopy with X-ray microanalysis and synchrotron radiation X-ray micro-techniques has provided invaluable valuable information on key particle characteristics, such as particle size, structure, element distribution and actinide oxidation state distribution.

Bioavailability and sequential extraction experiments conducted in the course of the project have clearly demonstrated that failure to recognise the presence of these particles and their weathering characteristics may lead to analytical inconsistencies, irreproducible results and, ultimately, to erroneous conclusions regarding the mobility of these radionuclides in a given ecosystem.

It is recommended that any realistic assessment of the short- and long-term impact of actinide releases to a particular ecosystem includes, in addition to a programme to evaluate the radionuclide distribution in the ecosystem's compartments, a suitable strategy to identify, isolate and characterise radioactive particles present at the site. Information on the physical and chemical characteristics of the particles, and kinetic information on processes influencing particle weathering, mobility and bioavailability of released radionuclide species associated with these particles should also form a key part of any such study.

Characterisation of source-terms, including radioactive particles in the submicrometer to micrometer range, certainly represents an analytical challenge. However, as demonstrated in the course of the ADVANCE project, application of emerging, state-of-the-art, advanced technologies, in conjunction with more traditional techniques, can provide much of the needed information.

As demonstrated in the ADVANCE project, the application of these techniques should contribute to the strengthening of European scientific competence in the field of radioecology, and may help to revitalise the interest in this important field, particularly amongst young scientists.

2.4. References

- Aarkrog, A. (1977), 'Environmental behaviour of plutonium accidentally released at Thule, Greenland', *Health Phys.* **32**, 271-284.
- Aarkrog, A. (1995), 'Inventory of nuclear releases in the World', In: *Proc. NATO Advanced Study Institute Advanced Course on Radioecology*, Zarechny, Russia, 19-28 June 1995, 12 pp.
- Aarkrog, A., Dahlgaard, H., Nilsson, K. and Holm, E. (1984), 'Further studies of plutonium and americium at Thule, Greenland', *Health Phys.* **46**, 29-44.
- Adams, F., Janssens, K. and Snigirev, A. (1998), 'Microscopic X-ray fluorescence analysis and related methods with laboratory and synchrotron radiation sources', *J. Anal. Atomic Spectr.* **13**, 319-331.
- Andersson, P.S., Porcelli, D., Wasseburg, G.J. and Ingri, J. (1998), 'Particle transport of ^{234}U - ^{238}U in the Kalix River and the Baltic Sea', *Geochim. Cosmochim. Acta* **62**, 385-392.
- Antón, M.P., Gascó, C., Sánchez-Cabeza, J.A. and Pujol, Ll. (1994), 'Geochemical association of plutonium in marine sediments from Palomares (Spain)', *Radiochim. Acta* **66/67**, 443-446.
- Antón, M.P., Gascó, C. and Pozuelo, M. (1995), 'Chemical partitioning of plutonium and americium in sediments from the Palomares marine ecosystem', *Rapp. Comm. Int. Mer Med.* **34**, 223.
- Beasley, T.M., Kelley, J.M., Orlandini, K.A., Bond, L.A., Aarkrog, A., Trapeznikov, A.P. and Pozolotina, V.N. (1998), 'Np-237/Pu-239 atom ratios in integrated global fallout: a reassessment of the production of Np-237', *J. Environ. Radioactivity* **39**(2), 215-230.
- Bennett, B.B., De Geer, L.E. and Doury, A. (2000), 'Nuclear weapons test programmes of the different countries', In: *Nuclear Test Explosions: Environmental and Human Impacts*, Sir F. Warner and R.J.C. Kirchmann (Eds.), Scientific Committee on Problems of the Environment (SCOPE) of the International Council for Science (ICSU), SCOPE 59, John Wiley & Sons, Chichester, Chapter 3, pp. 13-32.
- Bertsch, P.M., Hunter, D.B., Sutton, S.R., Bajt, S. and Rivers, M.L. (1994), 'In situ chemical speciation of uranium in soils and sediments by Micro-X-ray absorption-spectroscopy', *Env. Sci. Technol.* **28**, 980-985.
- BNFL (1980-2001), 'Annual Reports on Radioactive Discharges and Monitoring of the Environment, 1979; 1980; 1981; 1982; 1983; 1984; 1985; 1986; 1987; 1988; 1989; 1990; 1991; 1992; 1993; 1994; 1995; 1996; 1997; 1998, 1999, 2000', British Nuclear Fuels plc., Risley.
- Burns, P.A., Cooper, M.B., Lokan, K.H., Wilks, M.J. and Williams, G.A. (1995). 'Characterisation of plutonium and americium contamination at the former U.K. atomic weapons test ranges at Maralinga and Emu', *Applied Radiation and Isotopes* **46**(11), 1099-1107.
- Danesi, P.R., Bleise, A., Burkart, W., Cabianna, T., Campbell, M.J., Makarewicz, M. and Moreno, J. (2003a), 'Isotopic composition and origin of uranium and plutonium in selected soil samples collected in Kosovo', *J. Environ. Radioactivity* **64**, 121-131.
- Danesi, P.R., Markowicz, A., Chinea-Cano, E., Burkart, W., Salbu, B., Donohue, D., Ruedenauer, F., Hedberg, M., Vogt, S., Zaharadnik, P. and Ciurapinski, A. (2003b), 'Depleted uranium particles in selected Kosovo samples', *J. Environ. Radioactivity* **64**, 143-154.

Devell, L., Tovedall, U., Bergström, U., Applegren, A., Chussler, J. and Andersson, L. (1986), 'Initial observations of fallout from the reactor accident at Chernobyl', *Nature* **321**, 817–819.

Ericsson, M. (2002). *On Weapons Plutonium in the Arctic Environment* (150 pp.), PhD Thesis, Risø-R-1321(EUN), Roskilde: Risø National Laboratory.

Facer, G. (1980), 'Quantities of transuranic elements in the environment from operations relating to nuclear weapons', In: *Transuranic Elements in the Environment*, Wayne C. Hanson (Ed.), US DOE/TIC-22800, Office of Health and Environmental Research, p. 86.

Gascó, C., Iranzo, E. and Romero, L. (1992), 'Transuranics transfer in a Spanish marine ecosystem', *J. Radioanal. Nucl. Chem.* **156**, 151–163.

Gascó, C. and Antón, M.P. (1997), 'Influence of the submarine orography on the distribution of long-lived radionuclides in the Palomares marine ecosystem', *J. Environ. Radioactivity* **34**, 111–125.

Gray, J., Jones, S.R. and Smith, A.D. (1995), 'Discharges to the environment from the Sellafield site, 1951-1992', *J. Radiol. Prot.* **15**(2), 99–131.

Gouzy, A., Boust, D., Connan, O., Billon, G., León Vintrol, L., Lucey, J.A., Bowden, L., Agarande, M., Lesourd, S., Lesueur, P., Klein, A. and Kershaw, P.J. (submitted), 'Diagenetic reactivity of plutonium in marine anoxic sediments (Cumbrian mud patch – Eastern Irish Sea)', In: *ECORAD 2004: The Scientific Basis for Environmental Protection Against Radioactivity*, Aix-en-Provence, France, 6–10 September 2004.

Gunter, F. (1972), '*Principles of Isotope Geology*', Wiley & Sons, New York.

Hakam, O.K., Choukri, A., Reyss, J.L. and Lferde, M. (2001), 'Determination and comparison of uranium and radium isotopes activities and activity ratios in samples from some natural water sources in Morocco', *J. Environ. Radioactivity* **57**, 175–189.

Hamilton, E.I. (1981), 'Alpha-particle radioactivity of hot particles from the Esk Estuary', *Nature* **290**, 690–693.

Hamilton-Taylor, J., Kelly, M., Mudge, S., and Bradshaw, K. (1987), 'Rapid remobilisation of plutonium from estuarine sediments', *Journal of Environmental Radioactivity* **5**, 409–423.

Hetherington, J.A. (1978), 'The uptake of plutonium nuclides by marine sediments', *Mar. Sci. Comm.* **4**, 239-274.

Hill, P., Hille, R., Bouisset, P., Calmet, D., Kluson, J.m Smagulov, S. and Seysebaev, A. (1996), '*Radiological Assessment of Long-Term Effects at the Semipalatinsk Test Site: NATO-Semipalatinsk Project 1995/96*', Berichte des Forschungszentrums Jülich – 3325, March 1998, 115 pp.

Holden, N.E. (1981), '*The Uranium Half-Lives: A Critical Review*', National Nuclear Data Center, Brookhaven National Laboratory, New York, BNL-NCS-51320, 27 pp.

IAEA (1998), '*Radiological Conditions at the Semipalatinsk Test Site, Kazakhstan: Preliminary Assessment and Recommendations for Further Studies*', Radiological Assessment Report Series, International Atomic Energy Agency, Vienna, 43 pp.

Ivanovich, M., Fröhlich, K. and Hendry, M.J. (1991), 'Uranium-series radionuclides in fluids and solids, Milk River aquifer, Alberta, Canada', *Appl. Geochem.* **6**, 405–418.

Izrael, Yu U. (2002), 'Radioactive Fallout after Nuclear Explosions and Accidents', Radioactivity in the Environment Series, Vol. 3, Elsevier, Amsterdam, 281 pp.

Izrael, Yu A., Stukin, E.D., Petrov, V.N., Anspaugh, L., Doury, A., Kirchmann, R.J.C. and Van der Stricht, E. (2000), 'Nuclear explosions and their environmental contamination', In: *Nuclear Test Explosions: Environmental and Human Impacts*, Sir F. Warner and R.J.C. Kirchmann (Eds.), Scientific Committee on Problems of the Environment (SCOPE) of the International Council for Science (ICSU), SCOPE 59, John Wiley & Sons, Chichester, Chapter 3, pp. 33–98.

Jiménez Nápoles, H., León Víntró, L., Mitchell, P.I., Omarova, A., Burkitbayev, M., Priest, N.D., Artemyev, O. and Lukashenko, S. (2004), 'Source-term characterisation and solid speciation of plutonium at the Semipalatinsk NTS, Kazakhstan', *Appl. Radiat. Isot.* **61**, 325–331.

JNERG (1997), 'Sources Contributing to Radioactive Contamination of the Techa River and Areas Surrounding the Mayak Production Association, Urals, Russia. Programme of the Joint Norwegian-Russian Investigations of Possible Impacts of the Mayak PA Activities on Radioactive Contamination of the Barents and Kara Seas', Joint Norwegian-Russian Expert Group, Østerås, ISBN 82-993979-6-1.

Kashparov, V.A., Oughton, D.H., Zvarich, S.I., Protsak, V.P. and Levchuck, S.E. (1999), 'Kinetics of fuel particle weathering and ^{90}Sr mobility in the Chernobyl 30-km exclusion zone', *Health Phys.* **76**(3), 251–259.

Kennedy, V.H., Sanches, A.L., Oughton, D.H. and Rowland, A.P. (1997), 'Use of single and sequential chemical extractants to assess radionuclide and heavy metal availability from soils for root uptake', *Analyst* **122**, R98-R100.

Kershaw, P.J., Pentreath, R.J., Harvey, B.R., Lovett, M.B. and Boggis, S.J. (1986), 'Apparent distribution coefficients of transuranium elements in U.K. coastal waters', In: *Application of Distribution Coefficients to Radiological Assessment Models*, T.H. Sibley and C. Myttenaere (Eds.), Elsevier, London, pp. 277–287.

Kershaw, P.J., Swift, D.J. and Senoon, D.C. (1988), 'Evidence of recent sedimentation in the eastern Irish Sea', *Marine Geology* **85**, 1–14.

Kershaw, P.J., Denoon, D.C. and Woodhead, D.S. (1999), 'Observations on the redistribution of plutonium and americium in the Irish Sea sediments, 1978 to 1996: concentrations and inventories', *J. Environ. Radioactivity* **44**, 191–221.

Krey, P.W., Hardy, E.P., Pachucky, C., Rourke, F., Coluzza, J. and Benson, W.K. (1976), 'Mass isotopic composition of global fallout plutonium in soil', In: *Transuranium Nuclides in the Environment*, IAEA-SM-199/39, International Atomic Energy Agency, Vienna, pp. 671–678.

Kuriny, V.D., Ivanov, Y.A., Kashparov, V.A., Loschilov, N.A., Protsak, V.P., Yudin, E.B., Zurba, M.A. and Parshakov, A.E. (1993), 'Particle associated Chernobyl fallout in the local and intermediate zones', *Ann. Nucl. Energy* **20**, 415–420.

Langmuir, D. (1978), 'Uranium solution – mineral equilibria at low temperatures with application to sedimentary ore deposits', *Geochim. Cosmochim. Acta* **42**, 547–551.

Lee, M.H., Choi, G.S., Cho, Y.H., Lee, C.W. and Shin, H.S. (2001), 'Concentrations and activity ratios of uranium isotopes in the groundwater of the Okchun Belt in Korea', *J. Environ. Radioactivity* **57**, 105–116.

- León Vintró, L., Mitchell, P.I., Condren, O.M., Moran, M., Vives i Batlle, J. and Sánchez-Cabeza, J.A. (1996), 'Determination of the $^{240}\text{Pu}/^{239}\text{Pu}$ atom ratio in low activity environmental samples by alpha spectrometry and spectral deconvolution'. *Nucl. Instr. and Meth. Phys. Res. A* **369**, 597–602.
- Leonard, K.S., McCubbin, D. and Lovett, M.B. (1995), 'Physico-chemical characterisation of radionuclides discharged from a nuclear establishment', *Sci. Total Environ.* **175**, 9–24.
- Lind, O.C., Salbu, B., Janssens, K. and Simionovici, A. (2002), 'Radioactive particle characterisation by means of synchrotron radiation-based X-ray micro beam techniques', In: P. Strand (Ed.), *Proceedings of the 5th Int. Conference on Environmental Radioactivity in the Arctic & Antarctic*, St. Petersburg, Russia, 16-20 June 2002, Østerås, Norwegian Radiation Protection Authority, pp. 260-263.
- Lovett, M.B. and Nelson, D.M. (1981), 'Determination of some oxidation states of plutonium in sea water and associated particulate matter', In: *Techniques for Identifying Transuranic Speciation in Aquatic Environments*, Ispra. International Atomic Energy Agency, Vienna, STI/PUB/613, pp. 27–35.
- Loshilov, N.A., Kashparov, V.A., Yudin, E.B., Protsak, V.P., Zhurba, M.A. and Parshakov, A.E. (1991), 'Experimental assessment of radioactive fallout from the Chernobyl accident', *Sicurezza e Protezione* **46**, 25-26.
- Loshilov, N.A., Kashparov, V.A., Polakov, V.D., Protsak, V.P., Yudin, E.B. Zhurba, M.A. and Parshakov, A.E. (1992), 'Nuclear-physical properties of hot particles formed as a result of accident at ChNPP', *Radiochemistry* **4**, 113-119 (in Russian).
- Lucey, J.A. (2003), '*Solid Speciation of Plutonium in the Irish Sea by Sequential Extraction Analysis*', PhD Thesis, National University of Ireland, Dublin.
- MacKenzie, A.B., Scott, R.D. and Williams, T.M. (1987). 'Mechanisms for northwards dispersal of Sellafield waste', *Nature* **299**, 613–616.
- Manjón, G., García León, M., Ballestra, S. and Lopez, J.J. (1995), 'The presence of man-made radionuclides in the marine environment in the south of Spain', *J. Environ. Radioactivity* **28**(2), 171-189.
- McMahon, C.A., León Vintró, L., Mitchell, P.I. and Dahlgard, H. (2000), 'Oxidation state distribution of plutonium in surface and subsurface waters at Thule, NW Greenland', In: Proc. 12th ICRM Conference and International Symposium on Radionuclide Metrology and its Applications, Prague, 7–11 June 1999. *Appl. Radiat. Isot.* **52**, 697–703.
- Mitchell, P.I., Vives Batlle, J., Ryan, T.P., Schell, W.R., Sánchez-Cabeza, J.A. and Vidal-Quadras, A. (1991), 'Studies on the speciation of plutonium and americium in the western Irish Sea', In: *Radionuclides in the Study of Marine Processes*, P.J. Kershaw and D.S. Woodhead (Eds.), Elsevier, London, pp. 37–51.
- Mitchell, P.I., Vives i Batlle, J., Downes, A.B., Condren, O.M., León Vintró, L. and Sánchez-Cabeza, J.A. (1995), 'Recent observations on the physico-chemical speciation of plutonium in the Irish Sea and the western Mediterranean', *Appl. Radiat. Isot.* **46**(11), 1175–1190.
- Mitchell, P.I., Kershaw, P.J. and León Vintró, L. (1996), 'Radioactivity in the Irish Sea: Past Practices, Present Status and Future Perspectives'. In: *Radionuclides in the Oceans: Inputs and Inventories* (Proc. International Symposium on Radionuclides in the Oceans - RADOc 96-97. Part 1: Inventories, Behaviour and Processes. Cherbourg - Octeville, France, 7–11 October 1996), Pierre Guéguénat, Pierre Germain and Henri Métivier (Co-ordinators), *Les Éditions de Physique*, Les Ulis (ISBN 2-86883-285-7), Chapter 7, pp. 155–175.

Mitchell, P.I., Condren, O.M., León Vintró, L. and McMahon, C.A. (1999), 'Trends in plutonium, americium and radiocaesium accumulation and long-term bioavailability in the western Irish Sea mud basin', *J. Environ. Radioactivity* **44**(3), 221–249.

Mitchell, P.I., León Vintró, L., Smith, K.J., Sickel, M., Gerland, S., Brown, J., Oughton, D. and Lind, O.C., (2002), 'Size fractionation of plutonium in Arctic waters and implications for its mobility'. In: *Proc. 5th International Conference on Environmental Radioactivity in the Arctic and Antarctic*, Per Strand, Torun Jolle and Ase Sand (Eds.), 16–20 June 2002, St Petersburg, pp. 39–42.

NEA (1981), '*The environmental and Biological Behaviour of Plutonium and Some Other Transuranium Elements*', Report by an Expert Group, Nuclear Energy Agency, 116 pp.

Nelson, D.M., Larse, R.P. and Penrose, W.P. (1987), 'Chemical speciation of plutonium in natural waters', In: *Environmental Research on Actinide Elements*, J.E. Pinder III, J.J. Alberts, K.W. McLeod and R.G. Schreckise (Eds.), US Department of Energy, pp. 27–48.

Nitsche, H. (1995), 'Synchrotron X-ray-absorption spectroscopy - a new tool for actinide and lanthanide speciation in solids and solution', *J. Alloys Compounds* **223**, 274-279.

Osmond, J.K. and Ivanovich, M. (1992), 'Uranium-series mobilization and surface hydrology', In: *Uranium-series Disequilibrium: Applications to Earth, Marine, and Environmental Sciences*, M. Ivanovich and R.S. Harmon (Eds.), 2nd Edition, Chapter 8, Clarendon Press, Oxford, pp. 259–289.

Osmond, J.K., Cowart, J.B. and Ivanovich, M. (1983), 'Uranium isotope disequilibrium in ground waters as an indicator of anomalies', *Appl. Radiat. Isot.* **34**, 283–308.

Oughton, D.H., Salbu, B., Brand, T.L., Day, J.P. and Aarkrog, A. (1993), 'Under-determination of strontium-90 in soils containing particles of irradiated uranium oxide fuel', *Analyst* **118**, 1101-1105.

Oughton, D.H., Fifield, L.K., Day, J.P., Cresswell, R.C., Skipperud, L., Di Tada, M.L., Salbu, B., Strand, P., Drozcho, E. and Mokrov, Y. (2000), 'Plutonium from Mayak: measurements of isotope ratios and activities using accelerator mass spectrometry', *Environ. Sci. Technol.* **34**, 1938–1945.

Pentreath, R.J., Harvey, B.R. and Lovett, M.B. (1985), 'Chemical speciation of transuranium nuclides discharged into the marine environment'. In: R.A. Bullman & J.R. Cooper (Eds.), *Seminar on Speciation of Fission and Activation Products in the Environment*, Elsevier Applied Science, Oxford, pp. 312–325.

Pentreath, R.J., Woodhead, D.S., Kershaw, P.J., Jeffries, D.F. and Lovett, M.B. (1986), 'The behaviour of plutonium and americium in the Irish Sea', *Rap. P.-v. Reun. Cons. int. Explor. Mer.* **186**, 60-69.

Porcelli, D., Andersson, P.S., Wasserburgh, G.J., Ingri, J. and Baskaran, M. (1997), 'The importance of colloids and mires for the transport of uranium isotopes through the Kalix River watershed and Baltic Sea', *Geochim. Cosmochim. Acta* **61**, 4095–4113.

Priest, N.D., Burkitbayev, M., Artemyev, O., Lukashenko, S. and Mitchell, P.I. (2003), '*Investigation of the Radiological Situation in the Sarzhai Region of the Semipalatinsk Nuclear Test Site*', Final Report, NATO SEMIRAD Project, Science for Peace Programme, Contract No. Sfp-976046(99), February 2003, 103 pp.

Pulford, I.D., Allan, R.L., Cook, G.T. and MacKenzie, A.B. (1998), 'Geochemical associations of Sellafield-derived radionuclides in saltmarsh deposits of the Solway Firth', *Environmental Geochemistry and Health* **20**, 95–101.

Risø (1970), 'Project Crested Ice: A Joint Danish-American Report on the Crash Near Thule Air Base on 21 January 1968 of a B-52 Bomber Carrying Nuclear Weapons', Risø Report No. 213, 97 pp.

Romero, L. (1991), 'Estudios del Transporte Tierra-Mar de Elementos Transuránicos. Aplicación al Accidente de Palomares (Almería) de 1966', PhD Thesis. University of Madrid (in Spanish).

Romero, L., Lobo, A.M., Holm, E. and Sánchez, J.A. (1991), 'Transuranics contribution off Palomares coast: tracing history and routes to the marine environment', In: *Radionuclides in the study of Marine Processes*, P.J. Kershaw and D.S. Woodhead (Eds.), Elsevier Applied Science, London, pp. 245-254.

Ryan, T.P., Mitchell, P.I., Sánchez-Cabeza, J.A., Smith, V. and Vives i Batlle, J. (1995), 'Distribution of Radioactive Fallout throughout Ireland', In: Proc. Int. Tyndall School and National Environmental Week, Carlow (Ireland), 11-19 September 1993. *Science, Green Issues and the Environment: Ireland and the Global Crisis*, pp. 276-282.

Salbu, B. (2000), 'Speciation of Radionuclides in the Environment'. In: *Encyclopedia of Analytical Chemistry: Instrumentation and Applications, Part II, Radio-chemical Analysis*, Robert A. Meyers (Ed.), John Wiley and Sons Ltd., Chichester, England, Vol. 14, pp. 12993-13016.

Salbu, B., Bjørnstad, H.E., Sværen, I., Prosser, R.A., Bulman, R.A., Harvey, B.R. and Lovett, M.B. (1993), 'Size distribution of radionuclides in nuclear fuel reprocessing liquids after mixing with seawater', *Sci. Tot. Environ.* **130/131**, 51-63.

Salbu, B., Krekling, T., Oughton, D.H., Østby, G. Kashparov, V.A., Brand, T.L. and Day, J.P. (1994), 'Hot particles in accidental releases from Chernobyl and Windscale nuclear installations', *Analyst* **119**, 125-130.

Salbu, B., Krekling, T. and Oughton, D.H. (1998), 'Characterisation of radioactive particles in the environment', *Analyst* **123**, 843-849.

Salbu, B., Janssens, K., Krekling, T., Simionovici, A., Drakopoulos, M., Raven, C., Snigireva, I., Snigirev, A., Lind, O.C., Oughton, D.H., Adams, F. and Kashparov, V.A. (2000), 'μ-XAS-tomography and μ-XANES for characterisation of fuel particles', In: *ESRF Highlights 1999*, European Synchrotron Research Facility, Grenoble.

Salbu, B., Krekling, T., Lind, O.C., Oughton, D.H., Drakopoulos, M., Simionovici, A., Snigireva, I., Snigirev, A., Weitkamp, T., Adams, F., Janssens, K. and Kashparov, V.A. (2001), 'High energy X-ray microscopy for characterisation of fuel particles', *Nucl. Instr. Meth. Phys. Res. A* **467**(21), 1249-1252.

Salbu, B., Lind, O.C., Børretzen, P. and Oughton, D.H. (2001), 'Advanced speciation techniques for radionuclides associated with colloids and particles', In: F. Brechignac & B. Howard (Eds.), *Radioactive pollutants – Impact on the environment*, Les Ulis Cedex A, pp. 243-260.

Salbu, B., Janssens, K., Lind, O.C., Proost, K. and Danesi, P.R. (2003), 'Oxidation states of uranium in DU particles from Kosovo', *J. Environ. Radioactivity* **64**, 163-167.

Salbu, B., Janssens, K., Lind, O.C., Proost, K., Gijssels, L. and Danesi, P.R. (in press), 'Oxidation states of uranium in DU particles from Kuwait', *Journal of Environmental Radioactivity*.

Sánchez-Cabeza, J.A., Merino, J., Masqué, P., Mitchell, P.I., León Vintrolá, L., Schell, W.R., Cross, L. and Calbet, A. (2003), 'Concentrations of plutonium and americium in plankton from the western Mediterranean Sea', *The Science of the Total Environment* **311**, 233-245.

SCOPE (1993), 'Radioecology after Chernobyl: Biogeochemical Pathways of Artificial Radionuclides', Sir F. Warner and R.M. Harrison (Eds.), Scientific Committee on Problem on the Environment, John Wiley and Sons, Chichester, 367 pp.

Smith, J.N., Ellis, K.M., Aarkrog, A., Dahlggaard, H. and Holm, E. (1994), 'Sediment mixing and burial of the $^{239,240}\text{Pu}$ pulse from the 1968 Thule, Greenland nuclear weapons accident', *J. Environ. Radioactivity* **25**, 135-159.

Smith, K.J., León Vintó, L., Mitchell, P.I., Bally de Bois, P. and Boust, D. (2004), 'Uranium-thorium disequilibrium in North East Atlantic waters'. *Journal of Environmental Radioactivity* **74**, 199–210.

Stukin, E. and Izrael, Yu A. (1998), 'Radionuclide deposition over the territories adjacent to the Semipalatinsk test site according to the data of geophysical surveys carried out in 1960s and 1990s', In: *Atmospheric Nuclear Tests: Environmental and Human Consequences*, C.S. Shapiro (Ed.), NATO ASI Series, Partnership Sub-Series, 2. Environment, Vol. 35, Springer Verlag, Berlin, pp. 105–112.

Swift, D.J. (1993), 'The macrobenthic infauna off Sellafield, Cumbria (north-east Irish Sea) with special reference to bioturbation', *J. Mar. Biol. Assos. U.K.* **73**, 143–162.

Tessier, A., Campbell, P.G.C. and Bisson, M. (1979), 'Sequential extraction procedure for the speciation of particulate trace metals', *Analytical Chemistry* **51**(7), 844–851.

US Army Material Command (2000), 'Tank-Automotive and Armaments Comand (TACOM) and Army Material Command (AMC) Review of Transuranics (TRU) in Depleted Uranium Armor'. 19 January 2000. Memorandum. ATTN:AMCSF (Mr. Pittenger), 5001 Eisenhower Avenue, Alexandria, VA.

USEPA (2003), US Environmental Protection Agency Radiation Information Home Page, 7 January 2003; updated 13 August 2003. (<http://www.epa.gov/safewater/standard/pp/radnucpp.html>).

Victorova, N.V. and Geiger, E.K. (1990), 'Investigation of the Deposition and Spread of Radioactive Aerosol Particles in the Chernobyl Zone Based on Biological Monitoring', Report EU 13574, Commission of the European Communities, Luxembourg, 223–236.

Yamamoto, M., Tsukatani, T. and Katayama, Y. (1996a), 'Residual radioactivity in the soil of the Semipalatinsk nuclear test site in the former USSR', *Health Phys.* **71**(2), 142–148.

Voigt, G.M., Semiochkina, N., Dodd, B., Howard, B.J., Karabalin, B., Mukuschewa, M., Rosner, G., Sanchez, A., Singleton, D.L. and Strand, P. (2001), 'The present radiological situation at the nuclear weapons test site at Semipalatinsk in Kazakhstan with regard to plutonium contamination', In: *Plutonium in the Environment*, A. Kudo (Ed.), Radioactivity in the Environment Series, Vol. 1, Elsevier Science, pp. 363–373.

WHO (2003), 'Guidelines for Drinking Water Quality', Third Edition, Chapter 9 Draft, 17th February 2003. World Health Organisation, Geneva, Switzerland (http://www.who.int/docstore/water_sanitation_health/GDWQ/Updating/draftguidel/draftchap9.htm).

Yamamoto, M., Tsumura, A., Katayama, Y. and Tsukatani, T. (1996b), 'Plutonium isotopic composition in soil from the former Semipalatinsk Nuclear Test Site', *Radiochimica Acta* **72**, 209–215.